UNIVERSITY OF CALIFORNIA SAN DIEGO

Targeting Bacterial Pore Forming Toxins: Implications for Virulence Based Adjunctive Therapy for Invasive Bacterial Infections

A dissertation submitted in partial satisfaction of the requirements for the degree Doctor of Philosophy

in

Biomedical Sciences

by

Tamara Escajadillo

Committee in charge:

Professor Victor Nizet, Chair
Professor Lawrence Prince
Professor Tariq Rana
Professor Sharon Reed
Professor Liangfang Zhang

2018

This dissertation of Tamara Escajadillo is approved, and is acceptable in quality and form for publication on microfilm and electronically:

Chair

University of California San Diego

2018

DEDICATION

To my family, especially Robert as we navigate adulthood together, and my siblings Paul and Natasha, for always making sure I don’t grow up too much. And to all those who have mentored me along the way, my achievements are commensurate with your steadfast dedication to my success.

EPIGRAPH

“No great thing is created suddenly, any more than a bunch of grapes or a fig. If you tell me that you desire a fig, I answer that there must be time. Let it first blossom, then bear fruit, then ripen.”

- Epictetus

TABLE OF CONTENTS

LIST OF FIGURES

LIST OF TABLES

ACKNOWLEDGEMENTS

I would like to acknowledge my advisor and chair of my committee Victor Nizet, for being the type of mentor we should all aspire to be. Thank you for all your help and support during my time as a member of your scientific team, and for helping along my path beyond the laboratory as well.

I would also like to thank my thesis committee, Dr. Lawrence Prince, Dr. Tariq Rana, Dr. Sharon Reed, and Dr. Liangfang Zhang, for supporting me during my PhD career and helping me achieve this milestone.

I would like to say a special thank you to the Nizet lab members, past and present, for making it feel like a second home, especially on the days when there were more failures than successes. To my Bay E (“E Bay”) members Samira, Satoshi and Josh Sun and all those who came and went along the way, thank you for putting up with all my antics and endless decorations.

Chapter 1 is a portion from a review article that is being prepared for submission to the journal Toxins (Escajadillo T, Nizet V). The dissertation author is the primary author of this paper.

Chapter 2, in full, is a reprint of the material as it appears in: Escajadillo T, Olson J, Luk B, Zhang L, Nizet V. 2017. A red blood cell-camouflaged nanoparticle counteracts streptolysin O-mediated virulence phenotypes of invasive group A Streptococcus. *Frontiers in Pharmacology*. 8 (477) ISSN 1663-9812. The dissertation author is the primary investigator and author of this paper.

Chapter 3, in full, is a reprint of the material as it appears in: Thamphiwatana KS*, Angsantikul P*, Escajadillo T*, Zhang Q, Olson J, Luk BT, Zhang S, Fang RH, Gao W, Nizet V, Zhang L. 2017. Macrophage-like nanoparticles concurrently absorbing endotoxins and proinflammatory cytokines for sepsis management. *PNAS*. 114:11488-11493. The dissertation author was one of the primary investigators and authors of this paper.

Chapter 4 is a prepared manuscript ready for submission: Tamara Escajadillo, Lauren Popov, Samira Dahesh, Jan E Carette, Victor Nizet. Novel role for Sterol Regulatory Element Binding Protein-2 (SREBP-2) in the regulation of host cell susceptibility to the streptococcal toxin streptolysin-O. The dissertation author is one of the primary investigators and authors of this paper.

Chapter 5 is a portion from a review article that is being prepared for submission to the journal Toxins (Escajadillo T, Nizet V). The dissertation author is the primary author of this paper.

VITA

2014	Bachelor of Science, California State University, Dominguez Hills
2015-2017	Training Grant in Cellular and Molecular Pharmacology
2018	PhRMA Foundation Pre-Doctoral Fellowship
2018	Doctor of Philosophy, University of California, San Diego

PUBLICATIONS

Escajadillo T, Olson J, Luk B, Zhang L, Nizet V. 2017. A red blood cell-camouflaged nanoparticle counteracts streptolysin O-mediated virulence phenotypes of invasive group A Streptococcus. *Frontiers in Pharmacology*. 8 (477) ISSN 1663-9812.

Thamphiwatana KS*, Angsantikul P*, **Escajadillo T***, Zhang Q, Olson J, Luk BT, Zhang S, Fang RH, Gao W, Nizet V, Zhang L. 2017. Macrophage-like nanoparticles concurrently absorbing endotoxins and proinflammatory cytokines for sepsis management. *PNAS*. 114:11488-11493.

Escajadillo T, Wang H, Li L, Li D, Sewer, M. 2016. Oxysterol-Related-Binding-Protein Related Protein-2(ORP2) Regulates Steroid Hormone Metabolism and Cholesterol Homeostasis in H295R Adrenocortical Cells. *Molecular and Cellular Endocrinology*. 427: 73-85.

Lin AE, Autran CA, Szyszka A, **Escajadillo T**, Huang M, Godula K, Prudden AR, Boons GJ, Lewis AL, Doran KS, Nizet V, Bode L. 2017. Human milk oligosaccharides inhibit growth of group B Streptococcus. *Journal of Biological Chemistry*. 292 (27): 11243-11249. jbc.M117.789974.

Zhang Y, Gao W, Chen Y, **Escajadillo T**, Ungerleider J, Fang R, Christman KL, Nizet V, Zhang L. Self-Assembled Colloidal Gel Using Cell Membrane-Coated Nanosponges as Building Blocks. 2017. *ACS Nano*. **DOI:** 10.1021/acsnano.7b06968.

Chen Y, Chen M, Zhang Y, Lee JH, **Escajadillo T**, Gong H, Fang RH, Gao W, Nizet V, Zhang L. 2018. Broad-Spectrum Neutralization of Pore-Forming Toxins with Human Erythrocyte Membrane-Coated Nanosponges. *Advanced Healthcare Materials*. DOI: 10.1002/adhm.201701366.

ABSTRACT OF THE DISSERTATION

Targeting Bacterial Pore Forming Toxins: Implications for Virulence Based Adjunctive Therapy for Invasive Bacterial Infections

by

Tamara Escajadillo

Doctor of Philosophy in Biomedical Sciences

University of California San Diego, 2018

Professor Victor Nizet, Chair

While there is pressing concern over the development of antibiotic resistance, many non-resistant pathogens are capable of causing diseases of such severity that antibiotic treatment alone is insufficient for the development of optimal clinical outcomes. It is therefore imperative to explore new avenues for treatment of bacterial disease states. All bacterial pathogens have developed an arsenal of specialized virulence factors though which they are

capable of causing damage, and death, to host cells. Research focused neutralization of bacterial virulence factors as potential mechanisms for non-antibiotic therapy could help to address these concerns.

For this PhD dissertation project, I began by exploring the mechanisms of streptolysin O (SLO) induced host cell damage and examined the effects of utilizing red blood cell camouflaged nanoparticles (nanosponges) as a decoy capture platform for SLO. RBC derived nanosponges were capable of neutralizing SLO mediated toxicity and increasing immune cell function. The therapeutic potential of a toxin decoy capture platform was further expanded utilizing macrophage membrane derived nanoparticles in models of LPS driven bacteremia and were capable of absorbing bacterial LPS and several pro-inflammatory cytokines. Lastly, I focused on expanding the knowledge of host factors involved in mediating SLO toxicity through the use of gene-trap mutagenesis and CRISPR-Cas9 deletions, and explored potential pharmacological applications based on these results.

Altogether, this dissertation furthered our understanding of the mechanisms involved in bacterial toxin induced host cell damage and provides evidence for selecting toxin neutralization as a viable option for addressing bacterial disease, both through the use of engineered nanoparticles and through the application of knowledge derived from gene-trap mutagenesis strategies.

CHAPTER 1

INTRODUCTION

The rapid emergence of antimicrobial resistant strains of bacteria has exceeded the rate at which anti-bacterial therapies are currently being produced. While the classical approach to drug development has focused on the enhancement of bactericidal properties of antibiotics, over-prescription coupled with non-adherence to treatment regimens has further contributed to the development of widespread resistance (Alanis 2005, Boucher et al. 2009, Spellberg et al. 2008), underscoring the overarching need for the development of novel methods for combating bacterial infections. One possible approach that has gained attention over the past few years involves selecting bacterial virulence mechanisms as targets for therapy.

All bacteria rely on specialized virulence factors with which they can cause damage to host cells. While there exists a plethora of virulence mechanisms utilized by pathogenic bacteria to cause disease, the majority produce toxins that induce damage to either gain access to host cells for further proliferation, derive nutrients from host cells, or disrupt host cell immune function to increase their own survival, all of which may ultimately lead to host cell death. Pore forming toxins (PFTs) comprise about 25% of all known bacterial toxins, making them one of the largest classes of bacterial virulence factors (Gonzalez et al. 2008, Los et al. 2013, Dal Peraro and van der Goot 2016). All PFTs require binding in some way to a receptor on the host cell plasma membrane, where they oligomerize, form pores and alter membrane integrity(Kao et al. 2011, Bischofberger, Iacovache and van der Goot 2012, Gonzalez et al. 2008). While the mechanism of PFT pore formation may seem deceptively simple, PFTs can affect intracellular signaling cascades, dependent in part on the membrane structure the are bound to, and therefore can produce a variety of downstream responses, enhancing the pathogenicity of the bacteria that secrete them (Dal Peraro and van der Goot 2016, Bischofberger et al. 2012, Los et al. 2013, Griffitts et al. 2005, Giddings et al. 2004, Diep et al. 1998, Tweten 2005).

By preserving cell membrane integrity and viability of all host cells, including immune cells, PFT virulence factor neutralization could aid in facilitating pathogen elimination by normal immunity, while preserving the beneficial host microbiome. Given that anti-virulence strategies do not focus on directly killing the pathogen, they could provide the additional benefit of exerting less selective pressure, which may in turn result in a decreased need by the bacteria to develop resistance (Muhlen and Dersch 2016, Rasko and Sperandio 2010, Clatworthy, Pierson and Hung 2007).

1.CLASSIFICATION OF PORE FORMING TOXINS

PFTs can be generally classified into two large groups based on the secondary structure used to traverse the host cell plasma membrane, and are termed α-PFTs, for the creation of α-helixes, and β-PFTs, for the creation of β-barrels (Gouaux 1997). α-PFTs use clusters of amphipathic and hydrophobic helices to form pores on the host cell, (Parker and Feil 2005, Rojko et al. 2013) and the archetypal members of this class of PFTs are the colicins produced by Escherichia coli (Cascales et al. 2007, Lakey, van der Goot and Pattus 1994, Parker et al. 1989). Other α-PFT members include Cry toxins produced by *Bacillus thuringiensis (Grochulski et al. 1995), diphtheria toxin produced by Corynebacterium diphtheriae (Choe et al. 1992), and* exotoxin A produced by *Pseudomonas aeruginosa* (Allured et al. 1986).

β-PFTs comprise the majority of currently known bacterial PFTs and have been more extensively studied compared to α-PFTs owing to the possibility of establishing more precise classifications due to the high stability of their inter-strand hydrogens (Ros and Garcia-Saez 2015, Walker and Bayley 1995, Tilley and Saibil 2006). Some β-PFTs can further classified into three separate groups, including hemolysins, aerolysins, and cholesterol-dependent cytolysins (CDCs)(Dal Peraro and van der Goot 2016). CDCs require the presence of cholesterol during at least one step of their activity, and are also known as thiol-activated cytolysins due to their reported sensitivity to oxygen (Tweten, Parker and Johnson 2001).

CDCs are large family of over 20 PFTs that are secreted by many Gram-positive and gram-negative bacteria that share common structural motifs. Among the most widely studied are streptolysin-O (SLO) from *Streptococcus pyogenes* (Palmer et al. 1998), *pneumolysin (PLY)* from *Streptococcus pneumoniae (Sowdhamini et al. 1997), intermedilysin (ILY)* from *Streptococcus intermedius (Macey et al. 2001), listeriolysin O (LLO)* from *Listeria monocytogenes (Geoffroy et al. 1989, Mengaud et al. 1988), anthrolysin O (ALO)* from *Bacillus anthracis (Shannon et al. 2003)* and perfingolysin-O (PFO) from *Clostridium perfringens* (*Ro*ssjohn et al. 1997*).* Other commonly studied non CDC β-PFTs include aerolysin from *Aeromonas hydrophila (Parker et al. 1994),* and *α*-hemolysin (Hla) from *Staphylococcus aureus (Song et al. 1996).*

Following activation of attack or defense mechanisms, β-PFT monomers are secreted by their corresponding bacteria. The PFT then binds to a receptor on the plasma membrane of the host cell, where it oligomerizes to form a pre-pore complex. This complex subsequently becomes a transmembrane pore wall when it inserts itself into the host cell plasma membrane. Extensive details of the mechanisms of pore formation have previously been reviewed in detail (Rojko and Anderluh 2015, Iacovache, van der Goot and Pernot 2008, Parker and Feil 2005, Parker 2003, Tweten et al. 2001, Ros and Garcia-Saez 2015, Tilley and Saibil 2006, Los et al. 2013).

2.OVERVIEW OF PHARMACOLOGICAL APPROACHES TO PORE-FORMING TOXIN INHIBITION

Given the various components of pore formation after secretion of a PFT, there exist multiple candidate stages in which the PFT toxin can be targeted for inhibition, both directly and indirectly. While direct toxin inhibition involves physical binding to the monomer to preclude interaction with the host cell or interruption of the oligomerization process, multiple indirect methods have been described including prevention of binding to the receptor on the host cell

and the increase in host ability to resist toxin activity. The categories used for the purposes of this dissertation that will be described in further detail relate to direct binding/inhibition of toxin assembly by 1) antibodies or 2) other small molecules 3) decoy capture, and 4) alterations of host cell receptors/uptake inhibition 5) Pore blockage 6) increasing host resilience to effects of toxin activity (Figure 1.1).

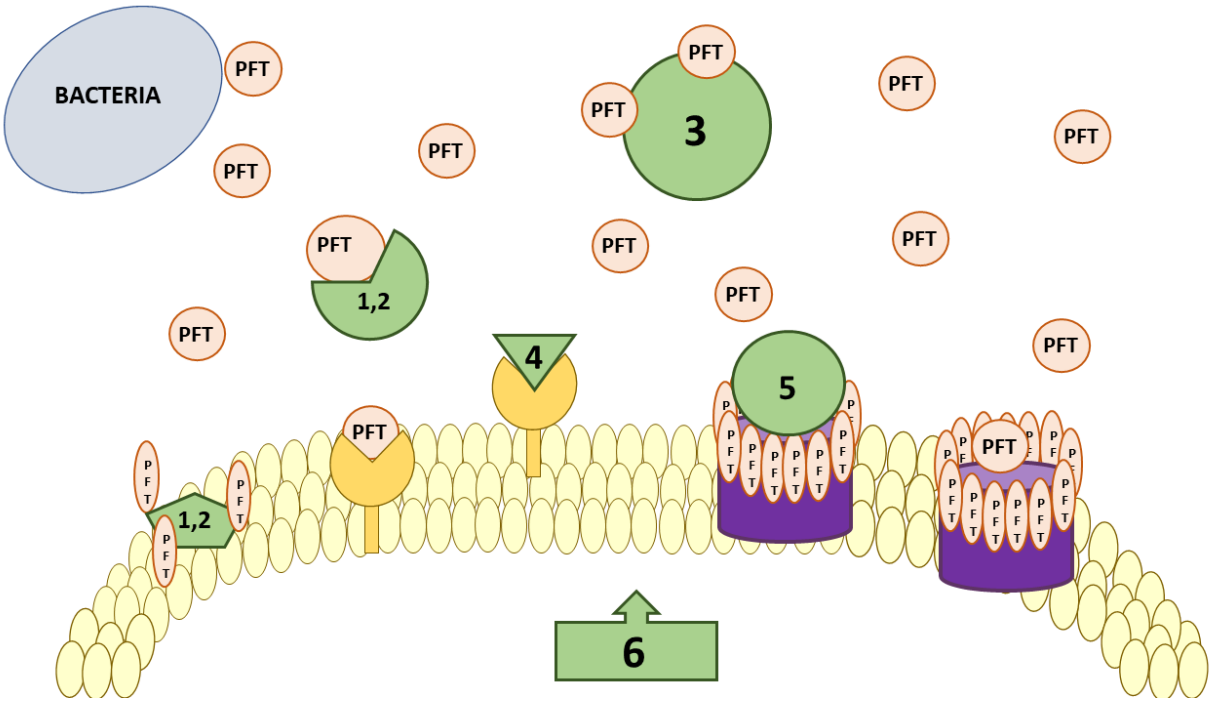

Figure 1.1 Stages of PFT secretion as potential targets for inhibition.

3. DIRECT BINDING OR SEQUESTRATION OF PORE FORMING TOXINS

Direct binding to the secreted PFT monomer constitutes one of the most straightforward approaches to neutralization and has been one of the most extensively explored within the realm of bacterial infections. In addition, the process of pore formation is dynamic, with different structural and functional states existing in the path to pore formation (Sonnen and Henneke 2013). Once the PFT has bound to its receptor on the host cell, it undergoes conformational

changes and oligomerizes to form a lytic transmembrane pore domain and insert itself into the plasma membrane.

3.1 Antibody Neutralization of Pore-Forming Toxins

A variety of small molecules have been discovered that are capable of binding to PFTs, including monoclonal antibodies (mAbs). Despite being one of the largest categories of PFT neutralizing agents, mAb therapies have not been as extensively explored in the realm of bacterial infections as they have in other areas of medicine, such as oncology and viral infections (Chames et al. 2009). mAbs can be isolated from a single B-cell clone expressing a single isotope, and is selected for superior activity against a target due to higher specificity (DiGiandomenico and Sellman 2015, Lang et al. 1993, Khazaeli, Conry and LoBuglio 1994).

Several monoclonal antibodies targeting Staphylococcus aureus' Hla have been developed using large scale libraries and high throughput screening methods. ASN-1 was isolated by screening a human IgG1 antibody library using a yeast selection system and was shown to bind Hla and four members of the S. aureus leukotoxin family of cytotoxins LukSF-PV, LukED, HlgAB, HlgCB and (Rouha et al. 2015); ASN-2 was shown to neutralize additional leukotoxin LukGH, and ASN-1 and ASN-2 mAb were then combined into ASN-100 (Rouha et al. 2018), with no dose limiting toxicity observed to date (Magyarics et al.) and is currently marketed by Arsanis, Inc.

MEDI4893 was developed by MedImmune LLC and binds Hla by recognizing a novel epitope in the "rim" domain and exerts its neutralizing effect through a dual mechanism that also involves inhibition of binding to the ADAM10 receptor (Foletti et al. 2013, Oganesyan et al. 2014, Hua et al. 2015), whose safety, tolerability, pharmacokinetics, anti-alpha-toxin-neutralizing activity save been explored (Yu et al. 2017).

AR-301 (Salvecin™) from Aridis Pharmaceuticals, Inc is a fully human monoclonal IgG1 antibody which reported promising results from a Phase 2a trial used as an adjunct therapy for severe pneumonia caused by *Staphylococcus aureus*. Another mAb, LTM14, was found to be a high affinity antibody derived from a phage display library which was shown during i*n vitro* studies to dose-dependently block the lytic activity of Hla in rabbit erythrocyte lysis assays (Foletti et al. 2013). Other mAbs against Hla include 2A3 and its affinity-optimized variant LC10, which were evaluated in a murine model of *S. aureus* pneumonia model (Tkaczyk et al. 2012, Hua et al. 2014), and mAbs 7B8 and 1A9 generated against the nontoxic Hla_{H35L} mutant which provided a high degree of protection against Hla-mediated injury by preventing oligomerization (Ragle and Bubeck Wardenburg 2009). Passive immunization strategies using rabbit polyclonal Hla-specific antisera generated using purified Hla_{H35L} as an immunogen have also been reported (Bubeck Wardenburg and Schneewind 2008, Kennedy et al. 2010).

Humanized heavy chain-only antibodies (HCAb) generated against S. aureus leukocidins LukS-PV and LukF-PV have been tested *in vitro* and *in vivo* and were shown to prevent toxin binding and pore formation for γ-hemolysin C (HlgC) as well(Laventie et al. 2011). Passive transfer of rabbit immunoglobulin raised against LukS-PV was also shown to protect against *S. aureus* sepsis (Karauzum et al. 2013).

Various molecules which directly target Streptococcus pneumoniae pneumolysin (PLY) include the murine monoclonal antibodies PLY-4 and PLY-7, directed against various epitopes on the toxin which also have dual modes of action by reducing cytolytic activity and blocking binding to eukaryotic cells, although they have not been used in clinical trials yet (Suarez-Alvarez et al. 2003, Garcia-Suarez Mdel et al. 2004). In addition to cholesterol, LeX/sLeX glycans have been described to be receptors for Ply and therefore mediate lysis of RBCs. When RBCs were preincubated with anti-sLeX and anti-LeX monoclonal antibodies hemolytic activity was inhibited (Shewell et al. 2014).

Nakouzi et al reported that the passive administration of monoclonal antibodies to Anthrolysin O (ALO) may contribute to host protection under specific circumstances. One mAb (64F8) slowed the toxicity of rALO *in vitro* and the combination of mAbs 64F8 and 80C9 was more effective than either mAb alone in prolonging survival in a murine model of infection (Nakouzi et al. 2008).

Moreover, polyclonal antibodies raised in rabbits against mutated Y30A-Y196A *C. perfringens* Epsilon toxin (Etx), a PFT that causes enterotoxemia, provided protection against wild type toxin in an *in vitro* neutralisation assay. (Bokori-Brown et al. 2014)

3.2 Small Molecules that Bind or Inhibit Toxin Assembly

While there are many small molecule natural compounds that have been found to inhibit α-toxin secretion (Qiu et al. 2010, Shah, Stapleton and Taylor 2008, Upadhyay et al. 2015), there are a few that have been studied for their direct toxin binding activity, including baicalin. Baicalin is a flavonoid compound isolated from the traditional Chinese medicinal herb *Scutellaria baicalensis*a which in addition to binding Hla directly also inhibits the hemolytic activity by restraining the conformation change of the binding cavity (Qiu et al. 2012). Other flavonoids have been reported to inhibit Hla include apigenin, chrysin, kaempferol, luteolin, and quercetin as well as the natural compounds *trans*-resveratrol and betulinic acid (Cho et al. 2015). Oroxylin A (ORO) was found to inhibit the hemolytic activity of Hla by binding to the active site (Thr11, Thr12, Ile14, Gly15 and Lys46) and inhibiting self-assembly of the heptameric transmembrane pore (Dong et al. 2013). Molecular Dynamics simulations and results of principal component analysis have indicated that Oroxylin A 7-O-glucuronide (OLG) and Oroxin B (ORB) also inhibit this conformational transition (Qiu et al. 2013). In silico based approaches based on key residues involved in the formation of the pore complex were used to design potential peptides for Hla inhibition, revealing the IYGSKANRQTDK peptide to both efficiently bind and disturb dimer formation(Rani et al. 2014). Morin hydrate, another bioflavonoid, was predicted to bind

to residues I107 and T109 and induce a conformational change which leads to inhibition of the self-assembly of the heptameric transmembrane pore (Wang et al. 2015b)

Several natural product derived compounds have been shown to interfere with the oligomerisation of PLY on cell membranes, although their actions have not yet been evaluated in the clinical setting. Amentoflavone (AMF; 4′,4‴,5,5″,7,7″-hexahydroxy-3‴,8-bi- flavone), is a flavonoid compound that is widely used in traditional Chinese medicine, extracted from Selaginella tamariscina and other plants. AMF blocks the PLY oligomerization process and inhibit its cytolytic activity by binding to PLY at the cleft between domains 3 and 4. (Zhao et al. 2017). Verbascoside (VBS) is a phenylpropanoid glycoside that does not exhibit bacteriostatic activity and has been shown through molecular dynamics simulations and mutational analysis to inhibit PLY-mediated cytotoxicity by also binding to the cleft between domains 3 and 4 of PLY (Zhao et al. 2016). In vitro studies of the flavonoid apigenin, demonstrated direct interaction with PLY and significantly attenuated hemolytic activity in a dose dependent manner and further showed a protective effect in a murine model of pneumococcal pneumonia (Song et al. 2016). β-sitosterol, a plant-derived cholesterol mimic was also shown to bind PLY with high affinity through Thr-459 and Leu-460 residues, and does not intervene in oligomerization (Li et al. 2015).

Inhibition of streptolysin O (SLO) by allicin, the most abundant thiosulfinate molecule found in garlic extract, was shown *in vitro* to inhibit SLO hemolytic activity likely through binding to the cysteine residue in the toxin's binding site (Arzanlou and Bohlooli 2010). Other studies by Shewell et al involving glycan array analysis determined that SLO displayed significant binding to 47 glycan structures, and upon flow cytometric analysis, it was found that free lacto-*N*-neotetraose (LNnT) blocked SLO binding to the RBC surface by binding to domain 4 of SLO, revealing glycans to be other possible inhibitors of PFT function (Shewell et al. 2014).

Through molecular modeling and mutational analysis, Wang et al demonstrated that fisetin, a dietary flavonoid, directly engages loop 2 and loop 3 of LLO, which leads both to the blockage of cholesterol binding and the reduction of its oligomerization, thus inhibiting its hemolytic activity (Wang et al. 2015a). Using a library containing 200,000 drug-like compounds against LLO, Ghafari et al discovered that modified compound (1-(4-Cyclopent-3-enyl-6, 7-dihydroxy-8-hydroxymethyl-nona-2, 8-dienylideneamino)-penta-1,4-dien-3-one) inhibited oligomerization of LLO fitting binding properties with no undesirable pharmacological properties such as toxicity by inhibiting (Ghafari et al. 2017).

3.3 Inhibition of Pore-Forming Toxins through Decoy Capture

A characteristic that all β-PFTs have in common is the need to bind to the plasma membrane of the host cell in some capacity. Therefore, this principle has been used as inspiration for developing liposomal targets that can be used as decoys for toxins by mimicking the lipid composition of natural host membranes. Liposomes are synthetic, spherical, nanoscale multilamellar or unilamellar bilayer vesicles composed of a variety of lipids that have been used for various commercial applications including enhancing drug delivery and enhancing signaling for medical diagnostics (Bitounis et al. 2012, Kshirsagar et al. 2005). Henry et al. described modeling these lipid layers after distinct microdomains termed lipid rafts which, while unstable *in vivo*, can be stably artificially created in liposomes. They reported that by tailoring liposomes toward enhanced selectivity for bacterial toxins by using higher than *in vivo* relative concentrations of cholesterol:sphingolyelin (Ch:Sm) liposomes (66mol/% cholesterol), these liposomes were able to bind CDCs and Hla, while a mixture of cholesterol:sphingolyelin liposomes (66mol/% cholesterol) with sphingomyelin only liposomes (Ch:Sm+Sm) efficiently sequestered a larger array of bacterial toxins. In addition, they demonstrated improved therapeutic efficacy of antibiotics when used in combination with their liposomal formulations as adjunctive therapy during *in vivo S. aureus* and *S. pneumoniae* bacteremia models (Henry et al.

2015). These studies served as the basis for the development of CAL02, a new liposomal formulation marketed by the Swiss based company Combioxin SA. CAL02 has recently completed Phase I clinical trials for the neutralization of a large panel of bacterial toxins by recognizing the artificially engineered lipid rafts on the liposomes.

Despite the promising nature of liposomal toxin decoy capture platforms, these artificial nanoparticle formulations face many challenges including rapid opsonization and clearance by macrophages and the need to tailor liposomal formulations to specific concentration ranges (Yoo, Chambers and Mitragotri 2010, Alexis et al. 2008). In addition, various attempts to circumvent this problem by applying stealth coatings have raised the issue of off-target immunological responses (Knop et al. 2010). This led to the development of host cell membrane coated camouflaged nanoparticles, which significantly enhanced bioavailability, essential for absorbing toxins in the bloodstream, while providing the same complex surface chemistry of a biological cell (Hu et al. 2011).

Red blood cell (RBC) membrane derived nanoparticles internally stabilized with a poly(lactic-co-glycolic-acid) (PLGA) core have been demonstrated to exhibit toxin binding and retention for a variety of toxins including SLO, LLO and Hla (Hu et al. 2013a). The ability to retain bacterial toxins on the nanoparticle therefore precludes interaction of the toxin with the host cell. Nanoparticles are therefore capable of reducing damage both *in vitro* and *in vivo (Escajadillo et al. 2017, Zhang Y 2017, Chen et al. 2018, Hu et al. 2013a)*, with the potential for detoxification of all membrane damaging bacterial toxins.

4.INHIBITION OF HOST CELL RECEPTORS OR UPTAKE OF PORE-FORMING TOXINS

PFTs recognize target cells by binding to different receptors including sugars, lipids and proteins on the plasma membrane yet not all receptors have been identified, leaving this to be an ongoing area of research (Dal Peraro and van der Goot 2016).

Research into mechanism of action of α-hemolysin revealed that the protein receptor ADAM10, a zinc-dependent metalloprotease, is required for Hla binding to the eukaryotic cells and consequent toxicity (Wilke and Bubeck Wardenburg 2010). The hydroxamate inhibitor GI254023X was found to inhibit ADAM10 by fitting into the S1 specificity pocket (Ludwig et al. 2005), and was found to both attenuate epithelial barrier disfunction and prevent E-cadherin cleavage (Inoshima, Wang and Bubeck Wardenburg 2012) and to significantly decrease lesion size in a murine model of *S. aureus* skin infection (Sampedro et al. 2014). Co-receptors for another *S. aureus* PFT, leukocidin LukED, include the human immunodeficiency virus (HIV) co-receptor or CC-chemokine receptor type 5 (CCR5) and CXC-chemokine receptor type 1 and 2 (CXCR1 and CXCR2). Activity of LukED has been reportedly efficiently blocked using CCR5 receptor agonists and HIV drug maraviroc (Alonzo et al. 2013, Reyes-Robles et al. 2013).

Intermedilysin (ILY), a CDC from *Streptococcus intermedius,* in addition to binding cholesterol, is capable of binding to the human complement regulator CD59, a clycosylphosphatidylinositol (GPI)-anchored cell-surface receptor, thereby promoting oligomerization and pore formation on the membrane of host cells (Dowd, Farrand and Tweten 2012, Giddings et al. 2004, LaChapelle, Tweten and Hotze 2009). The crystal structure of CD59 bound to ILY was solved and allowed for the synthesis of a peptide based on the binding site and comprised of ILY residues 438-452, which successfully competed for CD59 binding and inhibited ILY pore formation *in vitro* (Johnson et al. 2013). Another study using non-small lung carcinoma cells characterized the mechanism of a novel CD59 inhibitor: the 114-amino acid recombinant form of the 4th domain of intermedilysin (rILYd4). They showed that upon binding to rILYd4, CD59 is internalized and undergoes massive degradation in lysosomes within minutes., while the remaining rILYd4·CD59 complexes are shed from the cell, supporting a novel role for rILYd4 in promoting internalization and rapid degradation of the complement inhibitor CD59 (Cai et al. 2014). The major binding targets for the *Aeromonas* PFT aerolysin

have also been reported to be GPI-anchored surface receptors, including T-lymphocyte protein (Thy-1) (Diep et al. 1998). Given the ability of synthetic analogs of GPIs to inhibit binding of related toxin CAMP factor, this approach could be applicable to aerolysin as well (Wu and Guo 2010).

Cholesterol has widely been described to be essential for pore formation of CDCs and appears to play multiple roles including targeting, promotion of oligomerization, triggering a membrane insertion competent form, and stabilizing the membrane pore (Rossjohn et al. 1997). In addition, it has been suggested that the extent of toxin binding and size of the oligomers is dependent on the cholesterol concentration in the membrane (Ohno-Iwashita et al. 1992). Therefore, it is possible that targeting membrane cholesterol could have an advantageous effect against PFT pore formation, especially with CDCs PFTs. Statins, competitive inhibitors of 3-hydroxy 3-methylglutaryl coenzyme A (HMG-CoA) the rate limiting enzyme in cholesterol biosynthesis, are widely used in cardiovascular disease (Maron, Fazio and Linton 2000). Studies in a mouse model of sickle cell disease (SCD) suggested that simvastatin protected host cells from the cytotoxic effects of the PLY and extended to other CDCs SLO and tetanolysin, and was suggested to be due to lack of support for pore formation required for cytotoxicity after binding to membrane cholesterol of endothelial cells (Rosch et al. 2010). Although studies by Statt et al. on human airway epithelial cells treated with physiological serum concentration ranges of simvastatin *in vitro* showed protection from PLY and Hla, this was not reproducible in other cell lines. In addition, statins are known to have pleiotropic effects on cells, and data from this study suggested the protective effect might be related to reduced pore formation after cholesterol binding of enhanced cellular membrane repair (Statt et al. 2015). These results could suggest further benefit from the experimentation with cholesterol modifying agents in the context of PFTs.

5. BLOCKADE OF PORE-FORMAITON

Once the PFT has oligomerized and inserted into the host cell membrane, the pores that are formed have a characteristic size and shape depending on the PFT inducing the damage (Henning-Knechtel, Knechtel and Magzoub 2017). The pore then becomes a permeable channel and pathway for the flux of ions and other charged or polar molecules to cross the plasma membrane, which can result in alterations of host downstream signaling cascades at sub-cytolytic or in complete lysis of the host cell (Kao et al. 2011, Alouf 2000, Los et al. 2013, Dal Peraro and van der Goot 2016, Majd S 2010, Bischofberger, Gonzalez and van der Goot 2009). Considering this deceptively simple outcome of PFT action, the creation of a hole in the membrane, an equally simple approach to combat this insult it to disable the action of the pore by directly physical obstruction (Bezrukov and Nestorovich 2016, Nestorovich and Bezrukov 2012).

One method of blocking oligomeric pores that has been explored is the use of cyclodextrins, cyclic oligomers of glucose that for water-soluble inclusion complexes with small and large molecules and have been used for a variety of biotechnology applications (Davis and Brewster 2004). Studies on selectively blocking α-hemolysin using β-cyclodextrin derivatives demonstrated that symmetry, size of the inhibitor and the pore are important (Yannakopoulou et al. 2011, Karginov et al. 2007). Yannakopoulou et al. found that only β-cyclodextrin derivatives, and not α- or γ-derivatives, effectively inhibited Hla by mirroring the symmetry of the heptameric toxin. In other studies, ANBOβCD blocked the Hla channels irreversibly (Karginov et al. 2007), while modified hepta-6-substituted β-cyclodextrin compound termed IB201 was reported to block the assembled Hla pore and decrease mortality in a murine model of S. aureus pneumonia(Ragle, Karginov and Bubeck Wardenburg 2010). A slightly different approach found two different salts of a isatin-Schiff base copper(II) complex, Cu(isapn) and perclorate—$[Cu(isapn)](ClO_4)_2$—or sulfonate—$[Cu(isapn)](SO_4)_2$, possessed significant activity against Hla

by interacting with the constriction region of the pore and blocking it in a potential dependent manner (Melo et al. 2016).

A high-throughput screening of a 151,616-compound library by Lewis et al identified three compounds, N-cycloalkylbenzamide, furo[2,3-b]quinoline, and 6H- anthra[1,9-cd]isoxazol, that were suggested to inhibit C. perfringens Etx toxin by blocking the active pore, given that there was a decrease in the effect of the toxin yet no direct effect on the binding or oligomerization process of the toxin(Lewis M 2010).

6.INCREASING HOST CELL RESILIENCY AGAINST PORE-FORMING TOXIN ACTION

After attack by a PFT, the host cell can respond to this aggression by a number of pathways that are dependent upon both the type and concentration of the PFT and the type of host cell affected, which leads to different downstream signaling events (Bischofberger et al. 2012). Although at high concentrations PFTs cause host cell lysis, and at lower concentrations of toxin, survival of intoxicated host cells is well documented and reviewed (Cassidy and O'Riordan 2013, Dal Peraro and van der Goot 2016, Bischofberger et al. 2012). Mechanisms by which the host cell overcomes PFT damage have the potential to be a target for pharmacological intervention.

Resealing of the membrane pore through regulation of membrane lipids, control of cytoskeletal dynamics, enhancement of blebbling or microvesicle shedding are attractive options for further investigation (Mesquita et al. 2017, McNeil and Kirchhausen 2005, Romero et al. 2017, Keyel et al. 2011). The decrease in cytoplasmic potassium after pore formation has been reported to promote inflammasome activation through caspase-1, leading to activation of the inflammatory pathway to combat infection, but has also been reported to influence lipid membrane biogenesis gene regulator sterol regulatory element binding protein 1 (SREBP1) (Gurcel et al. 2006). Another study reported that the pretreatment of lung epithelial cells with

interferon IFN-α before treatment with Hla prevents cell-death via regulation of lipid metabolism and increases in protein synthesis and fatty acid activity, although it was reported to be independent of caspase-1 or mitogen-activated protein kinases (Yarovinsky et al. 2008).

A host cellular defense mechanism that has been suggested as a potential therapeutic target for PFTs is the process of autophagy, a lysosomal process involved in maintaining cellular homeostasis through turnover of damaged or redundant proteins and organelles (Meijer and Codogno 2009) and can result in autophagic cell death (Levine and Yuan 2005). Numerous bacterial pathogens interfere with the autophagy process, but the interaction between autophagy and bacteria is often dependent on the type of bacteria and the type of PFT they secrete (Mostowy 2013). A review of selected FDA approved drugs and pharmacological agents that modulate autophagy and could help improve the outcome of antibiotic treatment can be found here (Mathieu 2015).

A mutagenized screen in *Caenorhabditis elegans* for Crystal (Cry) protein PFT resistant mutants revealed that hypoxia and the induction of Hypoxia-inducible factor-1 (HIF-1), a transcription factor that is expressed by all metazoan species and functions as a master regulator of oxygen homeostasis (Semenza 2010), can protect cells against PFTs. (Bellier et al. 2009) HIF has been found to induce the transcription of genes involved in the inflammatory response such as IL-1β, IL-8, TNFα, iNOS and cathelicidin (LL-37), which could explain the enhanced survival after PFT intoxication (Peyssonnaux et al. 2005) Under normoxic conditions, HIF is hydroxylated by prolyl hydroxylases (PHDs) consequently degraded by a ubiquitin-ligase complex (Bruick and McKnight 2001). AKB-4924, a PHD2 inhibitor licensed to Akebia Therapeutics has been found to stabilize HIF-1 and increase skin innate defense against S. aureus, Pseudomonas aeruginosa and Acimetobacter baumanii infections (Okumura et al. 2012), making it an attractive possibility for continued research into host defense against PFTs.

When analyzing the effect of different PFTs on host cell function, a key characteristic of PLY is the ability to impair pulmonary barrier integrity and function, leading to altered alveolar permeability and epithelial tight junction integrity in the lung (Rayner et al. 1995). Recent studies by Lucas et al. revealed two peptides derived from host mediators that can counteract negative effects of PLY, the first is the Growth Hormone-Releasing-Hormone (GHRH) agonist JI-34 which enhances both epithelial sodium channel (ENaC) function and capillary resistance in a cAMP-dependent manner, and the second a TNF-derived TIP peptide, AP301, currently in phase 2a clinical trials, capable of blunting the activation of the enzymes protein kinase C-α and arginase 1, which are involved in the induction of hyperpermeability in the capillary endothelium, both *in vitro and in an in vivo murine model(Lucas et al. 2013)*.

The knowledge derived from decades of studying the PFT structure and pore architecture elucidated in great part by ongoing crystallization studies, have enabled the design of toxoid vaccines that to prime the host immune system without inducing the deleterious effects of the toxin itself (Cockeran, Anderson and Feldman 2005, Dal Peraro and van der Goot 2016). Pneumococcal conjugate vaccines (PCVs), including the seven-valent pneumococcal conjugate vaccine (PCV7) have helped decrease the burden of disease in many populations (Grijalva et al. 2007). But the development of broader protection is needed due to the shifts in serotype epidemiology, and PLY has long been regarded as a pneumococcal protein vaccine candidate (Crisinel et al. 2010, Leroux-Roels et al. 2014, Cockeran et al. 2005). Two candidate antigens for a protein-based pneumococcal vaccine are pneumolysin toxoid (dPly) and histidine-triad protein D (PhtD), and were originally shown to provide protection against pneumococcal infection in animal models (Alexander et al. 1994, Ogunniyi et al. 2001, Denoel et al. 2011) Further phase I clinical trials in adults and toddlers showed that vaccine formulations containing dPly and PhtD were well tolerated and immunogenic when administered as standalone protein

vaccines or combined with PHiD-CV conjugates (Leroux-Roels et al. 2014, Prymula et al. 2014, Alexander et al. 1994).

Another promising toxoid candidate is ΔA146 PLY, generated by deletion of alanine 146 and arginine 147 in the pore-forming region of wild-type PLY (Kirkham et al. 2006), that was promisingly not shown to produce a pro-inflammatory response in neutrophils (Cockeran et al. 2011). Other studies showed that a fusion protein created using L460D, a noncytolytic PLY toxoid incapable of binding cholesterol (Farrand et al. 2010), together with choline-binding protein A (CbpA) was broadly protective against pneumococcal infection, with the potential for additional protection against other meningeal pathogens(Mann et al. 2014).

In a murine model of S. aureus pneumonia, immunization with an Hla mutant possessing a single amino acid substitution, Hla_{H35L} , was capable of decreasing bacterial burden and overall mortality (Bubeck Wardenburg and Schneewind 2008). Protection using Hla_{H35L} was further confirmed to reduce skin lesions caused by S. aureus strain USA300 and prevented dermonecrosis in a murine skin infection model (Kennedy et al. 2010).

Given that a single point mutation in Hla is not considered ideally safe for use in a clinical setting, Adhikari et al. designed additional truncation mutants as vaccine candidates using a rational, structure based approach. Based on results of molecular modeling, they generated a lead Hla vaccine candidate, AT-62aa, which exhibited strong immunogenicity in mice when used with two clinically tested adjuvants ($AlPO_4$ and GLA-SE), in models of S. aureus skin and soft tissue infections (Adhikari et al. 2012, Adhikari et al. 2016). A chimeric bivalent vaccine using Hla and S. aureus iron surface determinant B (IsdB), an iron-regulated cell wall-anchored surface protein, was shown to have a stronger protective immune response than either protein alone (Zuo et al. 2013). Attenuated subunit vaccines using mutant LukS-PV and LukF-PV subunits LukS-Mut9/LukF-Mut1 were highly immunogenic and demonstrate significant protection in a S. aureus murine model of sepsis (Karauzum et al. 2013)

A few noncytolytic LLO mutants (LLO W492A and LLO W491-492A) have been reported to still maintain the binding capacity to the cell membranes with high affinity and are catabolized, processed, and presented efficiently by APCs to CD4+ or CD8+ T cells (Hernandez-Flores and Vivanco-Cid 2015, Carrero, Vivanco-Cid and Unanue 2012, Michel et al. 1990), although LLO has been reported to be strongly immunogenic independently of its cytotoxic ability (Carrero et al. 2012), and its role has been explored more in the context of live vaccine vectors (Bahey-El-Din et al. 2010).

Initial studies on the *C. perfringens* Epsilon toxin (Etx) determined that the H149A mutation (Etx-H149A) could reduce, yet not abolish, toxicity (Bokori-Brown et al. 2013), and lead to the discovery of the site-directed mutant of Etx (Y30A-Y196A) as a potential recombinant vaccine candidate. Etx (Y30A-Y196A) significantly reduced cell binding and cytotoxic activities in MDCK.2 cells (Bokori-Brown et al. 2014).

Studies on SLO showed that a recombinant SLO derivate (rSLOmut) with mutated tryptophan residue in the membrane-binding loop W535A (Chiarot et al. 2013) elicits protective immunity against lethal GAS challenge. Mice immunized with rSLOmut were significantly protected against lethal systemic challenge with WT GAS M1 strain, further supporting the inactivated SLO antigen as an attractive component for future multivalent GAS vaccines (Uchiyama et al. 2015).

Finally, in an effort to maximize PFT vaccine potency and safety, alternative strategies employing non-denatured PFTs anchored to the previously mentioned RBC membrane coated nanoparticles in conjunction have been developed. Hu et al described Hla loaded nanotoxoids were capable of bestowing strong protective immunity in an α-haemolysin murine intoxication model. Nanotoxoids were efficiently cleared with no additional toxicity after a period of two weeks, and could potentially be used for a broad range of PFTs, and applied clinically either by

using nanotoxoids developed directly from patient blood or using O- donor blood (Hu et al. 2013b, Hu and Zhang 2014).

Recently, the use of high-throughput genetic screens using human cells to discover novel host factors required for bacterial PFT toxicity have emerged as promising ways to increase the number of potential targets available for therapeutic intervention during bacterial disease (Banks and Bradley 2007, Carette et al. 2009). Insertional mutagenesis screens in human haploid cells coupled with CRISPR-Cas9 gene deletion studies to discover novel host cell targets that modulate susceptibility to PFTs, revealed the plekstrin-homology domain containing protein 7 (PLEKHA7) to be a critical mediator for Hla cytotoxicity (Popov LM et al. 2015). Another gene-trap mutagenesis and RNA interference study concluded that Etx was capable of binding to the hepatitis A virus cellular receptor 1 (HAVCR1), providing valuable insights into the process of toxin induced cell death (Ivie et al. 2011).

Summary

Reduction of bacterial burden and increase in host cell resilience are key determining factors for favorable outcomes during bacterial infectious disease states. Although still in early stages of investigation, neutralization of clinically significant virulence factors has begun to emerge as a potential method of alleviating disease severity. One important class of virulence factors present in many leading bacterial pathogens, including several antibiotic-resistant strains, is the pore-forming toxins (PFTs). PFTs comprise about 25% of all known bacterial toxins and are produced by both Gram-positive and Gram-negative bacterial pathogens. Due to the deceptive simplicity of their mechanism of action, the downstream effects of these toxins on cell signaling and immune responses have been vastly understudied, but their involvement in key aspects of disease pathogenesis make them attractive therapeutic targets. Therefore, preventing or neutralizing interaction between bacterial toxins and the host cell could be an effective therapeutic strategy.

This dissertation will focus on specific, novel non-classical approaches toward reducing bacterial damage to host cells through inhibition of bacterial toxins, which have the potential to become powerful alternative pharmacological strategies for the treatment of disease, used either independently or as adjunctive therapy to classical antibiotic regimens.

ACKNOWLEDGEMENTS

Chapter 1 is a portion of a review article being prepared for submission as: Escajadillo T & Nizet V. Targeting bacterial pore forming toxins: implications for virulence based adjunctive therapy for invasive bacterial infections. The dissertation author is the primary author of this paper.

SPECIFIC AIMS

The main purpose of this dissertation is to identify and apply potentially novel strategies involving toxin neutralization for the treatment of bacterial infections. Because of the multifaceted role of bacterial toxins in disease pathogenesis, I hypothesize that infectious disease therapeutics that neutralize the ability of bacterial toxins to damage host cells can slow the development of bacterial resistance, since it is the virulence mechanism and not the viability of the pathogen that is targeted. This approach may confer an additional therapeutic advantage when compared to conventional antibiotics, as the normal microflora of the host would not be perturbed by the treatment. I will examine the following aims:

Aim 1. Absorption and detoxification of SLO in vitro and in vivo using red blood cell-derived nanoparticles or "nanosponges".

1A. Determine if RBC-derived nanosponges block GAS SLO-mediated hemolysis and keratinocyte cytotoxicity

1B. Determine if RBC nanosponges counteract GAS SLO-mediated toxicity to macrophages.

1C. Determine if RBC nanosponges mitigate GAS SLO-mediated impairment of neutrophil killing.

1D. Determine if RBC nanosponges reduce GAS disease severity in necrotizing skin infection model.

Aim 2. Detoxification of endotoxin (LPS) and concurrent absorption of cytokines by macrophage derived nanoparticles.

2A. Determine if macrophage derived nanoparticles are capable of binding LPS and proinflammatory cytokines.

2B. Determine if macrophage derived nanoparticles are capable of detoxifying LPS and proinflammatory cytokines in vitro.

2C. Determine if macrophage derived nanoparticles are capable of detoxifying LPS and proinflammatory cytokines in a murine bacteremia model.

Aim 3. Identification of novel host factors that reduce toxicity induced by the PFT SLO.

3A. Validate top novel “hits” by CRISPR KO in Hap1 cells and determine if the host cell protection is specific for the PFT SLO or is generalizable for other PFTs.

3B. Analyze membrane dynamics, cholesterol homeostasis and cell death pathways associated with the SLO resistance phenotype in the SREBP2 knockout.

3C. Determine if host cell protection conferred by SREBP2 inhibition is applicable to a macrophage cell line and the effect on inflammatory pathways

3D. Screen for potential pharmacological inhibitors of SREBP2 that will mirror the phenotype observed in the genetic knockout.

REFERENCES

1. Adhikari, R. P., H. Karauzum, J. Sarwar, L. Abaandou, M. Mahmoudieh, A. R. Boroun, H. Vu, T. Nguyen, V. S. Devi, S. Shulenin, K. L. Warfield & M. J. Aman (2012) Novel structurally designed vaccine for S. aureus alpha-hemolysin: protection against bacteremia and pneumonia. *PLoS One,* 7**,** e38567.

2. Adhikari, R. P., C. D. Thompson, M. J. Aman & J. C. Lee (2016) Protective efficacy of a novel alpha hemolysin subunit vaccine (AT62) against Staphylococcus aureus skin and soft tissue infections. *Vaccine,* 34**,** 6402-6407.

3. Alanis, A. J. (2005) Resistance to antibiotics: are we in the post-antibiotic era? *Arch Med Res,* 36**,** 697-705.

4. Alexander, J. E., R. A. Lock, C. C. Peeters, J. T. Poolman, P. W. Andrew, T. J. Mitchell, D. Hansman & J. C. Paton (1994) Immunization of mice with pneumolysin toxoid confers a significant degree of protection against at least nine serotypes of Streptococcus pneumoniae. *Infect Immun,* 62**,** 5683-8.

5. Alexis, F., E. Pridgen, L. K. Molnar & O. C. Farokhzad (2008) Factors affecting the clearance and biodistribution of polymeric nanoparticles. *Mol Pharm,* 5**,** 505-15.

6. Allured, V. S., R. J. Collier, S. F. Carroll & D. B. McKay (1986) Structure of exotoxin A of Pseudomonas aeruginosa at 3.0-Angstrom resolution. *Proc Natl Acad Sci U S A,* 83**,** 1320-4.

7. Alonzo, F., 3rd, L. Kozhaya, S. A. Rawlings, T. Reyes-Robles, A. L. DuMont, D. G. Myszka, N. R. Landau, D. Unutmaz & V. J. Torres (2013) CCR5 is a receptor for Staphylococcus aureus leukotoxin ED. *Nature,* 493**,** 51-5.

8. Alouf, J. E. (2000) Cholesterol-binding cytolytic protein toxins. *Int J Med Microbiol,* 290**,** 351-6.

9. Arzanlou, M. & S. Bohlooli (2010) Inhibition of streptolysin O by allicin - an active component of garlic. *J Med Microbiol,* 59**,** 1044-9.

10. Bahey-El-Din, M., P. G. Casey, B. T. Griffin & C. G. Gahan (2010) Expression of two Listeria monocytogenes antigens (P60 and LLO) in Lactococcus lactis and examination for use as live vaccine vectors. *J Med Microbiol,* 59**,** 904-12.

11. Banks, D. J. & K. A. Bradley (2007) SILENCE: a new forward genetic technology. *Nat Methods,* 4**,** 51-3.

12. Bellier, A., C. S. Chen, C. Y. Kao, H. N. Cinar & R. V. Aroian (2009) Hypoxia and the hypoxic response pathway protect against pore-forming toxins in C. elegans. *PLoS Pathog,* 5**,** e1000689.

13. Bezrukov, S. M. & E. M. Nestorovich (2016) Inhibiting bacterial toxins by channel blockage. *Pathog Dis,* 74.

14. Bischofberger, M., M. R. Gonzalez & F. G. van der Goot (2009) Membrane injury by pore-forming proteins. *Curr Opin Cell Biol,* 21**,** 589-95.

15. Bischofberger, M., I. Iacovache & F. G. van der Goot (2012) Pathogenic pore-forming proteins: function and host response. *Cell Host Microbe,* 12**,** 266-75.

16. Bitounis, D., R. Fanciullino, A. Iliadis & J. Ciccolini (2012) Optimizing Druggability through Liposomal Formulations: New Approaches to an Old Concept. *ISRN Pharm,* 2012**,** 738432.

17. Bokori-Brown, M., C. A. Hall, C. Vance, S. P. Fernandes da Costa, C. G. Savva, C. E. Naylor, A. R. Cole, A. K. Basak, D. S. Moss & R. W. Titball (2014) Clostridium perfringens epsilon toxin mutant Y30A-Y196A as a recombinant vaccine candidate against enterotoxemia. *Vaccine,* 32**,** 2682-7.

18. Bokori-Brown, M., M. C. Kokkinidou, C. G. Savva, S. Fernandes da Costa, C. E. Naylor, A. R. Cole, D. S. Moss, A. K. Basak & R. W. Titball (2013) Clostridium perfringens epsilon toxin H149A mutant as a platform for receptor binding studies. *Protein Sci,* 22**,** 650-9.

19. Boucher, H. W., G. H. Talbot, J. S. Bradley, J. E. Edwards, D. Gilbert, L. B. Rice, M. Scheld, B. Spellberg & J. Bartlett (2009) Bad bugs, no drugs: no ESKAPE! An update from the Infectious Diseases Society of America. *Clin Infect Dis,* 48**,** 1-12.

20. Bruick, R. K. & S. L. McKnight (2001) A conserved family of prolyl-4-hydroxylases that modify HIF. *Science,* 294**,** 1337-40.

21. Bubeck Wardenburg, J. & O. Schneewind (2008) Vaccine protection against Staphylococcus aureus pneumonia. *J Exp Med,* 205**,** 287-94.

22. Cai, B., S. Xie, F. Liu, L. C. Simone, S. Caplan, X. Qin & N. Naslavsky (2014) Rapid degradation of the complement regulator, CD59, by a novel inhibitor. *J Biol Chem,* 289**,** 12109-25.

23. Carette, J. E., C. P. Guimaraes, M. Varadarajan, A. S. Park, I. Wuethrich, A. Godarova, M. Kotecki, B. H. Cochran, E. Spooner, H. L. Ploegh & T. R. Brummelkamp (2009) Haploid genetic screens in human cells identify host factors used by pathogens. *Science,* 326**,** 1231-5.

24. Carrero, J. A., H. Vivanco-Cid & E. R. Unanue (2012) Listeriolysin o is strongly immunogenic independently of its cytotoxic activity. *PLoS One,* 7**,** e32310.

25. Cascales, E., S. K. Buchanan, D. Duche, C. Kleanthous, R. Lloubes, K. Postle, M. Riley, S. Slatin & D. Cavard (2007) Colicin biology. *Microbiol Mol Biol Rev,* 71**,** 158-229.

26. Cassidy, S. K. & M. X. O'Riordan (2013) More than a pore: the cellular response to cholesterol-dependent cytolysins. *Toxins (Basel),* 5**,** 618-36.

27. Chames, P., M. Van Regenmortel, E. Weiss & D. Baty (2009) Therapeutic antibodies: successes, limitations and hopes for the future. *Br J Pharmacol,* 157**,** 220-33.

28. Chen, Y., M. Chen, Y. Zhang, J. H. Lee, T. Escajadillo, H. Gong, R. H. Fang, W. Gao, V. Nizet & L. Zhang (2018) Broad-Spectrum Neutralization of Pore-Forming Toxins with Human Erythrocyte Membrane-Coated Nanosponges. *Adv Healthc Mater*.

29. Chiarot, E., C. Faralla, N. Chiappini, G. Tuscano, F. Falugi, G. Gambellini, A. Taddei, S. Capo, E. Cartocci, D. Veggi, A. Corrado, S. Mangiavacchi, S. Tavarini, M. Scarselli, R. Janulczyk, G. Grandi, I. Margarit & G. Bensi (2013) Targeted amino acid substitutions impair streptolysin O toxicity and group A Streptococcus virulence. *MBio,* 4**,** e00387-12.

30. Cho, H. S., J. H. Lee, M. H. Cho & J. Lee (2015) Red wines and flavonoids diminish Staphylococcus aureus virulence with anti-biofilm and anti-hemolytic activities. *Biofouling,* 31**,** 1-11.

31. Choe, S., M. J. Bennett, G. Fujii, P. M. Curmi, K. A. Kantardjieff, R. J. Collier & D. Eisenberg (1992) The crystal structure of diphtheria toxin. *Nature,* 357**,** 216-22.

32. Clatworthy, A. E., E. Pierson & D. T. Hung (2007) Targeting virulence: a new paradigm for antimicrobial therapy. *Nat Chem Biol,* 3**,** 541-8.

33. Cockeran, R., R. Anderson & C. Feldman (2005) Pneumolysin as a vaccine and drug target in the prevention and treatment of invasive pneumococcal disease. *Arch Immunol Ther Exp (Warsz),* 53**,** 189-98.

34. Cockeran, R., H. C. Steel, A. J. Theron, T. J. Mitchell, C. Feldman & R. Anderson (2011) Characterization of the interactions of the pneumolysoid, Delta6 PLY, with human neutrophils in vitro. *Vaccine,* 29**,** 8780-2.

35. Crisinel, P. A., I. Chevalier, F. Rallu, B. Tapiero, V. Lamarre, R. Thibault & P. Ovetchkine (2010) Invasive pneumococcal disease after implementation of a reduced three-dose pneumococcal conjugate vaccine program: a pediatric tertiary care center experience. *Eur J Pediatr,* 169**,** 1311-5.

36. Dal Peraro, M. & F. G. van der Goot (2016) Pore-forming toxins: ancient, but never really out of fashion. *Nat Rev Microbiol,* 14**,** 77-92.

37. Davis, M. E. & M. E. Brewster (2004) Cyclodextrin-based pharmaceutics: past, present and future. *Nat Rev Drug Discov,* 3**,** 1023-35.

38. Denoel, P., M. T. Philipp, L. Doyle, D. Martin, G. Carletti & J. T. Poolman (2011) A protein-based pneumococcal vaccine protects rhesus macaques from pneumonia after experimental infection with Streptococcus pneumoniae. *Vaccine,* 29**,** 5495-501.

39. Diep, D. B., K. L. Nelson, S. M. Raja, E. N. Pleshak & J. T. Buckley (1998) Glycosylphosphatidylinositol anchors of membrane glycoproteins are binding determinants for the channel-forming toxin aerolysin. *J Biol Chem,* 273**,** 2355-60.

40. DiGiandomenico, A. & B. R. Sellman (2015) Antibacterial monoclonal antibodies: the next generation? *Curr Opin Microbiol,* 27**,** 78-85.

41. Dong, J., J. Qiu, Y. Zhang, C. Lu, X. Dai, J. Wang, H. Li, X. Wang, W. Tan, M. Luo, X. Niu & X. Deng (2013) Oroxylin A inhibits hemolysis via hindering the self-assembly of alpha-hemolysin heptameric transmembrane pore. *PLoS Comput Biol,* 9**,** e1002869.

42. Dowd, K. J., A. J. Farrand & R. K. Tweten (2012) The cholesterol-dependent cytolysin signature motif: a critical element in the allosteric pathway that couples membrane binding to pore assembly. *PLoS Pathog,* 8**,** e1002787.

43. Escajadillo, T., J. Olson, B. T. Luk, L. Zhang & V. Nizet (2017) A Red Blood Cell Membrane-Camouflaged Nanoparticle Counteracts Streptolysin O-Mediated Virulence Phenotypes of Invasive Group A Streptococcus. *Front Pharmacol,* 8**,** 477.

44. Farrand, A. J., S. LaChapelle, E. M. Hotze, A. E. Johnson & R. K. Tweten (2010) Only two amino acids are essential for cytolytic toxin recognition of cholesterol at the membrane surface. *Proc Natl Acad Sci U S A,* 107**,** 4341-6.

45. Foletti, D., P. Strop, L. Shaughnessy, A. Hasa-Moreno, M. G. Casas, M. Russell, C. Bee, S. Wu, A. Pham, Z. Zeng, J. Pons, A. Rajpal & D. Shelton (2013) Mechanism of action and in vivo efficacy of a human-derived antibody against Staphylococcus aureus alpha-hemolysin. *J Mol Biol,* 425**,** 1641-54.

46. Garcia-Suarez Mdel, M., M. D. Cima-Cabal, N. Florez, P. Garcia, R. Cernuda-Cernuda, A. Astudillo, F. Vazquez, J. R. De los Toyos & F. J. Mendez (2004) Protection against pneumococcal pneumonia in mice by monoclonal antibodies to pneumolysin. *Infect Immun,* 72**,** 4534-40.

47. Geoffroy, C., J. L. Gaillard, J. E. Alouf & P. Berche (1989) Production of thiol-dependent haemolysins by Listeria monocytogenes and related species. *J Gen Microbiol,* 135**,** 481-7.

48. Ghafari, S., M. Komeilian, M. S. Hashemi, S. Oushani, G. Rigi, B. Rashidieh, K. Yarahmadi & F. Khoddam (2017) Molecular docking based screening of Listeriolysin-O for improved inhibitors. *Bioinformation,* 13**,** 160-163.

49. Giddings, K. S., J. Zhao, P. J. Sims & R. K. Tweten (2004) Human CD59 is a receptor for the cholesterol-dependent cytolysin intermedilysin. *Nat Struct Mol Biol,* 11**,** 1173-8.

50. Gonzalez, M. R., M. Bischofberger, L. Pernot, F. G. van der Goot & B. Freche (2008) Bacterial pore-forming toxins: the (w)hole story? *Cell Mol Life Sci,* 65**,** 493-507.

51. Gouaux, E. (1997) Channel-forming toxins: tales of transformation. *Curr Opin Struct Biol,* 7**,** 566-73.

52. Griffitts, J. S., S. M. Haslam, T. Yang, S. F. Garczynski, B. Mulloy, H. Morris, P. S. Cremer, A. Dell, M. J. Adang & R. V. Aroian (2005) Glycolipids as receptors for Bacillus thuringiensis crystal toxin. *Science,* 307**,** 922-5.

53. Grijalva, C. G., J. P. Nuorti, P. G. Arbogast, S. W. Martin, K. M. Edwards & M. R. Griffin (2007) Decline in pneumonia admissions after routine childhood immunisation with pneumococcal conjugate vaccine in the USA: a time-series analysis. *Lancet,* 369**,** 1179-86.

54. Grochulski, P., L. Masson, S. Borisova, M. Pusztai-Carey, J. L. Schwartz, R. Brousseau & M. Cygler (1995) Bacillus thuringiensis CryIA(a) insecticidal toxin: crystal structure and channel formation. *J Mol Biol,* 254**,** 447-64.

55. Gurcel, L., L. Abrami, S. Girardin, J. Tschopp & F. G. van der Goot (2006) Caspase-1 activation of lipid metabolic pathways in response to bacterial pore-forming toxins promotes cell survival. *Cell,* 126**,** 1135-45.

56. Henning-Knechtel, A., J. Knechtel & M. Magzoub (2017) DNA-assisted oligomerization of pore-forming toxin monomers into precisely-controlled protein channels. *Nucleic Acids Res,* 45**,** 12057-12068.

57. Henry, B. D., D. R. Neill, K. A. Becker, S. Gore, L. Bricio-Moreno, R. Ziobro, M. J. Edwards, K. Muhlemann, J. Steinmann, B. Kleuser, L. Japtok, M. Luginbuhl, H. Wolfmeier, A. Scherag, E. Gulbins, A. Kadioglu, A. Draeger & E. B. Babiychuk (2015) Engineered liposomes sequester bacterial exotoxins and protect from severe invasive infections in mice. *Nat Biotechnol,* 33**,** 81-8.

58. Hernandez-Flores, K. G. & H. Vivanco-Cid (2015) Biological effects of listeriolysin O: implications for vaccination. *Biomed Res Int,* 2015**,** 360741.

59. Hu, C. M., R. H. Fang, J. Copp, B. T. Luk & L. Zhang (2013a) A biomimetic nanosponge that absorbs pore-forming toxins. *Nat Nanotechnol,* 8**,** 336-40.

60. Hu, C. M., R. H. Fang, B. T. Luk & L. Zhang (2013b) Nanoparticle-detained toxins for safe and effective vaccination. *Nat Nanotechnol,* 8**,** 933-8.

61. Hu, C. M. & L. Zhang (2014) Nanotoxoid Vaccines. *Nano Today,* 9**,** 401-404.

62. Hu, C. M., L. Zhang, S. Aryal, C. Cheung, R. H. Fang & L. Zhang (2011) Erythrocyte membrane-camouflaged polymeric nanoparticles as a biomimetic delivery platform. *Proc Natl Acad Sci U S A,* 108**,** 10980-5.

63. Hua, L., T. S. Cohen, Y. Shi, V. Datta, J. J. Hilliard, C. Tkaczyk, J. Suzich, C. K. Stover & B. R. Sellman (2015) MEDI4893* Promotes Survival and Extends the Antibiotic Treatment Window in a Staphylococcus aureus Immunocompromised Pneumonia Model. *Antimicrob Agents Chemother,* 59**,** 4526-32.

64. Hua, L., J. J. Hilliard, Y. Shi, C. Tkaczyk, L. I. Cheng, X. Yu, V. Datta, S. Ren, H. Feng, R. Zinsou, A. Keller, T. O'Day, Q. Du, L. Cheng, M. Damschroder, G. Robbie, J. Suzich, C. K. Stover & B. R. Sellman (2014) Assessment of an anti-alpha-toxin monoclonal antibody for prevention and treatment of Staphylococcus aureus-induced pneumonia. *Antimicrob Agents Chemother,* 58**,** 1108-17.

65. Iacovache, I., F. G. van der Goot & L. Pernot (2008) Pore formation: an ancient yet complex form of attack. *Biochim Biophys Acta,* 1778**,** 1611-23.

66. Inoshima, N., Y. Wang & J. Bubeck Wardenburg (2012) Genetic requirement for ADAM10 in severe Staphylococcus aureus skin infection. *J Invest Dermatol,* 132**,** 1513-6.

67. Ivie, S. E., C. M. Fennessey, J. Sheng, D. H. Rubin & M. S. McClain (2011) Gene-trap mutagenesis identifies mammalian genes contributing to intoxication by Clostridium perfringens epsilon-toxin. *PLoS One,* 6**,** e17787.

68. Johnson, S., N. J. Brooks, R. A. Smith, S. M. Lea & D. Bubeck (2013) Structural basis for recognition of the pore-forming toxin intermedilysin by human complement receptor CD59. *Cell Rep,* 3**,** 1369-77.

69. Kao, C. Y., F. C. Los, D. L. Huffman, S. Wachi, N. Kloft, M. Husmann, V. Karabrahimi, J. L. Schwartz, A. Bellier, C. Ha, Y. Sagong, H. Fan, P. Ghosh, M. Hsieh, C. S. Hsu, L. Chen & R. V. Aroian (2011) Global functional analyses of cellular responses to pore-forming toxins. *PLoS Pathog,* 7**,** e1001314.

70. Karauzum, H., R. P. Adhikari, J. Sarwar, V. S. Devi, L. Abaandou, C. Haudenschild, M. Mahmoudieh, A. R. Boroun, H. Vu, T. Nguyen, K. L. Warfield, S. Shulenin & M. J. Aman (2013) Structurally designed attenuated subunit vaccines for S. aureus LukS-PV and LukF-PV confer protection in a mouse bacteremia model. *PLoS One,* 8**,** e65384.

71. Karginov, V. A., E. M. Nestorovich, F. Schmidtmann, T. M. Robinson, A. Yohannes, N. E. Fahmi, S. M. Bezrukov & S. M. Hecht (2007) Inhibition of S. aureus alpha-hemolysin and B. anthracis lethal toxin by beta-cyclodextrin derivatives. *Bioorg Med Chem,* 15**,** 5424-31.

72. Kennedy, A. D., J. Bubeck Wardenburg, D. J. Gardner, D. Long, A. R. Whitney, K. R. Braughton, O. Schneewind & F. R. DeLeo (2010) Targeting of alpha-hemolysin by active or passive immunization decreases severity of USA300 skin infection in a mouse model. *J Infect Dis,* 202**,** 1050-8.

73. Keyel, P. A., L. Loultcheva, R. Roth, R. D. Salter, S. C. Watkins, W. M. Yokoyama & J. E. Heuser (2011) Streptolysin O clearance through sequestration into blebs that bud passively from the plasma membrane. *J Cell Sci,* 124**,** 2414-23.

74. Khazaeli, M. B., R. M. Conry & A. F. LoBuglio (1994) Human immune response to monoclonal antibodies. *J Immunother Emphasis Tumor Immunol,* 15**,** 42-52.

75. Kirkham, L. A., A. R. Kerr, G. R. Douce, G. K. Paterson, D. A. Dilts, D. F. Liu & T. J. Mitchell (2006) Construction and immunological characterization of a novel nontoxic protective pneumolysin mutant for use in future pneumococcal vaccines. *Infect Immun,* 74**,** 586-93.

76. Knop, K., R. Hoogenboom, D. Fischer & U. S. Schubert (2010) Poly(ethylene glycol) in drug delivery: pros and cons as well as potential alternatives. *Angew Chem Int Ed Engl,* 49**,** 6288-308.

77. Kshirsagar, N. A., S. K. Pandya, G. B. Kirodian & S. Sanath (2005) Liposomal drug delivery system from laboratory to clinic. *J Postgrad Med,* 51 Suppl 1**,** S5-15.

78. LaChapelle, S., R. K. Tweten & E. M. Hotze (2009) Intermedilysin-receptor interactions during assembly of the pore complex: assembly intermediates increase host cell susceptibility to complement-mediated lysis. *J Biol Chem,* 284**,** 12719-26.

79. Lakey, J. H., F. G. van der Goot & F. Pattus (1994) All in the family: the toxic activity of pore-forming colicins. *Toxicology,* 87**,** 85-108.

80. Lang, A. B., S. J. Cryz, Jr., U. Schurch, M. T. Ganss & U. Bruderer (1993) Immunotherapy with human monoclonal antibodies. Fragment A specificity of polyclonal and monoclonal antibodies is crucial for full protection against tetanus toxin. *J Immunol,* 151**,** 466-72.

81. Laventie, B. J., H. J. Rademaker, M. Saleh, E. de Boer, R. Janssens, T. Bourcier, A. Subilia, L. Marcellin, R. van Haperen, J. H. Lebbink, T. Chen, G. Prevost, F. Grosveld & D. Drabek (2011) Heavy chain-only antibodies and tetravalent bispecific antibody neutralizing Staphylococcus aureus leukotoxins. *Proc Natl Acad Sci U S A,* 108**,** 16404-9.

82. Leroux-Roels, G., C. Maes, F. De Boever, M. Traskine, J. U. Ruggeberg & D. Borys (2014) Safety, reactogenicity and immunogenicity of a novel pneumococcal protein-based vaccine in adults: a phase I/II randomized clinical study. *Vaccine,* 32**,** 6838-46.

83. Levine, B. & J. Yuan (2005) Autophagy in cell death: an innocent convict? *J Clin Invest,* 115**,** 2679-88.

84. Lewis M, W. C., McClain MS (2010) Identification of Small Molecule Inhibitors of Clostridium perfringens ε-Toxin Cytotoxicity Using a Cell-Based High-Throughput Screen. *Toxins (Basel),* 2**,** 1825-1847.

85. Li, H., X. Zhao, J. Wang, Y. Dong, S. Meng, R. Li, X. Niu & X. Deng (2015) beta-sitosterol interacts with pneumolysin to prevent Streptococcus pneumoniae infection. *Sci Rep,* 5**,** 17668.

86. Los, F. C., T. M. Randis, R. V. Aroian & A. J. Ratner (2013) Role of pore-forming toxins in bacterial infectious diseases. *Microbiol Mol Biol Rev,* 77**,** 173-207.

87. Lucas, R., I. Czikora, S. Sridhar, E. Zemskov, B. Gorshkov, U. Siddaramappa, A. Oseghale, J. Lawson, A. Verin, F. G. Rick, N. L. Block, H. Pillich, M. Romero, M. Leustik, A. V. Schally & T. Chakraborty (2013) Mini-review: novel therapeutic strategies to blunt actions of pneumolysin in the lungs. *Toxins (Basel),* 5**,** 1244-60.

88. Ludwig, A., C. Hundhausen, M. H. Lambert, N. Broadway, R. C. Andrews, D. M. Bickett, M. A. Leesnitzer & J. D. Becherer (2005) Metalloproteinase inhibitors for the disintegrin-like metalloproteinases ADAM10 and ADAM17 that differentially block constitutive and phorbol ester-inducible shedding of cell surface molecules. *Comb Chem High Throughput Screen,* 8**,** 161-71.

89. Macey, M. G., R. A. Whiley, L. Miller & H. Nagamune (2001) Effect on polymorphonuclear cell function of a human-specific cytotoxin, intermedilysin, expressed by Streptococcus intermedius. *Infect Immun,* 69**,** 6102-9.

90. Magyarics, Z., F. Leslie, S. A. Luperchio, J. Bartko, C. Schörgenhofer, M. Schwameis, U. Derhaschnig, H. Lagler, L. Stiebellehner, B. Jilma, C. Stevens & E. Nagy. *Serum and Lung Pharmacokinetics of ASN100, a Monoclonal Antibody Combination for the Prevention and Treatment of Staphylococcus aureus Pneumonia*. Open Forum Infect Dis. 2017 Fall;4(Suppl 1):S310. doi:10.1093/ofid/ofx163.722.

91. Majd S, Y. E., Billeh YN, Macrae MX, Yang J, Mayer M (2010) Applications of biological pores in nanomedicine, sensing, and nanoelectronics. *Curr Opin Biotechnol,* 21**,** 439-476.

92. Mann, B., J. Thornton, R. Heath, K. R. Wade, R. K. Tweten, G. Gao, K. El Kasmi, J. B. Jordan, D. M. Mitrea, R. Kriwacki, J. Maisonneuve, M. Alderson & E. I. Tuomanen (2014) Broadly protective protein-based pneumococcal vaccine composed of pneumolysin toxoid-CbpA peptide recombinant fusion protein. *J Infect Dis,* 209**,** 1116-25.

93. Maron, D. J., S. Fazio & M. F. Linton (2000) Current perspectives on statins. *Circulation,* 101**,** 207-13.

94. Mathieu, J. (2015) Interactions between Autophagy and Bacterial Toxins: Targets for Therapy? *Toxins (Basel),* 7**,** 2918-58.

95. McNeil, P. L. & T. Kirchhausen (2005) An emergency response team for membrane repair. *Nat Rev Mol Cell Biol,* 6**,** 499-505.

96. Meijer, A. J. & P. Codogno (2009) Autophagy: regulation and role in disease. *Crit Rev Clin Lab Sci,* 46**,** 210-40.

97. Melo, M. C., L. R. Teixeira, L. Pol-Fachin & C. G. Rodrigues (2016) Inhibition of the hemolytic activity caused by Staphylococcus aureus alpha-hemolysin through isatin-Schiff copper(II) complexes. *FEMS Microbiol Lett,* 363**,** fnv207.

98. Mengaud, J., M. F. Vicente, J. Chenevert, J. M. Pereira, C. Geoffroy, B. Gicquel-Sanzey, F. Baquero, J. C. Perez-Diaz & P. Cossart (1988) Expression in Escherichia coli and sequence analysis of the listeriolysin O determinant of Listeria monocytogenes. *Infect Immun,* 56**,** 766-72.

99. Mesquita, F. S., C. Brito, D. Cabanes & S. Sousa (2017) Control of cytoskeletal dynamics during cellular responses to pore forming toxins. *Commun Integr Biol,* 10**,** e1349582.

100. Michel, E., K. A. Reich, R. Favier, P. Berche & P. Cossart (1990) Attenuated mutants of the intracellular bacterium Listeria monocytogenes obtained by single amino acid substitutions in listeriolysin O. *Mol Microbiol,* 4**,** 2167-78.

101. Mostowy, S. (2013) Autophagy and bacterial clearance: a not so clear picture. *Cell Microbiol,* 15**,** 395-402.

102. Muhlen, S. & P. Dersch (2016) Anti-virulence Strategies to Target Bacterial Infections. *Curr Top Microbiol Immunol,* 398**,** 147-183.

103. Nakouzi, A., J. Rivera, R. F. Rest & A. Casadevall (2008) Passive administration of monoclonal antibodies to anthrolysin O prolong survival in mice lethally infected with Bacillus anthracis. *BMC Microbiol,* 8**,** 159.

104. Nestorovich, E. M. & S. M. Bezrukov (2012) Obstructing toxin pathways by targeted pore blockage. *Chem Rev,* 112**,** 6388-430.

105. Oganesyan, V., L. Peng, M. M. Damschroder, L. Cheng, A. Sadowska, C. Tkaczyk, B. R. Sellman, H. Wu & W. F. Dall'Acqua (2014) Mechanisms of neutralization of a human anti-alpha-toxin antibody. *J Biol Chem,* 289**,** 29874-80.

106. Ogunniyi, A. D., M. C. Woodrow, J. T. Poolman & J. C. Paton (2001) Protection against Streptococcus pneumoniae elicited by immunization with pneumolysin and CbpA. *Infect Immun,* 69**,** 5997-6003.

107. Ohno-Iwashita, Y., M. Iwamoto, S. Ando & S. Iwashita (1992) Effect of lipidic factors on membrane cholesterol topology--mode of binding of theta-toxin to cholesterol in liposomes. *Biochim Biophys Acta,* 1109**,** 81-90.

108. Okumura, C. Y., A. Hollands, D. N. Tran, J. Olson, S. Dahesh, M. von Kockritz-Blickwede, W. Thienphrapa, C. Corle, S. N. Jeung, A. Kotsakis, R. A. Shalwitz, R. S. Johnson & V. Nizet (2012) A new pharmacological agent (AKB-4924) stabilizes hypoxia inducible factor-1 (HIF-1) and increases skin innate defenses against bacterial infection. *J Mol Med (Berl),* 90**,** 1079-89.

109. Palmer, M., R. Harris, C. Freytag, M. Kehoe, J. Tranum-Jensen & S. Bhakdi (1998) Assembly mechanism of the oligomeric streptolysin O pore: the early membrane lesion is lined by a free edge of the lipid membrane and is extended gradually during oligomerization. *Embo j,* 17**,** 1598-605.

110. Parker, M. W. (2003) Cryptic clues as to how water-soluble protein toxins form pores in membranes. *Toxicon,* 42**,** 1-6.

111. Parker, M. W., J. T. Buckley, J. P. Postma, A. D. Tucker, K. Leonard, F. Pattus & D. Tsernoglou (1994) Structure of the Aeromonas toxin proaerolysin in its water-soluble and membrane-channel states. *Nature,* 367**,** 292-5.

112. Parker, M. W. & S. C. Feil (2005) Pore-forming protein toxins: from structure to function. *Prog Biophys Mol Biol,* 88**,** 91-142.

113. Parker, M. W., F. Pattus, A. D. Tucker & D. Tsernoglou (1989) Structure of the membrane-pore-forming fragment of colicin A. *Nature,* 337**,** 93-6.

114. Peyssonnaux, C., V. Datta, T. Cramer, A. Doedens, E. A. Theodorakis, R. L. Gallo, N. Hurtado-Ziola, V. Nizet & R. S. Johnson (2005) HIF-1alpha expression regulates the bactericidal capacity of phagocytes. *J Clin Invest,* 115**,** 1806-15.

115. Popov LM, M. C., Philipp M. Starkl, Jennifer H. Lumb, J. S. , D. G. , , R. L. Cooper, C. M. , D. M. B. , W. M. , Hiroshi Kiyonari, M. T. , , b. Stephen J. Gallia, Fabio Bagnoli, S. C. & J. E. C. , and Manuel R. Amieva (2015) The adherens junctions control susceptibility to Staphylococcus aureus α-toxin. *PNAS,* 112**,** 14337-14342.

116. Prymula, R., P. Pazdiora, M. Traskine, J. U. Ruggeberg & D. Borys (2014) Safety and immunogenicity of an investigational vaccine containing two common pneumococcal proteins in toddlers: a phase II randomized clinical trial. *Vaccine,* 32**,** 3025-34.

117. Qiu, J., X. Niu, J. Dong, D. Wang, J. Wang, H. Li, M. Luo, S. Li, H. Feng & X. Deng (2012) Baicalin protects mice from Staphylococcus aureus pneumonia via inhibition of the cytolytic activity of alpha-hemolysin. *J Infect Dis,* 206**,** 292-301.

118. Qiu, J., D. Wang, H. Xiang, H. Feng, Y. Jiang, L. Xia, J. Dong, J. Lu, L. Yu & X. Deng (2010) Subinhibitory concentrations of thymol reduce enterotoxins A and B and alpha-hemolysin production in Staphylococcus aureus isolates. *PLoS One,* 5**,** e9736.

119. Qiu, J., D. Wang, Y. Zhang, J. Dong, J. Wang & X. Niu (2013) Molecular modeling reveals the novel inhibition mechanism and binding mode of three natural compounds to staphylococcal alpha-hemolysin. *PLoS One,* 8**,** e80197.

120. Ragle, B. E. & J. Bubeck Wardenburg (2009) Anti-alpha-hemolysin monoclonal antibodies mediate protection against Staphylococcus aureus pneumonia. *Infect Immun,* 77**,** 2712-8.

121. Ragle, B. E., V. A. Karginov & J. Bubeck Wardenburg (2010) Prevention and treatment of Staphylococcus aureus pneumonia with a beta-cyclodextrin derivative. *Antimicrob Agents Chemother,* 54**,** 298-304.

122. Rani, N., V. Saravanan, P. T. V. Lakshmi & A. Annamalai (2014) Inhibition of Pore Formation by Blocking the Assembly of Staphylococcus aureus α-Hemolysin Through a Novel Peptide Inhibitor: an In Silco Approach. *International Journal of Peptide Research and Therapeutics,* 20**,** 575-583.

123. Rasko, D. A. & V. Sperandio (2010) Anti-virulence strategies to combat bacteria-mediated disease. *Nat Rev Drug Discov,* 9**,** 117-28.

124. Rayner, C. F., A. D. Jackson, A. Rutman, A. Dewar, T. J. Mitchell, P. W. Andrew, P. J. Cole & R. Wilson (1995) Interaction of pneumolysin-sufficient and -deficient isogenic variants of Streptococcus pneumoniae with human respiratory mucosa. *Infect Immun,* 63**,** 442-7.

125. Reyes-Robles, T., F. Alonzo, 3rd, L. Kozhaya, D. B. Lacy, D. Unutmaz & V. J. Torres (2013) Staphylococcus aureus leukotoxin ED targets the chemokine receptors CXCR1 and CXCR2 to kill leukocytes and promote infection. *Cell Host Microbe,* 14**,** 453-9.

126. Rojko, N. & G. Anderluh (2015) How Lipid Membranes Affect Pore Forming Toxin Activity. *Acc Chem Res,* 48**,** 3073-9.

127. Rojko, N., K. C. Kristan, G. Viero, E. Zerovnik, P. Macek, M. Dalla Serra & G. Anderluh (2013) Membrane damage by an alpha-helical pore-forming protein, Equinatoxin II, proceeds through a succession of ordered steps. *J Biol Chem,* 288**,** 23704-15.

128. Romero, M., M. Keyel, G. Shi, P. Bhattacharjee, R. Roth, J. E. Heuser & P. A. Keyel (2017) Intrinsic repair protects cells from pore-forming toxins by microvesicle shedding. *Cell Death Differ,* 24**,** 798-808.

129. Ros, U. & A. J. Garcia-Saez (2015) More Than a Pore: The Interplay of Pore-Forming Proteins and Lipid Membranes. *J Membr Biol,* 248**,** 545-61.

130. Rosch, J. W., A. R. Boyd, E. Hinojosa, T. Pestina, Y. Hu, D. A. Persons, C. J. Orihuela & E. I. Tuomanen (2010) Statins protect against fulminant pneumococcal infection and cytolysin toxicity in a mouse model of sickle cell disease. *J Clin Invest,* 120**,** 627-35.

131. Rossjohn, J., S. C. Feil, W. J. McKinstry, R. K. Tweten & M. W. Parker (1997) Structure of a cholesterol-binding, thiol-activated cytolysin and a model of its membrane form. *Cell,* 89**,** 685-92.

132. Rouha, H., A. Badarau, Z. C. Visram, M. B. Battles, B. Prinz, Z. Magyarics, G. Nagy, I. Mirkina, L. Stulik, M. Zerbs, M. Jagerhofer, B. Maierhofer, A. Teubenbacher, I. Dolezilkova, K. Gross, S. Banerjee, G. Zauner, S. Malafa, J. Zmajkovic, S. Maier, R. Mabry, E. Krauland, K. D. Wittrup, T. U. Gerngross & E. Nagy (2015) Five birds, one stone: neutralization of alpha-hemolysin and 4 bi-component leukocidins of Staphylococcus aureus with a single human monoclonal antibody. *MAbs,* 7**,** 243-54.

133. Rouha, H., S. Weber, P. Janesch, B. Maierhofer, K. Gross, I. Dolezilkova, I. Mirkina, Z. C. Visram, S. Malafa, L. Stulik, A. Badarau & E. Nagy (2018) Disarming Staphylococcus aureus from destroying human cells by simultaneously neutralizing six cytotoxins with two human monoclonal antibodies. *Virulence,* 9**,** 231-247.

134. Sampedro, G. R., A. C. DeDent, R. E. Becker, B. J. Berube, M. J. Gebhardt, H. Cao & J. Bubeck Wardenburg (2014) Targeting Staphylococcus aureus alpha-toxin as a novel approach to reduce severity of recurrent skin and soft-tissue infections. *J Infect Dis,* 210**,** 1012-8.

135. Semenza, G. L. (2010) Oxygen homeostasis. *Wiley Interdiscip Rev Syst Biol Med,* 2**,** 336-361.

136. Shah, S., P. D. Stapleton & P. W. Taylor (2008) The polyphenol (-)-epicatechin gallate disrupts the secretion of virulence-related proteins by Staphylococcus aureus. *Lett Appl Microbiol,* 46**,** 181-5.

137. Shannon, J. G., C. L. Ross, T. M. Koehler & R. F. Rest (2003) Characterization of anthrolysin O, the Bacillus anthracis cholesterol-dependent cytolysin. *Infect Immun,* 71**,** 3183-9.

138. Shewell, L. K., R. M. Harvey, M. A. Higgins, C. J. Day, L. E. Hartley-Tassell, A. Y. Chen, C. M. Gillen, D. B. James, F. Alonzo, 3rd, V. J. Torres, M. J. Walker, A. W. Paton, J. C. Paton & M. P. Jennings (2014) The cholesterol-dependent cytolysins pneumolysin and streptolysin O require binding to red blood cell glycans for hemolytic activity. *Proc Natl Acad Sci U S A,* 111**,** E5312-20.

139. Song, L., M. R. Hobaugh, C. Shustak, S. Cheley, H. Bayley & J. E. Gouaux (1996) Structure of staphylococcal alpha-hemolysin, a heptameric transmembrane pore. *Science,* 274**,** 1859-66.

140. Song, M., L. Li, M. Li, Y. Cha, X. Deng & J. Wang (2016) Apigenin protects mice from pneumococcal pneumonia by inhibiting the cytolytic activity of pneumolysin. *Fitoterapia,* 115**,** 31-36.

141. Sonnen, A. F. & P. Henneke (2013) Role of pore-forming toxins in neonatal sepsis. *Clin Dev Immunol,* 2013**,** 608456.

142. Sowdhamini, R., T. J. Mitchell, P. W. Andrew & P. J. Morgan (1997) Structural and functional analogy between pneumolysin and proaerolysin. *Protein Eng,* 10**,** 207-15.

143. Spellberg, B., R. Guidos, D. Gilbert, J. Bradley, H. W. Boucher, W. M. Scheld, J. G. Bartlett & J. Edwards, Jr. (2008) The epidemic of antibiotic-resistant infections: a call to action for the medical community from the Infectious Diseases Society of America. *Clin Infect Dis,* 46**,** 155-64.

144. Statt, S., J. W. Ruan, L. Y. Hung, C. Y. Chang, C. T. Huang, J. H. Lim, J. D. Li, R. Wu & C. Y. Kao (2015) Statin-conferred enhanced cellular resistance against bacterial pore-forming toxins in airway epithelial cells. *Am J Respir Cell Mol Biol,* 53**,** 689-702.

145. Suarez-Alvarez, B., M. Garcia-Suarez Mdel, F. J. Mendez & J. R. de los Toyos (2003) Characterisation of mouse monoclonal antibodies for pneumolysin: fine epitope mapping and V gene usage. *Immunol Lett,* 88**,** 227-39.

146. Tilley, S. J. & H. R. Saibil (2006) The mechanism of pore formation by bacterial toxins. *Curr Opin Struct Biol,* 16**,** 230-6.

147. Tkaczyk, C., L. Hua, R. Varkey, Y. Shi, L. Dettinger, R. Woods, A. Barnes, R. S. MacGill, S. Wilson, P. Chowdhury, C. K. Stover & B. R. Sellman (2012) Identification of anti-alpha toxin monoclonal antibodies that reduce the severity of Staphylococcus aureus dermonecrosis and exhibit a correlation between affinity and potency. *Clin Vaccine Immunol,* 19**,** 377-85.

148. Tweten, R. K. (2005) Cholesterol-dependent cytolysins, a family of versatile pore-forming toxins. *Infect Immun,* 73**,** 6199-209.

149. Tweten, R. K., M. W. Parker & A. E. Johnson (2001) The cholesterol-dependent cytolysins. *Curr Top Microbiol Immunol,* 257**,** 15-33.

150. Uchiyama, S., S. Dohrmann, A. M. Timmer, N. Dixit, M. Ghochani, T. Bhandari, J. C. Timmer, K. Sprague, J. Bubeck-Wardenburg, S. I. Simon & V. Nizet (2015) Streptolysin O Rapidly Impairs Neutrophil Oxidative Burst and Antibacterial Responses to Group A Streptococcus. *Front Immunol,* 6**,** 581.

151. Upadhyay, A., S. Mooyottu, H. Yin, M. S. Nair, V. Bhattaram & K. Venkitanarayanan (2015) Inhibiting Microbial Toxins Using Plant-Derived Compounds and Plant Extracts. *Medicines (Basel),* 2**,** 186-211.

152. Walker, B. & H. Bayley (1995) Key residues for membrane binding, oligomerization, and pore forming activity of staphylococcal alpha-hemolysin identified by cysteine scanning mutagenesis and targeted chemical modification. *J Biol Chem,* 270**,** 23065-71.

153. Wang, J., J. Qiu, W. Tan, Y. Zhang, H. Wang, X. Zhou, S. Liu, H. Feng, W. Li, X. Niu & X. Deng (2015a) Fisetin inhibits Listeria monocytogenes virulence by interfering with the oligomerization of listeriolysin O. *J Infect Dis,* 211**,** 1376-87.

154. Wang, J., X. Zhou, S. Liu, G. Li, L. Shi, J. Dong, W. Li, X. Deng & X. Niu (2015b) Morin hydrate attenuates Staphylococcus aureus virulence by inhibiting the self-assembly of alpha-hemolysin. *J Appl Microbiol,* 118**,** 753-63.

155. Wilke, G. A. & J. Bubeck Wardenburg (2010) Role of a disintegrin and metalloprotease 10 in Staphylococcus aureus alpha-hemolysin-mediated cellular injury. *Proc Natl Acad Sci U S A,* 107**,** 13473-8.

156. Wu, Q. & Z. Guo (2010) Glycosylphosphatidylinositols are potential targets for the development of novel inhibitors for aerolysin-type of pore-forming bacterial toxins. *Med Res Rev,* 30**,** 258-69.

157. Yannakopoulou, K., L. Jicsinszky, C. Aggelidou, N. Mourtzis, T. M. Robinson, A. Yohannes, E. M. Nestorovich, S. M. Bezrukov & V. A. Karginov (2011) Symmetry requirements for effective blocking of pore-forming toxins: comparative study with alpha-, beta-, and gamma-cyclodextrin derivatives. *Antimicrob Agents Chemother,* 55**,** 3594-7.

158. Yarovinsky, T. O., M. M. Monick, M. Husmann & G. W. Hunninghake (2008) Interferons increase cell resistance to Staphylococcal alpha-toxin. *Infect Immun,* 76**,** 571-7.

159. Yoo, J. W., E. Chambers & S. Mitragotri (2010) Factors that control the circulation time of nanoparticles in blood: challenges, solutions and future prospects. *Curr Pharm Des,* 16**,** 2298-307.

160. Yu, X. Q., G. J. Robbie, Y. Wu, M. T. Esser, K. Jensen, H. I. Schwartz, T. Bellamy, M. Hernandez-Illas & H. S. Jafri (2017) Safety, Tolerability, and Pharmacokinetics of MEDI4893, an Investigational, Extended-Half-Life, Anti-Staphylococcus aureus Alpha-Toxin Human Monoclonal Antibody, in Healthy Adults. *Antimicrob Agents Chemother,* 61.

161. Zhang Y, G. W., Chen Y, Escajadillo T, Ungerleider J, Fang RH, Christman K, Nizet V, Zhang L (2017) Self-Assembled Colloidal Gel Using Cell Membrane-Coated Nanosponges as Building Blocks. *ACS Nano,* 11**,** 11923-11930.

162. Zhao, X., H. Li, J. Wang, Y. Guo, B. Liu, X. Deng & X. Niu (2016) Verbascoside Alleviates Pneumococcal Pneumonia by Reducing Pneumolysin Oligomers. *Mol Pharmacol,* 89**,** 376-87.

163. Zhao, X., B. Liu, S. Liu, L. Wang & J. Wang (2017) Anticytotoxin Effects of Amentoflavone to Pneumolysin. *Biol Pharm Bull,* 40**,** 61-67.

164. Zuo, Q. F., L. Y. Yang, Q. Feng, D. S. Lu, Y. D. Dong, C. Z. Cai, Y. Wu, Y. Guo, J. Gu, H. Zeng & Q. M. Zou (2013) Evaluation of the protective immunity of a novel subunit fusion vaccine in a murine model of systemic MRSA infection. *PLoS One,* 8**,** e81212.

CHAPTER 2

A red blood cell membrane-camouflaged nanoparticle counteracts streptolysin O-mediated virulence phenotypes of invasive group A *Streptococcus*

Tamara Escajadillo[1,2], Joshua Olson[2], Brian T. Luk[3], Liangfang Zhang[3*], Victor Nizet[1,2,4*]

Biomedical Sciences Graduate Program[1], Department of Pediatrics, Division of Host-Microbe Systems and Therapeutics[2], Department of Nanoengineering[3], Skaggs School of Pharmacy and Pharmaceutical Sciences[4], UC San Diego, La Jolla, California

Published in *Frontiers in Pharmacology*

July 2017

Volume 8, Issue 477

Keywords: *Streptococcus pyogenes*, group A *Streptococcus*, streptolysin O, pore-forming toxin, neutrophil, macrophage, nanotherapeutic, nanoparticle, biomimetic, antivirulence therapy

PREFACE TO CHAPTER 2

Chapter 2 in full is a published journal article in *Frontiers in Pharmacology* in which I was the principal investigator and author. This works helps address Aims 1A-D: determine if RBC-derived nanosponges block GAS SLO-mediated hemolysis and keratinocyte cytotoxicity, determine if RBC nanosponges counteract GAS SLO-mediated toxicity to macrophages, determine if RBC nanosponges mitigate GAS SLO-mediated impairment of neutrophil killing, and determine if RBC nanosponges reduce GAS disease severity in necrotizing skin infection model. This was done by generating RBC derived nanoparticles derived from mouse and human blood and applying the nanosponges to models of SLO mediated GAS infection both *in vitro* and *in vivo*. The experiments revealed that neutralization of the GAS pore forming toxin SLO by nanosponges increases viability of cells and improves immune function *in vitro* and diminishes the severity of the disease in a murine model of infection.

ABSTRACT

Group A *Streptococcus* (GAS), an important human-specific Gram-positive bacterial pathogen, is associated with a broad spectrum of disease, ranging from mild superficial infections such as pharyngitis and impetigo, to serious invasive infections including necrotizing fasciitis and streptococcal toxic shock syndrome. The GAS pore-forming streptolysin O (SLO) is a well characterized virulence factor produced by nearly all GAS clinical isolates. High level expression of SLO is epidemiologically linked to intercontinental dissemination of hypervirulent clonotypes and poor clinical outcomes. SLO can trigger macrophage and neutrophil cell death and/or the inactivation of immune cell functions and promotes tissue injury and bacterial survival in animal models of infection. In the present work, we describe how the pharmacological presentation of red blood cell (RBC) derived biomimetic nanoparticles ("nanosponges") can sequester SLO and block the ability of GAS to damage host cells, thereby preserving innate immune function and increasing bacterial clearance *in vitro* and *in vivo*. Nanosponge administration protected human neutrophils, macrophages and keratinocytes against SLO-mediated cytoxicity. This therapeutic intervention prevented SLO-induced macrophage apoptosis and increased neutrophil extracellular trap formation, allowing increased GAS killing by the respective phagocytic cell types. In a murine model of GAS necrotizing skin infection, local administration of the biomimetic nanosponges was associated with decreased lesion size and reduced bacterial colony-forming unit recovery. Utilization of a toxin decoy and capture platform that inactivates the secreted SLO before it contacts the host cell membrane, presents a novel virulence factor targeted strategy that could be a powerful adjunctive therapy in severe GAS infections where morbidity and mortality are high despite antibiotic treatment.

INTRODUCTION

Streptococcus pyogenes, also known as group A *Streptococcus* (GAS), is a leading human-specific Gram-positive bacterial pathogen (Walker et al., 2014). GAS is responsible for significant disease morbidity and burden to the global healthcare system, producing an estimated 700 million cases of throat and skin infections annually. A clear increase in cases of severe invasive GAS infections, including sepsis, necrotizing fasciitis and toxic shock syndrome, has been documented in the last three or four decades, with mortality rates of 25% or higher (Wong and Stevens, 2013; Waddington et al., 2014). Coupled with its ability to trigger post-infectious immunologically-mediated syndromes of glomerulonephritis and rheumatic heart disease, GAS ranks among the top 10 causes of infection-associated mortality in humans (Ralph and Carapetis, 2013).

The capacity of GAS to produce invasive human disease is the byproduct of a diverse array of bacterial virulence determinants that coordinately promote tissue invasion and resistance to innate immune clearance by host phagocytic cells including neutrophils and macrophages (Cole et al., 2011; Walker et al., 2014; Hamada et al., 2015; Dohrmann et al., 2016). These include the anti-opsonophagocytic surface-anchored M protein (Oehmcke et al., 2010) and hyaluronic acid capsule (Dale et al., 1996), resistant mechanisms against host defense peptides (LaRock and Nizet, 2015) and reactive oxygen species (Henningham et al., 2015), and secreted toxins capable of lysing phagocytes and/or disrupting their critical antimicrobial functions (Barnett et al., 2015).

Among the best studied GAS virulence factors is a potent secreted pore-forming toxin, streptolysin O (SLO). SLO is a cholesterol-dependent cytolysin that disrupts cytoplasmic membrane integrity of multiple eukaryotic cell types through pore formation (Tweten et al., 2015), thereby triggering cell death through apoptosis (Timmer et al., 2009), pyroptosis (Keyel et al., 2013) or programmed necrosis (Chandrasekaran and Caparon, 2016). SLO promotes GAS

resistance to phagocyte killing (Sierig et al., 2003; Ato et al., 2008) and impairs critical phagocyte functions such as oxidative burst, migration, degranulation and neutrophil extracellular trap (NET) production (Uchiyama et al., 2015). Evolutionary genetic events associated with increased expression of SLO are associated with emergence of hypervirulent GAS clones and their rapid intercontinental dispersal (Zhu et al., 2015), as exemplified by the globally disseminated M1T1 clone that has emerged as the leading cause of severe, invasive infections in recent epidemiology (Aziz and Kotb, 2008; Nasser et al., 2014). Moreover, SLO expression is strongly upregulated by mutations in the *cov*R/S two-component transcriptional regulator that may arise *in vivo* and enhance systemic dissemination among M1T1 and other invasive GAS strains (Sumby et al., 2006; Cole et al., 2011). Mutation of the SLO gene or antibody-mediated inhibition of SLO toxin action is associated with reduced virulence in multiple murine models of invasive GAS infection (Limbago et al., 2000; Ikebe et al., 2009; Timmer et al., 2009; Chiarot et al., 2013; Uchiyama et al., 2015).

Anti-virulence strategies are gaining increased attention as a potential means to improve clinical outcomes in infections complicated by severe toxicity or antibiotic resistance (Clatworthy et al., 2007; Cegelski et al., 2008; Johnson and Abramovitch, 2017; Munguia and Nizet, 2017). Nanoparticle-based delivery systems have emerged as a key pharmacological platform for indications in diverse disease states including cancer (Schroeder et al., 2011) and diabetes (Sharma et al., 2015), and we and others have begun exploring their utility in counteracting bacterial toxin-mediated pathologies. Synthetic liposomal formulations can act as decoy targets for bacterial membrane-damaging toxins (Henry et al., 2015); however, a critical concern in nanotherapeutics is achievement of long circulation times to enhance clinical impact. Artificial nanocarriers may stimulate unwanted immunological responses or undergo relatively fast *in vivo* clearance (Luk and Zhang, 2015). Biomimetic nanotechnologies that utilize natural host cell membrane-coated nanoparticles may allay these concerns, bestowing stealth properties for

increased circulation time and providing efficient interfacing to exploit known biological interactions (Kroll et al., 2017).

We have developed nanoparticles displaying red blood cells (RBC) membranes derived by hypotonic treatment and coated onto negatively charged poly-($_{D,L}$-lactide-*co*-glycolide) (PLGA) polymeric cores by extrusion or sonication methods (Kroll et al., 2017). These RBC membrane-camouflaged nanoparticles maintain right-side-out membrane orientation due to electrostatic repulsion with the PLGA core, remain stable in phosphate buffered solution as determined by polydispersity index (PDI) and the surface zeta potential, and possess an elimination half-life of ~40 h before their clearance by hepatic macrophages without associated liver injury (Hu et al., 2011; Hu et al., 2014; Luk and Zhang, 2015). RBC membrane-camouflaged nanoparticles, or "nanosponges", have been shown to act as decoy targets for purified versions of pore-forming toxins, including α-toxin produced by *Staphylococcus aureus*. Nanosponge administration sequestered α-toxin, rendering it harmless to mammalian cellular targets (Hu et al., 2013).

The current study takes our analysis of the pharmacological potential of RBC nanosponges to another leading pathogen, GAS, and its pore-forming toxin virulence factor, SLO. Employing wild-type (WT) and isogenic SLO-deficient mutant GAS strains, we assessed the effects of nanosponge administration upon SLO-mediated cytotoxicity and modulation of phagocyte antimicrobial functions in the context of live bacterial infection and provide a first proof-of-principle of their therapeutic potential in a murine model of GAS necrotizing skin infection.

METHODS

Bacterial Strains

GAS M1T1 serotype M1T1 5448 was originally isolated from a patient with necrotizing fasciitis and toxic shock syndrome (Chatellier et al., 2000) and an animal passaged (AP) version of the

M1 5448 GAS parent strain (5448AP) containing a single inactivating adenine insertion at the 877-bp position of *covS* were used (Aziz et al., 2004). The isogenic M1T1 5448 ΔSLO mutant were described previously (Timmer et al., 2009). GAS strains were propagated using ToddHewitt broth (THB) or agar (THA) at 37 °C.

Collection of Human Blood and Purification of RBCs or Neutrophils

Phlebotomy was performed on healthy donors with full informed consent under a protocol approved by the University of California San Diego (UCSD) Human Research Protections Program. RBC were isolated for hemolysis assays or preparation of RBC nanosponges (see below). Neutrophils were isolated from freshly collected whole blood of healthy donors under a protocol approved by the, using PolyMorphPrep Kit (Fresenius Kabi) as previously described (Kristian et al., 2005).

Mammalian Cell Culture

Human keratinocyte cell line HaCaT, murine macrophage cell line J774 and human monocyte cell line THP1 were cultured in RPMI-1640 media (Invitrogen) + 10% heat-inactivated fetal bovine serum (FBS) at 37°C in humidified air with 5% CO_2. Primary bone marrow-derived macrophages (BMDM) were prepared as described (Hsu et al., 2004) with slight modification. Bone marrow cells were collected from mice and cultured in Dulbecco's modified Eagle's medium (high glucose) supplemented with 20% L-929 cell conditioned medium for 7 d. Adherent cells (BMDM) were then collected and cultured in Dulbecco's modified Eagle's medium (high glucose) with 10 ng/ml macrophage colony-stimulating factor (Pepro-Tech) overnight before bacterial infection.

Generation of Human RBC-Derived Nanoparticles

RBC nanoparticles were prepared following published methods (Hu et al., 2011). Briefly, ~100nm PLGA polymeric cores were prepared using 0.67 dl/g of carboxy-terminated 50:50

poly(DLlactide-co-glycolide) (LACTEL Absorbable Polymers) through a nanoprecipitation process. The PLGA polymer was first dissolved in acetone at a concentration of 10 mg/ml. One ml of the solution was then added rapidly to 3 ml of water, and the mixture placed in a vacuum for at least 3 h to evaporate the organic solvent. Human blood from healthy donors was washed with PBS + 1mM EDTA x 3 by centrifugation at 500 × *g* for 10 min. RBC membrane vesicles were then prepared via hypotonic treatment and centrifugation at 10°C at 800 x *g* for 12 min. RBC membrane coating was completed by fusing RBC membrane vesicles with PLGA particles via sonication using an FS30D bath sonicator at frequency = 42 kHz and power = 100 W for 2 min.

Bacterial Growth in Human Whole Blood

Blood was drawn from healthy donors after informed consent, and 2 x 10^5 CFU of bacteria at OD_{600} = 0.4 were added to 400 µL heparinized whole blood in siliconized tubes. Tubes were placed on a rotator at 37°C for 1 h, then diluted and plated for colony forming unit (CFU) enumeration. Growth index was calculated as the ratio of surviving CFU after incubation vs. the initial inoculum.

Macrophage and Neutrophil Killing Assays

J774 murine macrophages were seeded at ~5 x 10^5 cells in 350 µl of RPMI–2% FBS in a 24-well plate. Overnight bacterial cultures were diluted 1:10, subcultured for 3 h, resuspended and serially diluted in RPMI-2% FBS, and used to inoculate J774 cells at a multiplicity of infection (MOI) = 10 bacteria/cell. Freshly purified human neutrophils in serum-free RPMI were added to 96-well plates at a density of 1 × 10^6 cells/well and infected with GAS at MOI = 1. Plates were centrifuged at 600 x *g* for 5 min to facilitate bacterial contact with cells. To assess total killing, macrophages were incubated at 37°C for 2 h and neutrophils for 15 min, washed three times with PBS, detached with 100 µl of 0.05% trypsin, and lysed with 900 µl of 0.025% Triton X-100

in PBS. Samples were serially diluted in PBS and plated on THA overnight for CFU enumeration.

Cell Viability Assays

For quantification of cellular ATP as an indicator of metabolic activity and cell viability, opaque-walled 96-well plates with were prepared using THP-1 cells seeded at density 2 x 10^4 cells/well, and infected with GAS WT or ΔSLO mutant strains at MOI = 25 for 2 h at 37°C. After incubation, 100 µl of CellTiter-Glo® reagent was added to contents of wells, mixed for 2 min on an orbital shaker to induce cell lysis, and incubated at RT x 10 min to stabilize luminescent signal. Luminescence was recorded using SpectraMax plate reader and software. Live-Dead staining of HaCaT cells and murine BMDMs were performed by growing cells to 70% confluency in 96-well plates and infecting with WT GAS at MOI = 50 for 2 h, or 0.2 µg purified SLO for 30 minutes. Cells were then washed with PBS and treated with the viability assay mixture from the LIVE/DEAD Viability/Cytotoxicity Kit for mammalian cells (Molecular Probes, Invitrogen) for 30 min at 37°C, and imaged using an Olympus BX51 fluorescent microscope.

Apoptosis Measurement

THP1 monocytes were plated at 1 x 10^6 cells/well in 12-well plates and infected with GAS strains at MOI = 20:1. Plates were centrifuged at 2,000 rpm for 5 min to ensure bacterial contact with cells and then incubated at 37 °C, 5% CO2. One h after infection, penicillin (5 µg/ml) and gentamicin (100 µg/ml) were added to the media to kill residual extracellular bacteria. At 4 h after infection, cells were collected, fixed, and permeabilized for apo-bromodeoxyuridine TUNEL assay per manufacturer's (BD Bioscience) instructions.

Western Immunoblot Analysis

In a 6-well plate, 1 x 10^6 J774 macrophages were seeded per well in 2 ml of RPMI + 2% FBS. Cells were infected with WT GAS at MOI = 10 for 2 and 4 h. To harvest whole-cell lysates, cells

were washed 3 times with PBS and treated with radioimmunoprecipitation assay (RIPA) lysis buffer. Nuclear and cytoplasmic fractions were isolated using the NER-PER Extraction Kit (Pierse, Rockford, IL) according to manufacturer's protocol. Protein abundances were determined in cell fraction lysates with bicinchoninic acid assay (BCA) colorimetric assay. Aliquots containing 30 µg of protein were separated on 10% SDS-PAGE gels and transferred onto nitrocellulose membranes. Blots were probed using rabbit anti-Caspase 1 (Santa Cruz Technologies, diluted 1:500 in Tris-buffered saline–Tween 20 (TBST). Enhanced chemiluminescence reagent (PerkinElmer) was used for detection.

IL-1β Measurement and Caspase-1 Activity Assays

J774 macrophages were infected at MOI = 10 for 2 h, supernatant collected and replaced with fresh media, then supernatant collected again 24 h post infection. Skin from infected mice were homogenized in 1 ml PBS and centrifuged at 4°C, and the resulting supernatant used in ELISA for for IL-1β release (R & D Systems), via absorbance at 450 nm on a SpectraMax M3 plate reader and SoftMax Pro software. Caspase-1 activation was determined by Fam-YVAD-FMK (ImmunoChemistry Technologies) staining of THP-1 macrophages infected in 96-well plates per manufacturer's specifications. Caspase-dependent apoptosis was determined in J774 murine macrophages using the APO-Caspase 3/7 activity assay (Promega) following the manufacturer's protocol. Briefly, 100µL of J774 cells were cultured in a white opaque 96-well plate at semi-confluency 1d prior to infection with GAS at MOI = 20:1. Penicillin (5 µg/ml) and gentamicin (100 µg/ml) were added to the media 1 h after infection to kill residual extracellular bacteria. At 4 h after infection, caspase activity was quantified by adding 100 µL of detecting reagent per well, shaking gently for 5 min and incubating at room temperature x 1 h. Fluorescence at 520 nm was red on a Molecular Devices SpectraMax M3 reader to detect the level of caspase 3/7.

Murine Infection Model

Mouse infections with GAS were performed based on modifications to a previously described model (Nizet et al., 2001) under a protocol approved by the UCSD Institutional Animal Care and Use Committee (IACUC). Twenty-four hours prior to infection, the backs of 8 C57Bl6 mice were shaved and hair was removed by chemical depilation (Nair). Mice were infected subcutaneously with 50 µL of a sublethal dose of log-phase GAS ($1x10^7$ CFU) in PBS, and 15 minutes later subsequently treated with vehicle only (10% sucrose) or vehicle plus 50 mg/kg of nanosponges in an area proximal to the site of the infection. Digital photographs of skin lesions were taken and lesion size was measured using NIH Imager software. Lesions were biopsied on day 3 post-infection. Excised lesions were placed into 2 ml screw cap tubes containing 1 ml PBS + 1 mm silica/zirconia beads (Biospec Products). Tissue was homogenized by shaking twice with the mini-beadbeater-8 (Biospec Products) at full for speed for 1 min, placing on ice in between. The homogenate was serially diluted in sterile PBS and plated on THA for enumeration. Dilutions were plated on THA agar and cultured overnight at 37°C for enumeration of CFU. Hematoxylin-and-eosin (H&E) staining was performed by the UCSD Histology Core Facility. Images were obtained using an Olympus BX41 microscope.

Immunostaining of NETs and Elastase Release

Neutrophils ($2 x10^5$) were plated in 96 wells and infected with WT GAS and ΔSLO mutant at MOI = 1 in 37°C/5% CO_2 for 4 h. Cells were fixed with 4% paraformaldehyde and stained with anti-myeloperoxidase (MPO) antibody (1:300 dilution, Calbiochem) in PBS + 2% bovine serum albumin (BSA, Sigma) at room temperature for 1 h, followed by incubation with goat anti-rabbit Alexa 488 antibody (1:500 dilution, Life Technologies). Cells were counterstained with ProlongGold + 4',6'-diamidino-2-phenylindole (DAPI, Invitrogen) and imaged on a fluorescent microscope. Representative, randomized images (n=3) were taken for each condition and individualized experiment. Ratio of NET-releasing cells to non-NET releasing cells was determined as % of total cells. Elastase release from neutrophils infected with GAS at MOI = 5

for 30 min into the supernatant was indirectly determined using 20 μM peptide substrate N(Methoxysuccinyl)-Ala-Ala-Pro-Val 4-nitroanilide (Sigma) for 20 min at RT and absorbance 405 nm (SpectraMax M3 plate reader/ SoftMax Pro). Statistical Analysis Experiments were performed in triplicate and repeated at least twice. Error data represent standard errors of the means (SEM) of the results from experimental duplicates, triplicates, or quadruplets. Statistical analysis was performed using Student's unpaired two-tailed t test. Comparisons among three or more samples were evaluated using one-way analysis of variance (ANOVA) followed by the nonparametric Tukey's post-test. Comparisons of multiple samples were evaluated using ANOVA followed by Dunnett's or Tukey's test (Graph Pad Prism).

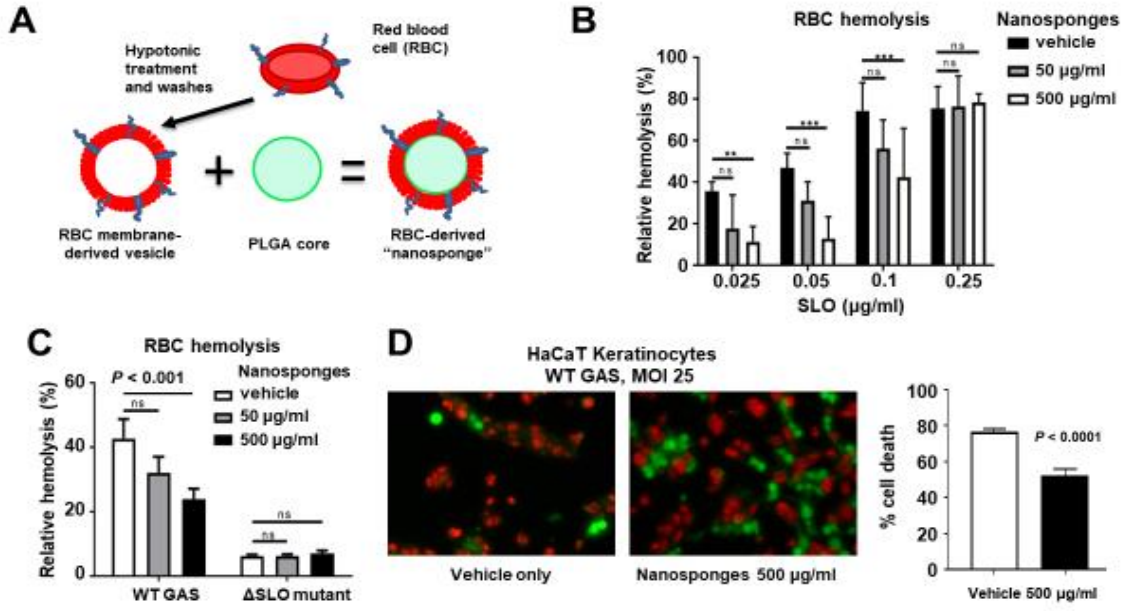

Figure 2.1 RBC nanosponges decrease GAS SLO-induced hemolysis and keratinocyte cytotoxicity. (A) Schematic showing fusion of RBC-derived ghost membrane vesicle and PLGA core to create nanosponge therapeutic. Human whole blood was centrifuged and washed with PBS + 1% EDTA to purify RBCs, then subjected to hypotonic treatment and centrifugation to rupture the membrane and remove intracellular content. PLGA cores were prepared from a 0.67 dL/g carboxy-terminated PLGA polymer by solvent displacement and resulting nanoparticles fused with RBC membranes by sonication. (B) RBC nanosponges inhibit purified SLO-induced RBC in a dose-dependent manner. (C) RBC nanosponges inhibit hemolysis induced by SLO produced by live WT GAS bacteria; isogenic SLO-deficient mutant serves as control. (D) Coincubation with RBC nanosponges increases survival of HaCaT keratinocytes infected with WT GAS at MOI = 25 bacteria/cell; live/dead cell staining illustrates viable (green) or dead (red) cells. Results are from experiments performed in triplicate and reported as mean ± SEM from at least three experiments.

RESULTS

RBC-derived nanosponges block GAS SLO-mediated hemolysis and keratinocyte injury.

Creation of RBC-camouflaged nanoparticles involves two main steps: membrane vesicle derivation from RBCs followed by fusion of the membrane vesicle with the polymeric nanoparticle core (**Figure 2.1A**), as previously reported in detail (Desilets et al., 2001; Cheng et al., 2007; Hu et al., 2011; Pang et al., 2015). The RBC-derived nanoparticles, hereafter termed "nanosponges", have an approximate particle size of 80 nm, right side out orientation, and other physical characteristics and physiochemical properties that lead to favorable pharmacokinetics and biodistribution (Hu et al., 2011). We determined that RBC nanosponges (50 or 500 μg/ml) could significantly inhibit the hemolytic action of purified SLO in a dose-dependent manner to an SLO concentration of 0.1 μg/ml (**Figure 2.1B**). Dot blot analysis confirmed sequestration of SLO from the media to the nanosponges (**Supplementary Figure 2.1**). These findings mirrored prior observations with *S. aureus* α-toxin, in which RBC nanosponges absorbed α-toxin to limit its interaction with subsequent cellular targets, a finding that was absent when using just RBC membranes or polymeric cores individually (Hu et al., 2013). We then tested the ability of RBC-derived nanosponges to block hemolysis induced by coincubation of freshly isolated human RBC with a high level SLO-producing WT GAS strain (**Supplementary Figure. 2.2**) compared to its isogenic ΔSLO mutant as a control. Paralleling results with the purified toxin, 500 μg/ml nanosponges produced a significant (~50%) reduction of hemolysis induced by the WT strain, but had no effect on the low level of hemolysis seen in the ΔSLO mutant control (**Figure 2.1C**). SLO can also trigger membrane damage and cytolytic cell death in keratinocytes, which may play a role in the severe tissue injury of invasive GAS necrotizing skin infection (Ruiz et al., 1998; Sierig et al., 2003). As measured by LIVE/DEAD immunofluorescent staining, we found that administration of RBC nanosponges allowed a significant increase in survival of

keratinocytes upon coincubation of the cells with the WT SLO-producing GAS strain at MOI = 25 (50% survival vs. 20% untreated, **Figure 2.1D**).

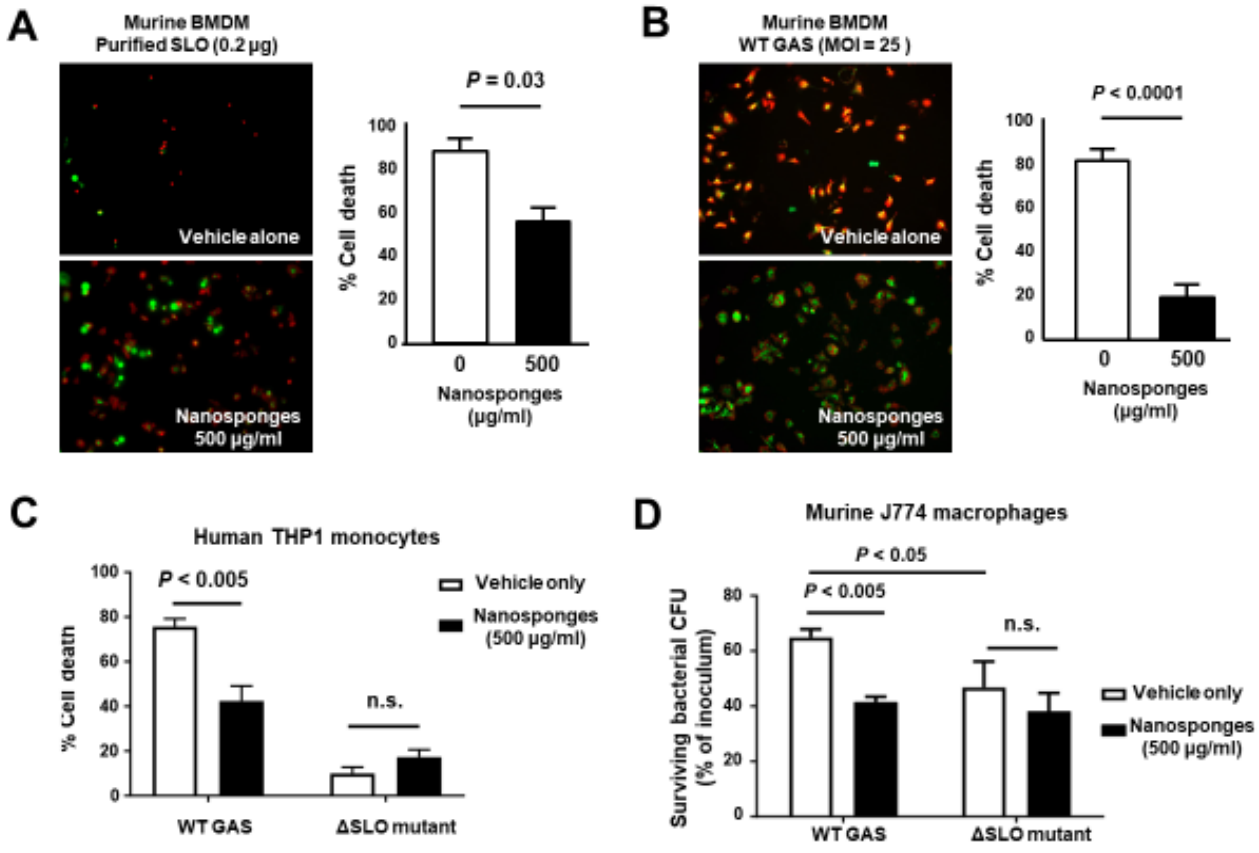

Figure 2.2 RBC nanosponges counteract GAS SLO-mediated toxicity to macrophages. RBC nanosponges significantly reduced cell death of murine BMDM following exposure to 0.2 µg purified SLO toxin (A) or infection with WT GAS at MOI = 25 bacteria/cell (B); live/dead cell staining illustrates viable (green) or dead (red) cells. (C) RBC-derived nanosponges increased viability of human THP-1 macrophages exposed to WT GAS in a SLO-dependent manner. (D) RBC nanosponges enhanced murine macrophage killing of WT GAS to the level of killing observed with the isogenic GAS 1SLO mutant. Results are from experiments performed in triplicate, and reported as mean ± SEM from at least three experiments

RBC nanosponges counteract GAS SLO-mediated toxicity to macrophages

Macrophages contribute directly to bacterial clearance and produce cytokines and other inflammatory signals that can orchestrate downstream immune responses. As measured by live-dead staining, we found that RBC nanosponges significantly reduced cell death of murine BMDM following exposure to purified SLO toxin (**Figure 2.2A**) or WT GAS (**Figure 2.2B**).

Similarly, RBC nanosponges increased viability of human THP-1 macrophages following incubation with GAS in a SLO-dependent manner (**Figure 2.2C**). RBC nanosponges also enhanced murine macrophage killing of WT GAS to the level of killing observed with the GAS ΔSLO mutant (**Figure 2.2D**).

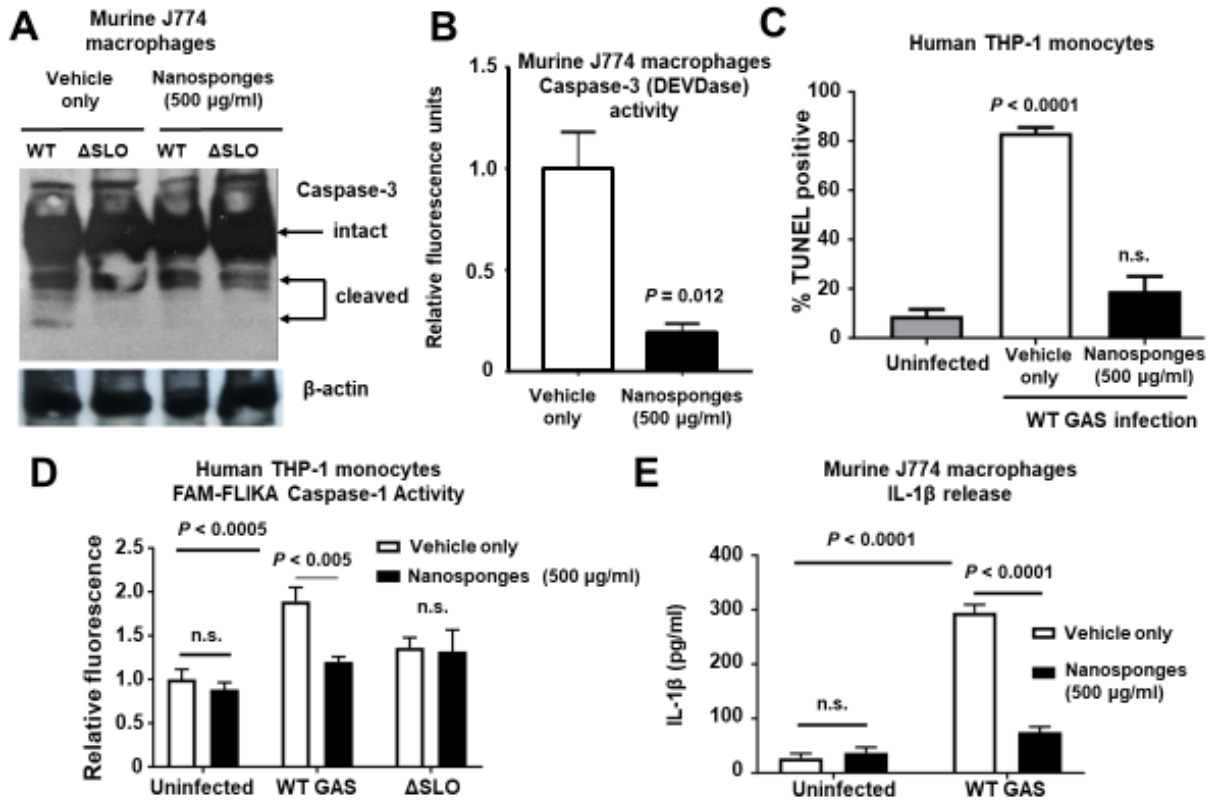

Figure 2.3 RBC nanosponges reduce GAS SLO-induced apoptosis and inflammasome activation in macrophages. Treatment with RBC-derived nanosponges reduced WT GASinduced macrophage apoptosis as measured by caspase-3 cleavage (A) and activity assays (B) performed in murine J774 macrophages, as well as TUNEL assay in human THP1 monocytes (C). Treatment with RBC-derived nanosponges reduced GAS SLO-induced inflammasome activation measured by caspase-1 activity in human THP1 mononcytes (D) and IL-1β secretion in J774 macrophages (E). Results are from experiments performed in triplicate and reported as mean +/- SEM from at least 3 experiments.

Treatment with nanosponges reduced WT GAS-induced macrophage apoptosis as measured by caspase-3 cleavage (**Figure 2.3A**), caspase-3 activity assay (**Figure 2.3B**) and TUNEL assay (**Figure 2.3C**). Nanosponge treatment also blocked GAS SLO-induced inflammasome activation (measured by caspase-1 activity, **Figure 2.3D**) and IL-1β secretion

(**Figure 2.3E**). In sum, RBC nanosponges improved macrophage viability in the face of GAS SLO activation, enhancing their antibacterial function against the pathogen.

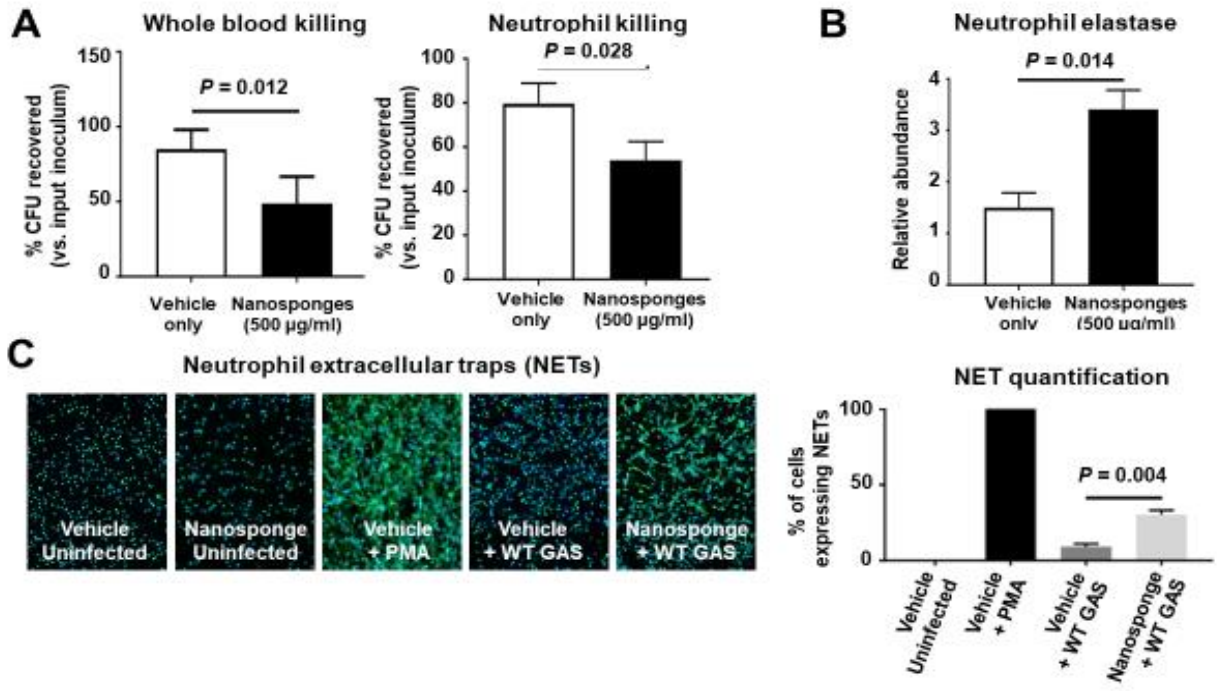

Figure 2.4 RBC nanosponges mitigates GAS SLO-mediated impairment of neutrophil killing. (A) Addition of 500 µg/ml of RBC nanosponges to freshly isolated human whole blood or purified human neutrophils significantly increases killing of WT GAS strain expressing SLO. (B) RBC nanosponge treatment increased neutrophil degranulation as measured by release of neutrophil elastase. (C) RBC-derived nanosponge treatment increased human neutrophil production of antibacterial NETs as detected by immunofluorescent staining and DNA quantification. Results are from experiments performed in triplicate and reported as mean +/- SEM from at least 3 experiments.

RBC nanosponges mitigate GAS SLO-mediated impairment of neutrophil killing

GAS production of SLO has been shown to impair neutrophil microbicidal activity, degranulation and release of DNA-based neutrophil extracellular traps, or NETs (Sierig et al., 2003; Ato et al., 2008; Uchiyama et al., 2015). We found that addition of 500 µg/ml of RBC nanosponges to freshly isolated human whole blood or purified human neutrophils significantly increased killing of the WT GAS strain expressing SLO (**Figure 2.4A**).

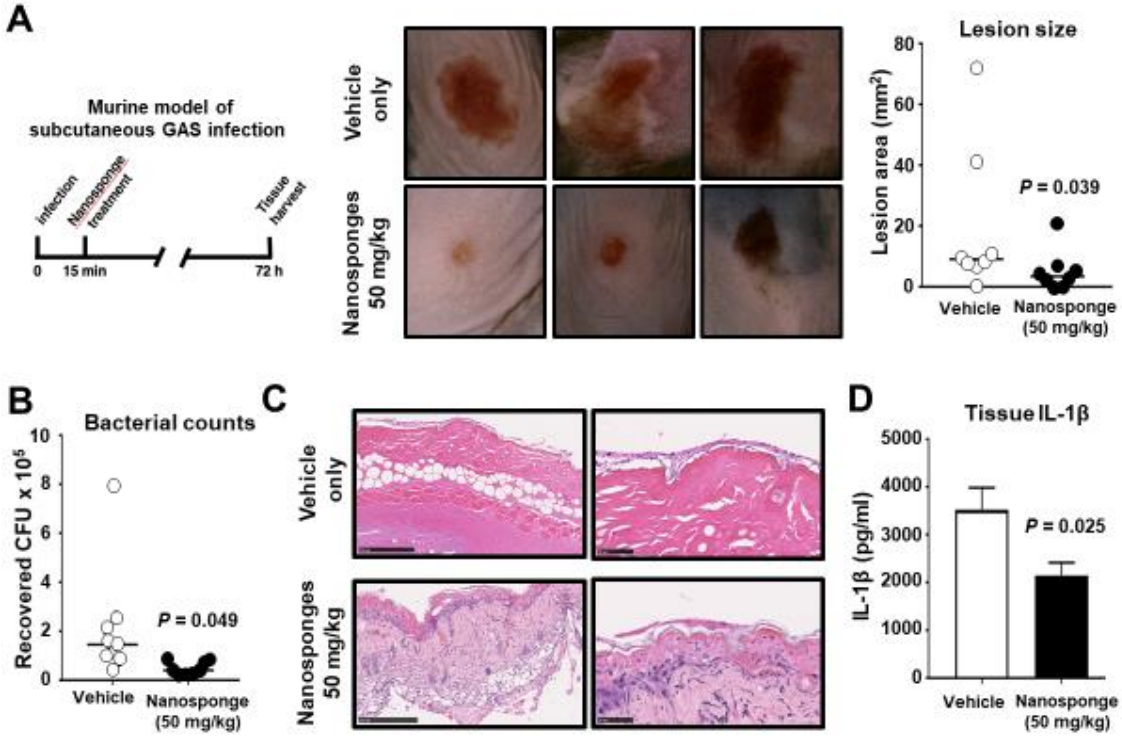

Figure 2.5 RBC nanosponges reduce GAS disease severity in necrotizing skin infection model. Invasive WT SLO-producing GAS strain subcutaneously into flanks of WT C57bl6 mice and mice were subsequently treated in the proximal tissues with either vehicle only control or vehicle + 50 mg/kg of RBC nanosponges (15 min post infection). (A) At 72 h post-infection, necrotic skin lesions in the nanosponge-treated group were significantly smaller than those in the control group. (B) Quantitative bacterial cultures showed nanosponge-treated mice had significantly fewer GAS CFU recovered from wound tissue. (C) Representative histopathologic analysis of lesion biopsies showing reduced necrotic tissue injury in nanosponge-treated mice. (D) Levels of proinflammatory cytokine IL-1β produced in skin tissues in GAS-infected mice upon nanosponge administration. Statistical analyses performed using unpaired Student's *t* test. Results are shown as ± SEM.

Nanosponge treatment also increased neutrophil degranulation as measured by release of neutrophil elastase (**Figure 2.4B**), as well as the production of antibacterial NETs as detected by immunofluorescent staining and DNA quantification (**Figure 2.4C**). Coupled with the macrophage studies above, our in vitro analyses suggest that nanosponge sequestration of the GAS toxin can ameliorate damaging effects on innate immune phagocytes, allowing improved clearance of the pathogen.

RBC nanosponges reduce GAS disease severity in necrotizing skin infection model

GAS production of SLO has been shown to contribute to the severity of necrotizing skin lesions in murine experimental infection models (Limbago et al., 2000; Fontaine et al., 2003; Zhu et al., 2017). We injected the invasive WT SLO-producing GAS strain subcutaneously into the flanks of WT C57bl6 mice and then subsequently treated the mice proximally with either vehicle only control or vehicle + 50 mg/kg of RBC nanosponges at 15 minutes post infection, a dose known to be well tolerated by mice in studies of purified α-toxin neutralization (Hu et al., 2013). At 72 h post-infection, necrotic skin lesions in the nanosponge-treated group were significantly smaller than those in the control group (**Figure 2.5A**), and quantitative bacterial cultures showed that nanosponge-treated mice had significantly fewer GAS CFU recovered from the wound tissue (**Figure 2.5B**). Histopathologic analysis of lesion biopsies showed wholescale hemorrhagic necrosis and tissue destruction of the dermal and sucutaneous tissues in control (vehicle-treated) mice; in contrast, nansponge treatment preserved tissue architecture with markedly reduced necrotic changes and diminished neutrophil infiltration (**Figure 2.5C**). Furthermore, levels of proinflammatory cytokine IL-1β associated with inflammasome activation and pyroptotic cell death were reduced in the infected mice upon nanosponge administration (**Figure 2.5D**).

DISCUSSION

GAS infections continue to be a significant medical concern worldwide due in part to the high morbidity and mortality of severe invasive infections that require more aggressive care than antibiotics alone (Steer et al., 2008). Necrotizing fasciitis (aka “flesh-eating disease”) is an especially life-threatening form of invasive GAS infection that requires intensive supportive care and multiple modalities of treatment with limited established efficacy (Young et al., 2006). SLO is a critical GAS virulence factor linked epidemiologically and experimentally to tissue injury, resistance to immunological clearance and more severe pathology in necrotizing fasciitis and other forms of invasive GAS infection. Immune cell inhibition and destruction are major contributing factors to the progression of bacterial disease. Mice lacking macrophages or treated with inhibitors of macrophage phagocytosis cannot clear GAS infections even at low challenge doses (Goldmann et al., 2004), demonstrating their key front-line function in defense against the pathogen. GAS production of SLO damage macrophages (Ofek et al., 1972), including accelerating macrophage cell death pathways of apoptosis (Timmer et al., 2009) or oncosis (Goldmann et al., 2009). GAS expression of SLO may impair macrophage phagolysosomal fusion (Hakansson et al., 2005) and acidification (BastiatSempe et al., 2014), facilitate GAS escape from the phagosome into the cytoplasm (O'Neill et al., 2016), block autophagic/xenophagic killing (O'Seaghdha and Wessels, 2013), or activate the NLRP3 inflammasome and IL-1β production/pyroptosis (Harder et al., 2009; Keyel et al., 2013). Here we found that a biomimetic nanosponge constructed with a polymeric core wrapped in natural RBC bilayer membrane provided a substrate to absorb SLO, reduced its cytotoxic and immune inhibitory properties, promoted phagocyte clearance of GAS, and reduced disease pathology *in vivo* in a mouse necrotizing fasciitis model.

Neutralization of secreted toxins like SLO is an attractive anti-infective strategy, as it does not interfere directly with bacterial biochemical processes that exert selective pressure for antimicrobial resistance. Likewise, the antibiotic resistance profile of specific pathogen does not

alter their susceptibility to toxin neutralization. An additional advantage of the anti-virulence nanosponge therapeutic is high specificity to target only the pathogenic infection, without deleterious effects on the normal host microbiome inherent in conventional broad-spectrum antibiotic therapy. In principle, the biomimetic RBC membrane shell provides substrate mimicry of a human host cell target capable of absorbing a wide range of pore-forming toxins of GAS and other pathogens regardless of their molecular structures.

Our proof-of-principle studies indicate that RBC nanosponges can counteract multiple pathogenic processes attributed to SLO and that their local administration can reduce bacterial burden and disease progression in an *in vivo* model of GAS necrotizing fasciitis. These experiments suggest there is merit in expanded analysis of the detailed pharmacokinetic and pharmacodynamic properties of this nanotherapeutic platform to expand investigations to multiple models of invasive infection with GAS and other pathogens in which disease outcome is driven in significant part by the deleterious effects of secreted membrane-active toxins.

SUPPLEMENTARY METHODS AND FIGURES

Dot blot analysis

Control (10% sucrose) or nanosponges were incubated in 1.5 ml Eppendorf tubes in the presence or absence of purified streptolysin O (SLO) + 10 mM dithiothreitol (DTT). Samples were incubated at 37°C for 30 min, centrifuged at 2000 rpm for 5 min, supernatants transferred to new tubes, and the pellet re-suspended in PBS. Samples were dropped in 5 µl aliquots onto a nitrocellulose membrane and dried completely before blocking with 5% milk x 1 h. The membrane was washed x 3 with Tris-buffered saline + 0.1% tween (TBST), incubated with anti-SLO antibody (ABCAM ab188539) at 1:1000 for 16 h, washed with TBST x 3, secondary rabbit antibody added for 1 h, washed x 3 with TBST, and enhanced chemiluminescence reagent (PerkinElmer) was used for detection. Images were quantified using jPEG imaging software.

RBC Hemolysis Assay

Supernatants from bacterial cultures collected at OD600 = 0.4 were used to assay hemolysis activity of released SLO. Purified SLO toxin activity was assessed using 10 mM dithiothreitol (DTT) to stabilize the toxin. Assays were allowed to proceed for 30 min at 37°C, with PBS (0% hemolysis) and 0.025% Triton (100% hemolysis) as negative and positive controls, respectively. Supernatants were collected from assay wells after centrifugation at 3000 x g for 10 min, and hemolysis determined by absorbance with SpectraMax M3 plate reader at 541 nm using SoftMax Pro software. Each titer was recorded as the point where hemolysis reached half of the 100% RBC lysis (0.025% Triton) control.

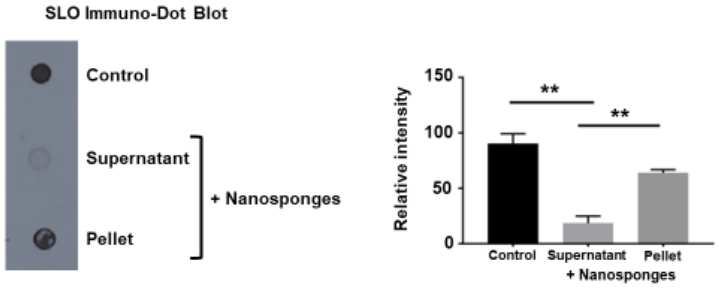

Figure S 2.1 RBC nanosponges absorb SLO toxin from solution. Vehicle alone (10% sucrose) or 500 µg/ml nanosponges suspended in vehicle were incubated in 1.5 ml Eppendorf tubes in the presence of purified streptolysin O (SLO) + 10 mM dithiothreitol (DTT). Samples were incubated at 37°C for 30 min, centrifuged at 2,000 rpm, and supernatants and pellet collected and resuspended in PBS. 5 µl aliquots were dropped onto a nitrocellulose membrane for immunoblot detection using an anti-SLO antibody and enhanced chemiluminescence quantified using JPEG imaging software.

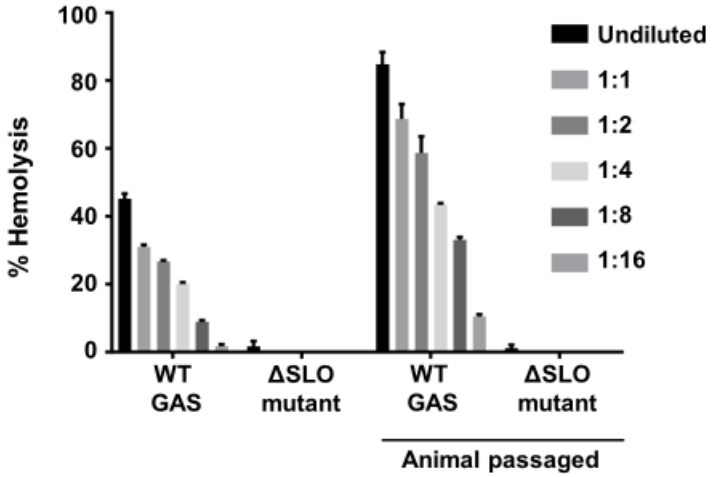

Figure S2.2 RBC nanosponges reduce GAS SLO-induced apoptosis and inflammasome activation in macrophages. Supernatants from bacterial cultures collected at OD600 = 0.4 were used to assay hemolysis activity of released SLO using 10 mM dithiothreitol (DTT) to stabilize the toxin. Assays proceeded for 30 min at 37°C, with PBS (0% hemolysis) and 0.025% Triton (100% hemolysis) as negative and positive controls, respectively. Supernatants were collected from assay wells 3000 x g centrifugation x 10 min, and hemolysis assayed by absorbance at 541 nm. Each titer was recorded as the point where hemolysis reached half of the 100% RBC lysis (0.025% Triton) control.

ACKNOWLEDGEMENTS

This work was supported by the National Institutes of Health under Award Numbers R01CA200574 (L.Z.), R01EY025947 (L.Z.), R01AI077780 (V.N.), and R01HL125352 (V.N.). T.E. was supported through the UCSD NIH/NIGMS Training Program in Molecular and Cellular Pharmacology (T32GM007752).

Chapter 2, in full, is a reprint of the material as it appears in: Escajadillo T, Olson J, Luk B, Zhang L, Nizet V. 2017. A red blood cell-camouflaged nanoparticle counteracts streptolysin O-mediated virulence phenotypes of invasive group A Streptococcus. *Frontiers in Pharmacology*. 8 (477) ISSN 1663-9812. The dissertation author is the primary investigator and author of this paper.

REFERENCES

Ato, M., Ikebe, T., Kawabata, H., Takemori, T., and Watanabe, H. (2008). Incompetence of neutrophils to invasive group A *Streptococcus* is attributed to induction of plural virulence factors by dysfunction of a regulator. *PLoS One* 3**,** e3455.

Aziz, R.K., and Kotb, M. (2008). Rise and persistence of global M1T1 clone of *Streptococcus pyogenes*. *Emerg Infect Dis* 14**,** 1511-1517.

Aziz, R.K., Pabst, M.J., Jeng, A., Kansal, R., Low, D.E., Nizet, V., and Kotb, M. (2004). Invasive M1T1 group A *Streptococcus* undergoes a phase-shift in vivo to prevent proteolytic degradation of multiple virulence factors by SpeB. *Mol Microbiol* 51**,** 123-134.

Barnett, T.C., Cole, J.N., Rivera-Hernandez, T., Henningham, A., Paton, J.C., Nizet, V., and Walker, M.J. (2015). Streptococcal toxins: role in pathogenesis and disease. *Cell Microbiol* 17**,** 1721-1741.

Bastiat-Sempe, B., Love, J.F., Lomayesva, N., and Wessels, M.R. (2014). Streptolysin O and NAD-glycohydrolase prevent phagolysosome acidification and promote group A Streptococcus survival in macrophages. *MBio* 5**,** e01690-01614.

Cegelski, L., Marshall, G.R., Eldridge, G.R., and Hultgren, S.J. (2008). The biology and future prospects of antivirulence therapies. *Nat Rev Microbiol* 6**,** 17-27.

Chandrasekaran, S., and Caparon, M.G. (2016). The NADase-negative variant of the S*treptococcus pyogenes* toxin NAD(+) glycohydrolase induces JNK1-mediated programmed cellular necrosis. *MBio* 7**,** e02215-02215.

Chatellier, S., Ihendyane, N., Kansal, R.G., Khambaty, F., Basma, H., Norrby-Teglund, A., Low, D.E., Mcgeer, A., and Kotb, M. (2000). Genetic relatedness and superantigen expression in group A *Streptococcus* serotype M1 isolates from patients with severe and nonsevere invasive diseases. *Infect Immun* 68**,** 3523-3534.

Cheng, J., Teply, B.A., Sherifi, I., Sung, J., Luther, G., Gu, F.X., Levy-Nissenbaum, E., RadovicMoreno, A.F., Langer, R., and Farokhzad, O.C. (2007). Formulation of functionalized PLGA-PEG nanoparticles for in vivo targeted drug delivery. *Biomaterials* 28**,** 869-876.

Chiarot, E., Faralla, C., Chiappini, N., Tuscano, G., Falugi, F., Gambellini, G., Taddei, A., Capo, S., Cartocci, E., Veggi, D., Corrado, A., Mangiavacchi, S., Tavarini, S., Scarselli, M., Janulczyk, R., Grandi, G., Margarit, I., and Bensi, G. (2013). Targeted amino acid substitutions impair streptolysin O toxicity and group A *Streptococcus* virulence. *MBio* 4**,** e00387-00312.

Clatworthy, A.E., Pierson, E., and Hung, D.T. (2007). Targeting virulence: a new paradigm for antimicrobial therapy. *Nat Chem Biol* 3**,** 541-548.

Cole, J.N., Barnett, T.C., Nizet, V., and Walker, M.J. (2011). Molecular insight into invasive group A streptococcal disease. *Nat Rev Microbiol* 9**,** 724-736.

Dale, J.B., Washburn, R.G., Marques, M.B., and Wessels, M.R. (1996). Hyaluronate capsule and surface M protein in resistance to opsonization of group A streptococci. *Infect Immun* 64**,** 1495-1501.

Desilets, J., Lejeune, A., Mercer, J., and Gicquaud, C. (2001). Nanoerythrosomes, a new derivative of erythrocyte ghost: IV. Fate of reinjected nanoerythrosomes. *Anticancer Res* 21**,** 1741-1747.

Dohrmann, S., Cole, J.N., and Nizet, V. (2016). Conquering neutrophils. *PLoS Pathog* 12**,** e1005682.

Fontaine, M.C., Lee, J.J., and Kehoe, M.A. (2003). Combined contributions of streptolysin O and streptolysin S to virulence of serotype M5 *Streptococcus pyogenes* strain Manfredo. *Infect Immun* 71**,** 3857-3865.

Goldmann, O., Rohde, M., Chhatwal, G.S., and Medina, E. (2004). Role of macrophages in host resistance to group A streptococci. *Infect Immun* 72**,** 2956-2963.

Goldmann, O., Sastalla, I., Wos-Oxley, M., Rohde, M., and Medina, E. (2009). *Streptococcus pyogenes* induces oncosis in macrophages through the activation of an inflammatory programmed cell death pathway. *Cell Microbiol* 11**,** 138-155.

Hakansson, A., Bentley, C.C., Shakhnovic, E.A., and Wessels, M.R. (2005). Cytolysindependent evasion of lysosomal killing. *Proc Natl Acad Sci U S A* 102**,** 5192-5197.

Hamada, S., Kawabata, S., and Nakagawa, I. (2015). Molecular and genomic characterization of pathogenic traits of group A *Streptococcus pyogenes*. *Proc Jpn Acad Ser B Phys Biol Sci* 91**,** 539-559.

Harder, J., Franchi, L., Munoz-Planillo, R., Park, J.H., Reimer, T., and Nunez, G. (2009). Activation of the Nlrp3 inflammasome by *Streptococcus pyogenes* requires streptolysin O and NF-κB activation but proceeds independently of TLR signaling and P2X7 receptor. *J Immunol* 183**,** 5823-5829.

Henningham, A., Dohrmann, S., Nizet, V., and Cole, J.N. (2015). Mechanisms of group A Streptococcus resistance to reactive oxygen species. *FEMS Microbiol Rev* 39**,** 488-508.

Henry, B.D., Neill, D.R., Becker, K.A., Gore, S., Bricio-Moreno, L., Ziobro, R., Edwards, M.J., Muhlemann, K., Steinmann, J., Kleuser, B., Japtok, L., Luginbuhl, M., Wolfmeier, H., Scherag, A., Gulbins, E., Kadioglu, A., Draeger, A., and Babiychuk, E.B. (2015). Engineered liposomes sequester bacterial exotoxins and protect from severe invasive infections in mice. *Nat Biotechnol* 33**,** 81-88.

Hsu, L.C., Park, J.M., Zhang, K., Luo, J.L., Maeda, S., Kaufman, R.J., Eckmann, L., Guiney, D.G., and Karin, M. (2004). The protein kinase PKR is required for macrophage apoptosis after activation of Toll-like receptor 4. *Nature* 428**,** 341-345.

Hu, C.M., Fang, R.H., Copp, J., Luk, B.T., and Zhang, L. (2013). A biomimetic nanosponge that absorbs pore-forming toxins. *Nat Nanotechnol* 8**,** 336-340.

Hu, C.M., Fang, R.H., Luk, B.T., and Zhang, L. (2014). Polymeric nanotherapeutics: clinical development and advances in stealth functionalization strategies. *Nanoscale* 6**,** 65-75.

Hu, C.M., Zhang, L., Aryal, S., Cheung, C., Fang, R.H., and Zhang, L. (2011). Erythrocyte membrane-camouflaged polymeric nanoparticles as a biomimetic delivery platform. *Proc Natl Acad Sci U S A* 108**,** 10980-10985.

Ikebe, T., Ato, M., Kobayashi, K., and Watanabe, H. (2009). [Mechanism behind streptococcus toxic shock-like syndrome onset--immune evasion and bacterial properties]. *Kansenshogaku Zasshi* 83**,** 485-489.

Johnson, B.K., and Abramovitch, R.B. (2017). Small molecules that sabotage bacterial virulence. *Trends Pharmacol Sci* 38**,** 339-362.

Keyel, P.A., Roth, R., Yokoyama, W.M., Heuser, J.E., and Salter, R.D. (2013). Reduction of streptolysin O (SLO) pore-forming activity enhances inflammasome activation. *Toxins (Basel)* 5**,** 1105-1118.

Kristian, S.A., Datta, V., Weidenmaier, C., Kansal, R., Fedtke, I., Peschel, A., Gallo, R.L., and Nizet, V. (2005). D-alanylation of teichoic acids promotes group A *Streptococcus* antimicrobial peptide resistance, neutrophil survival, and epithelial cell invasion. *J Bacteriol* 187**,** 6719-6725.

Kroll, A.V., Fang, R.H., and Zhang, L. (2017). Biointerfacing and applications of cell membrane-coated nanoparticles. *Bioconjug Chem* 28**,** 23-32.

Larock, C.N., and Nizet, V. (2015). Cationic antimicrobial peptide resistance mechanisms of streptococcal pathogens. *Biochim Biophys Acta* 1848**,** 3047-3054.

Limbago, B., Penumalli, V., Weinrick, B., and Scott, J.R. (2000). Role of streptolysin O in a mouse model of invasive group A streptococcal disease. *Infect Immun* 68**,** 6384-6390.

Luk, B.T., and Zhang, L. (2015). Cell membrane-camouflaged nanoparticles for drug delivery. *J Control Release* 220**,** 600-607.

Munguia, J., and Nizet, V. (2017). Pharmacological targeting of the host-pathogen interaction: alternatives to classical antibiotics to combat drug-resistant superbugs. *Trends Pharmacol Sci*. (online early)

Nasser, W., Beres, S.B., Olsen, R.J., Dean, M.A., Rice, K.A., Long, S.W., Kristinsson, K.G., Gottfredsson, M., Vuopio, J., Raisanen, K., Caugant, D.A., Steinbakk, M., Low, D.E., Mcgeer, A., Darenberg, J., Henriques-Normark, B., Van Beneden, C.A., Hoffmann, S., and Musser, J.M. (2014). Evolutionary pathway to increased virulence and epidemic group A *Streptococcus* disease derived from 3,615 genome sequences. *Proc Natl Acad Sci U S A* 111**,** E1768-1776.

Nizet, V., Ohtake, T., Lauth, X., Trowbridge, J., Rudisill, J., Dorschner, R.A., Pestonjamasp, V., Piraino, J., Huttner, K., and Gallo, R.L. (2001). Innate antimicrobial peptide protects the skin from invasive bacterial infection. *Nature* 414**,** 454-457.

O'neill, A.M., Thurston, T.L., and Holden, D.W. (2016). Cytosolic replication of group A *Streptococcus* in human macrophages. *MBio* 7**,** e00020-00016.

O'seaghdha, M., and Wessels, M.R. (2013). Streptolysin O and its co-toxin NAD-glycohydrolase protect group A *Streptococcus* from xenophagic killing. *PLoS Pathog* 9**,** e1003394.

Oehmcke, S., Shannon, O., Morgelin, M., and Herwald, H. (2010). Streptococcal M proteins and their role as virulence determinants. *Clin Chim Acta* 411**,** 1172-1180.

Ofek, I., Bergner-Rabinowitz, S., and Ginsburg, I. (1972). Oxygen-stable hemolysins of group A streptococci. 8. Leukotoxic and antiphagocytic effects of streptolysins S and O. *Infect Immun* 6**,** 459-464.

Pang, Z., Hu, C.M., Fang, R.H., Luk, B.T., Gao, W., Wang, F., Chuluun, E., Angsantikul, P., Thamphiwatana, S., Lu, W., Jiang, X., and Zhang, L. (2015). Detoxification of organophosphate poisoning using nanoparticle bioscavengers. *ACS Nano* 9**,** 6450-6458.

Ralph, A.P., and Carapetis, J.R. (2013). Group Astreptococcal diseases and their global burden. *Curr Top Microbiol Immunol* 368**,** 1-27.

Ruiz, N., Wang, B., Pentland, A., and Caparon, M. (1998). Streptolysin O and adherence synergistically modulate proinflammatory responses of keratinocytes to group A streptococci. *Mol Microbiol* 27**,** 337-346.

Schroeder, A., Heller, D.A., Winslow, M.M., Dahlman, J.E., Pratt, G.W., Langer, R., Jacks, T., and Anderson, D.G. (2011). Treating metastatic cancer with nanotechnology. *Nat Rev Cancer* 12**,** 39-50.

Sharma, G., Sharma, A.R., Nam, J.S., Doss, G.P., Lee, S.S., and Chakraborty, C. (2015). Nanoparticle based insulin delivery system: the next generation efficient therapy for type 1 diabetes. *J Nanobiotechnology* 13**,** 74.

Sierig, G., Cywes, C., Wessels, M.R., and Ashbaugh, C.D. (2003). Cytotoxic effects of streptolysin o and streptolysin S enhance the virulence of poorly encapsulated group Astreptococci. *Infect Immun* 71**,** 446-455.

Steer, A.C., Curtis, N., and Carapetis, J.R. (2008). Diagnosis and treatment of invasive group A streptococcal infections. *Expert Opin Med Diagn* 2**,** 289-301.

Sumby, P., Whitney, A.R., Graviss, E.A., Deleo, F.R., and Musser, J.M. (2006). Genome-wide analysis of group A streptococci reveals a mutation that modulates global phenotype and disease specificity. *PLoS Pathog* 2**,** e5.

Timmer, A.M., Timmer, J.C., Pence, M.A., Hsu, L.C., Ghochani, M., Frey, T.G., Karin, M., Salvesen, G.S., and Nizet, V. (2009). Streptolysin O promotes group A *Streptococcus* immune evasion by accelerated macrophage apoptosis. *J Biol Chem* 284**,** 862-871.

Tweten, R.K., Hotze, E.M., and Wade, K.R. (2015). The unique molecular choreography of giant pore formation by the cholesterol-dependent cytolysins of Gram-positive bacteria. *Annu Rev Microbiol* 69**,** 323-340.

Uchiyama, S., Dohrmann, S., Timmer, A.M., Dixit, N., Ghochani, M., Bhandari, T., Timmer, J.C., Sprague, K., Bubeck-Wardenburg, J., Simon, S.I., and Nizet, V. (2015). Streptolysin O

rapidly impairs neutrophil oxidative burst and antibacterial responses to group A *Streptococcus*. *Front Immunol* 6**,** 581.

Waddington, C.S., Snelling, T.L., and Carapetis, J.R. (2014). Management of invasive group A streptococcal infections. *J Infect* 69 Suppl 1**,** S63-69.

Walker, M.J., Barnett, T.C., Mcarthur, J.D., Cole, J.N., Gillen, C.M., Henningham, A., Sriprakash, K.S., Sanderson-Smith, M.L., and Nizet, V. (2014). Disease manifestations and pathogenic mechanisms of group A *Streptococcus*. *Clin Microbiol Rev* 27**,** 264-301.

Wong, C.J., and Stevens, D.L. (2013). Serious group A streptococcal infections. *Med Clin North Am* 97**,** 721-736, xi-xii.

Young, M.H., Engleberg, N.C., Mulla, Z.D., and Aronoff, D.M. (2006). Therapies for necrotising fasciitis. *Expert Opin Biol Ther* 6**,** 155-165.

Zhu, L., Olsen, R.J., Lee, J.D., Porter, A.R., Deleo, F.R., and Musser, J.M. (2017). Contribution of secreted NADase and streptolysin O to the pathogenesis of epidemic serotype M1 *Streptococcus pyogenes* infections. *Am J Pathol* 187**,** 605-613.

Zhu, L., Olsen, R.J., Nasser, W., Beres, S.B., Vuopio, J., Kristinsson, K.G., Gottfredsson, M., Porter, A.R., Deleo, F.R., and Musser, J.M. (2015). A molecular trigger for intercontinental epidemics of group A *Streptococcus*. *J Clin Invest* 125**,** 3545-3559.

CHAPTER 3

Macrophage-like nanoparticles concurrently absorbing endotoxins and proinflammatory cytokines for sepsis management

Soracha Thamphiwatana1,2,5,†, Pavimol Angsantikul1,2,†, Tamara Escajadillo3,4,†, Qiangzhe Zhang1,2, Joshua Olson3,4, Brian T. Luk1,2, Sophia Zhang1,2, Ronnie H. Fang1,2, Weiwei Gao1,2, Victor Nizet3,4*, Liangfang Zhang1,2,*

1Department of Nanoengineering, 2Moores Cancer Center, 3Department of Pediatrics, 4Skaggs School of Pharmacy and Pharmaceutical Sciences, University of California, San Diego, La Jolla, California 92093, USA. 5Institute of Biomedical Engineering, Faculty of Medicine, Prince of Songkla University, Songkhla 90110, Thailand.

† These authors contribute equally

Published in *PNAS*

September 2017

Issue 114, Pages 11488-11493

Keywords: biomimetic nanoparticle, detoxification, sepsis, lipopolysaccharide, proinflammatory cytokines

PREFACE TO CHAPTER 3

Chapter 3 in full is a published journal article in *PNAS* in which I was one of the principal investigators and authors. This works helps address Aims 2A-C: determine if macrophage derived nanoparticles are capable of binding LPS and proinflammatory cytokines, determine if macrophage derived nanoparticles are capable of detoxifying LPS and proinflammatory cytokines in vitro, and determine if macrophage derived nanoparticles are capable of detoxifying LPS and proinflammatory cytokines in a murine bacteremia model. This was done by generating white blood cell derived nanoparticles derived from mouse blood and applying the nanoparticles to models of LPS mediated infection both *in vitro* and *in vivo*. The experiments revealed that WBC derived nanoparticles are capable of absorbing and retaining the E. coli endotoxin, and a significant portion of pro-inflammatory cytokines. This dual detoxification decreased mortality and improved outcomes in a murine model of systemic infection.

ABSTRACT

Sepsis, resulting from uncontrolled inflammatory responses to bacterial infections, continues to cause high morbidity and mortality worldwide. Currently, effective sepsis treatment is unavailable in the clinic, and care remains primarily supportive. Herein, we report the development of biomimetic nanoparticles that mimic macrophages for the management of sepsis. The nanoparticles, made by wrapping polymeric cores with cell membrane derived from macrophages, possess an antigenic exterior the same as the source cells. By acting as macrophage decoys, these nanoparticles bind and neutralize endotoxins that would otherwise trigger immune activation. In addition, these macrophage-like nanoparticles are capable of binding with proinflammatory cytokines and inhibiting their ability to potentiate the sepsis cascade. By using a mouse bacteremia model, we demonstrate that treatment with macrophage mimicking nanoparticles, termed MΦ-NPs, reduces pro-inflammatory cytokine levels, inhibits bacterial colonization, and ultimately confers a higher survival rate for infected mice. Overall, employing MΦ-NPs as a new biomimetic detoxification strategy shows promise for improving patient outcomes, potentially shifting the current paradigm of sepsis management.

INTRODUCTION

Sepsis is a life-threatening complication characterized by systemic inflammatory response caused by bacterial infections (1). Uncontrolled inflammatory responses in sepsis result in the collapse of cardiovascular function, leading to multiple organ dysfunction syndrome and death (2, 3). Despite many efforts devoted to finding an effective treatment, sepsis continues to cause a high mortality rate, and the number of hospitalizations resulting from the condition continues to rise (4, 5). Endotoxin, an important pathogenic trigger of sepsis, induces a systemic inflammatory response characterized by production of proinflammatory cytokines and nitric oxide, fever, hypotension, and intravascular coagulation, which ultimately lead to septic shock (6). Endotoxin enters the bloodstream via infection sites or by the systemic spread of the bacteria. Emerging evidence suggests that the systemic spread of endotoxin, rather than bacteremia itself, is crucial in the pathogenesis of this dramatic immune dysregulation (7, 8). It has been found that a higher level of endotoxin correlates with worsened clinical outcomes (9, 10). Clearly, effective endotoxin removal is critical for successful sepsis management.

Endotoxin neutralization and removal face various challenges. While all endotoxins share a common architecture, they vary greatly in their structural motifs, which are dependent on bacterial genus, species, and strain (11, 12). Accordingly, their interactions with ligands can differ substantially, which poses challenges for structure-based neutralization strategies. Antibiotics effective in neutralizing endotoxin such as polymyxins only have limited clinical use due to their strong nephrotoxicity and neurotoxicity (13, 14). Attaching these molecules to solid-phase carriers for hemoperfusion can retain their endotoxin-binding properties while minimizing the toxic effects, but clinical evidence of therapeutic efficacy has yet to be established (15, 16). In addition, such solid-phase perfusion strategies are impractical in resource-limited environments (17).

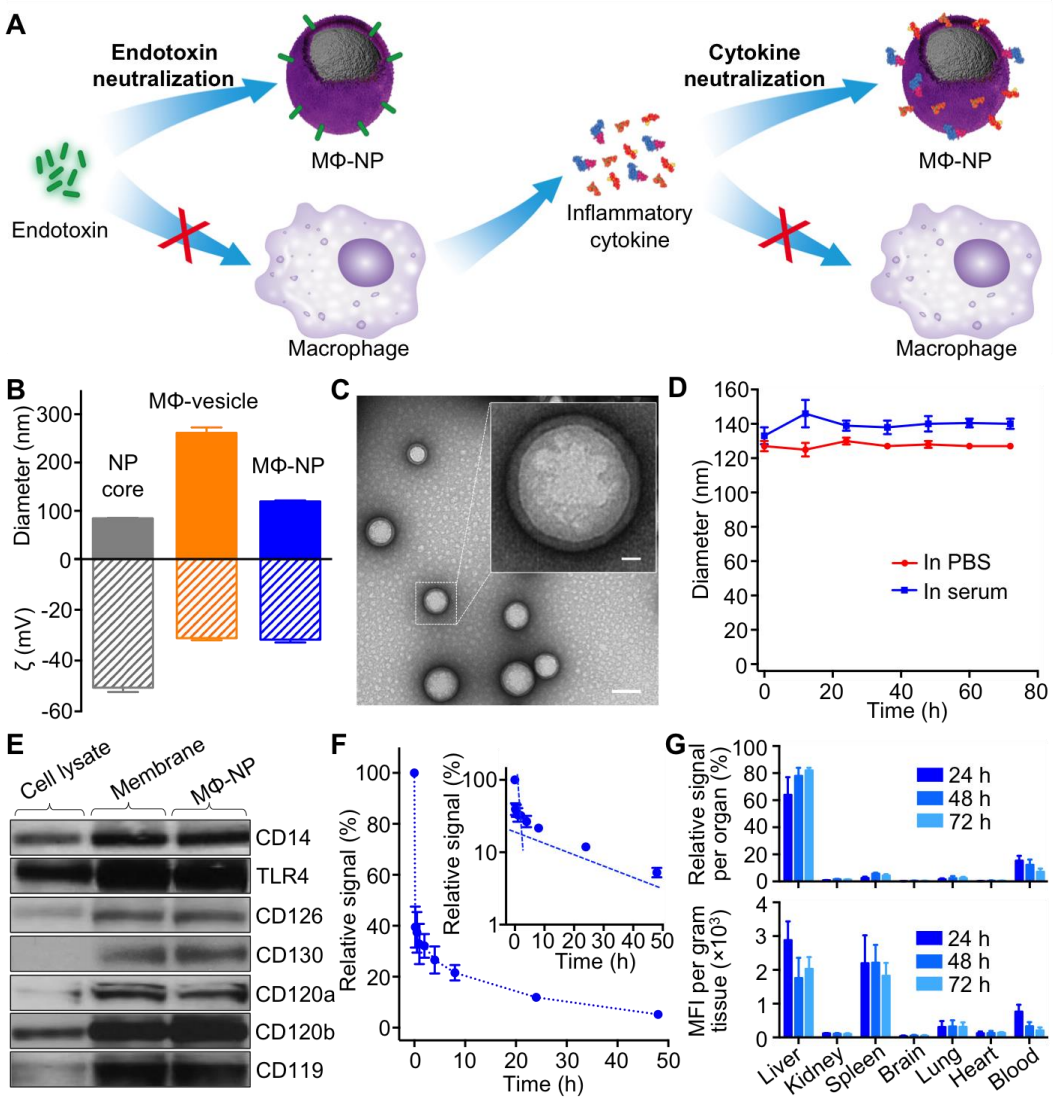

Figure 3.1. Formulation and characterization of macrophage membrane-coated nanoparticles (MΦ-NPs). (A) Schematic representation of using MΦ-NPs to neutralize endotoxin and proinflammatory cytokines as a two-step process for sepsis management. (B) Hydrodynamic size (diameter, nm) and surface zeta potential (ζ, mV) of PLGA polymeric cores before and after coating with macrophage membrane as measured by dynamic light scattering (n = 6). (C) TEM images of MΦ-NPs negatively stained with uranyl acetate. Scale bar = 100 nm. Inset: the roomed-in view of a single MΦ-NP. Scale bare = 10 nm. (D) Stability of MΦ-NPs in 1× PBS or 50% FBS, determined by monitoring particle size (diameter, nm), over a span of 72 h. (E) Representative protein bands of macrophage cell lysate, membrane vesicles, and MΦ-NPs resolved using western blotting. (F) DiD-labeled MΦ-NPs were injected intravenously via the tail vein of mice. At various time points, blood was collected and measured for fluorescence (excitation/emission = 644/670 nm) to evaluate the systemic circulation lifetime of the nanoparticles (n = 6). Inset: the semilog plot of fluorescence signal at various time points. (G) Biodistribution of the MΦ-NPs collected by injecting DiD-labeled MΦ-NPs intravenously into the mice. At each time point (24, 48, and 72 h), the organs from a randomly grouped subset of mice were collected, homogenized, and quantified for fluorescence. Fluorescence intensity per gram of tissue and relative signal per organ were compared (n = 6).

Recently, cell membrane-coated nanoparticles have emerged as a new biomimetic nanomedicine platform, enabling a broad range of biodetoxification applications (18, 19). In particular, nanoparticles coated with membranes derived from red blood cells (RBC nanosponges) have taken advantage of functional similarities shared by various pore-forming toxins to neutralize their hemolytic activity regardless of molecular structure (20). This unique core-shell nanoparticle exhibits prolonged systemic circulation, preventing further bioactivity of the toxins that it absorbs and diverting them away from their intended cellular targets. RBC nanosponges have also been developed as therapeutic detoxification agents to neutralize pathological antibodies in autoimmune diseases (21) as well as organophosphate nerve agents (22).

The therapeutic potential of membrane-coated nanoparticles for broad-spectrum detoxification inspired us to develop biomimetic nanoparticles for endotoxin removal, potentially enabling effective sepsis management. In sepsis, endotoxin, also referred to as lipopolysaccharide (LPS), is released from the bacteria during cell division, cell death, or under antibiotic treatment, and it is subsequently recognized by monocytes and macrophages (23, 24). In the blood, LPS-binding protein (LBP) binds with high affinity to LPS via lipid A, and the LPS-LBP complex subsequently engages CD14 present on the surface of macrophages (25, 26). Following the binding interaction, LPS can induce various changes in cellular activity. For example, LPS is cytotoxic to the cells, attributable to the excessive production of nitric oxide; LPS-treated macrophages demonstrate dose-dependent production of nitric oxide in culture (10). In addition, LPS-macrophage binding activates toll-like receptor 4 (TLR4) and subsequently enhances phagocytosis (27). TLR4 activation has been considered to play a significant role in the regulation of bacterial uptake, translocation, and cell death (28, 29). Furthermore, LPS-induced engagement of TLR4 also activates the nuclear factor-κB (NF-κB) transcription factor, which results in the production and secretion of proinflammatory cytokines

such as tumor necrosis factor- α (TNF-α), interleukin 6 (IL-6), and interleukin 8 (IL-8) (30, 31).

Compelled by the critical roles played by macrophages in endotoxin signaling, herein, we develop biomimetic nanoparticles consisting of a biodegradable polymeric nanoparticle core coated with cell membrane derived from macrophages (denoted MΦ-NPs, **Figure 3.1A**). MΦ-NPs possess an antigenic exterior the same as the source macrophage cells, thus inheriting their capability to bind with endotoxins. In addition, MΦ-NPs also act as decoys to bind with cytokines, inhibiting their ability to potentiate downstream inflammation cascades. These two steps together enable effective intervention during uncontrollable immune activation, providing a therapeutic strategy with significant potential for the management of sepsis.

RESULTS AND DISCUSSION

The preparation of MΦ-NPs was divided into two steps. In the first step, cell membranes from J774 mouse macrophages were derived and purified using a process involving hypotonic lysis, mechanical disruption, and differential centrifugation. In the second step, we used a sonication method to form membrane vesicles and subsequently fused them onto poly(lactic-*co*-glycolic acid) (PLGA) cores to form MΦ-NPs. Following membrane fusion, the diameter of the nanoparticles measured with dynamic light scattering (DLS) increased from 84.5 ± 1.9 nm to 102.0 ± 1.5 nm, corresponding to the addition of a bilayered cell membrane onto the polymeric cores (**Figure 3.1B**). Meanwhile, the surface zeta potential changed from −41.3 ± 3.6 mV to −26.7 ± 3.1 mV, which was likely due to charge screening by the membrane. The resulting MΦ-NPs were then stained with uranyl acetate and visualized by transmission electron microscopy (TEM). Under the microscope, nanoparticles showed a spherical core-shell structure, in which the PLGA core was wrapped with a thin shell (**Figure 3.1C**). Following the formulation, MΦ-NPs were suspended in 1× PBS and 50% serum, respectively. Within 72 h, their sizes were monitored with DLS and showed negligible changes, suggesting an excellent stability conferred by membrane coating (**Figure 3.1D**). Improved colloidal stability is attributable to the stabilizing

effect by the macrophage membrane's hydrophilic surface glycans. Together, these results demonstrate the successful coating of PLGA cores with unilamellar macrophage membranes.

Through membrane coating, MΦ-NPs are expected to inherit biological characteristics of the source cells. By using western blotting analysis, we verified that MΦ-NPs preserved critical membrane proteins responsible for LPS binding, including CD14 and TLR4 (**Figure 3.1E**). Representative cytokine-binding proteins were also preserved, including CD126 and CD130 for interleukin 6 (IL-6), CD120a and CD120b for tumor necrosis factor (TNF), and CD119 for interferon gamma (IFN-γ). Notably, the membrane derivation process not only preserved these proteins, but also resulted in significant protein enrichment. We also studied the systemic circulation time of MΦ-NPs by labeling the nanoparticles with a hydrophobic DiD fluorophore (**Figure 3.1F**). At 24 h and 48 h, MΦ-NPs showed 29% and 16% retention in the blood, respectively. Based on a two-compartment model that has been applied in previous studies to fit the circulation results of nanoparticles, the elimination half-life was calculated as 17.2 h. We investigated the in vivo tissue distribution of the MΦ-NPs to further evaluate their potential for systemic applications (**Figure 3.1G**). When analyzed per organ, MΦ-NPs were distributed mainly in the blood and the liver. Per gram of tissue, MΦ-NPs were mainly contained in the liver and spleen, two primary organs of the reticuloendothelial system (RES). Meanwhile, significant fluorescence was also observed in the blood. As the blood fluorescence decreased, a corresponding increase in signal was observed in the liver, suggesting the uptake of MΦ-NPs by the RES over time.

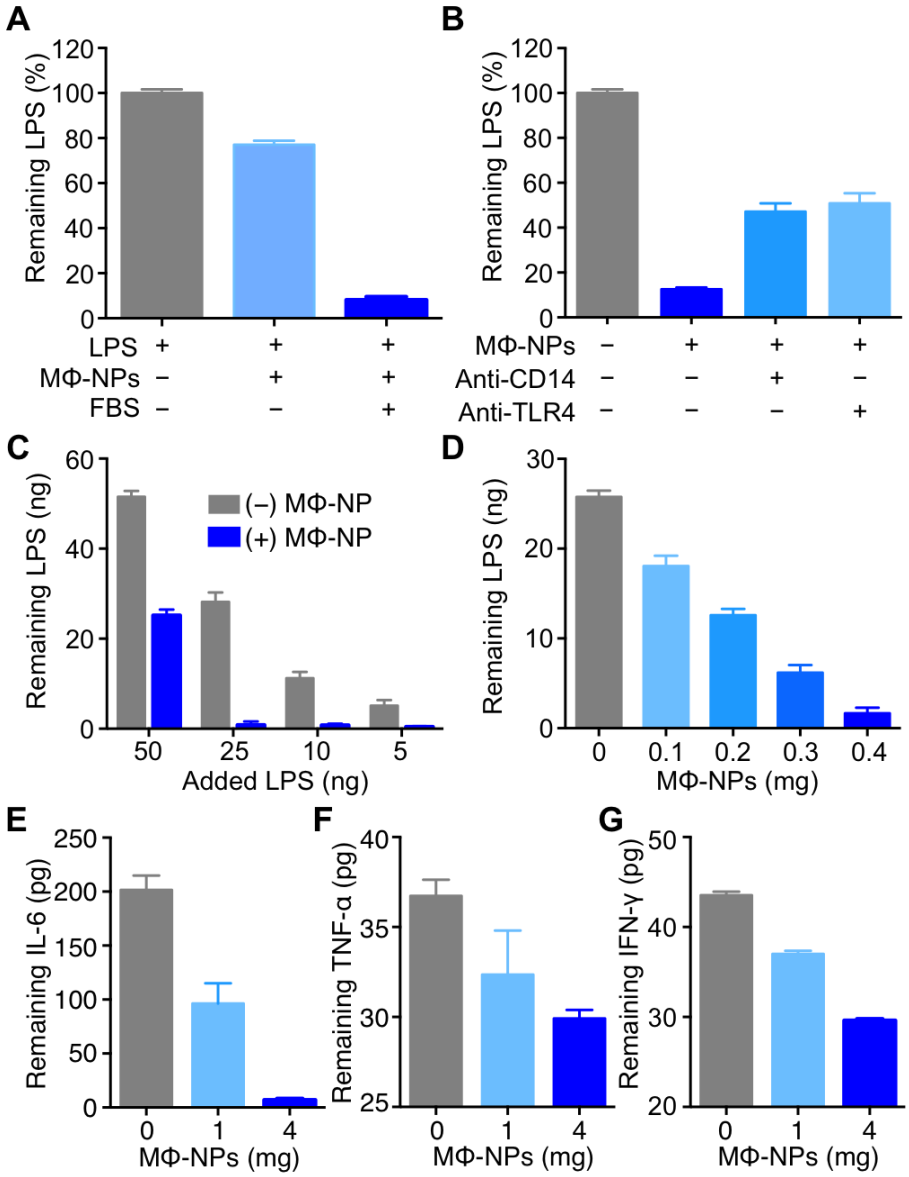

Figure 3.2. In vitro LPS and proinflammatory cytokines removal with MΦ-NPs**.** (A) LPS removal with MΦ-NPs with and without LPS binding protein (LBP) supplemented from fetal bovine serum (FBS). (B) LPS removal with MΦ-NPs with and without antibodies blocking CD14 and TLR4, respectively. (C) Quantification of LPS removal with a fixed amount of MΦ-NPs (0.4 mg) while varying the amount of added LPS. (D) Quantification of LPS removal with a fixed amount of LPS (25 ng) while varying the amount of added MΦ-NPs. (E-G) Removal of proinflammatory cytokines, including (E) IL-6, (F) TNF-α, and (G) IFN-γ, with MΦ-NPs. In all studies, three samples were used in each group.

We next examined the ability of MΦ-NPs to bind with LPS, which is known to first form high-affinity complexes with LPS-binding protein (LBP). These complexes then bind to TLR4 through CD14, which are both present on the cell surface of macrophages. We first tested the effect of LBP on LPS binding to MΦ-NPs. In the study, we mixed MΦ-NPs with FITC-LPS conjugate and incubated the mixture at 37°C. Following the incubation, MΦ-NPs were removed with ultracentrifugation and binding was evaluated by comparing FITC fluorescence intensity from the supernatant. As shown in **Figure 3.2A**, with the absence of LBP, nearly 80% of LPS remained in the solution. However, when LBP was supplemented, only 10% of LPS was left, suggesting a significant increase of LPS binding with MΦ-NPs. We then examined whether LPS binding with MΦ-NPs was dependent on surface markers known to mediate LPS binding with macrophages including CD14 and TLR4. In the study, we used anti-TLR4 or anti-CD14 to block these surface markers. Following each blockade, the amount of unbound LPS remaining in the supernatant increased compared to samples without added antibodies, indicating the decrease of binding interactions between MΦ-NPs and LPS (**Figure 3.2B**). The study suggests that LPS binding with MΦ-NPs is indeed mediated by CD14 and TLR4. Overall, compared to macrophages, MΦ-NPs show similar dependence on LBP, TLR4, and CD14 in binding with LPS, suggesting that MΦ-NPs inherit the biological characteristics of the source cells.

Next, we quantified LPS removal capability of MΦ-NPs through two sets of experiments. First, we fixed the total amount of MΦ-NPs at 0.4 mg and incubated it with various amounts of LPS (5, 10, 25, and 50 ng, respectively). After removing nanoparticles with ultracentrifuge, it was found that the added amount of MΦ-NPs was able to neutralize up to 25 ng LPS, translating to a LPS removal capacity of 62.5 ng LPS /mg MΦ-NPs (**Figure 3.2C**). In the second experiment, we fixed the total amount of LPS at 25 ng and varied the amounts of MΦ-NPs (0, 0.1, 0.2, 0.3, 0.4 mg, respectively). When MΦ-NP concentration was increased from 0.1 to 0.4 mg, a linear decrease of remaining LPS in the supernatant was observed. The measurement showed that 0.4 mg MΦ-NPs are needed to neutralize 25 ng LPS, corresponding to a removal

capacity of 62.5 ng LPS /mg MΦ-NPs (**Figure 3.2D**), which was consistent with the results of the first experiment.

The ability of MΦ-NPs to bind with proinflammatory cytokines, including IL-6, TNF-α, and IFN-γ, was also investigated. In the study, cytokine solutions with known initial concentrations were added with different concentrations of MΦ-NPs and allowed for incubation at 37°C for 30 min. Following the incubation, nanoparticles were removed with ultracentrifugation and the amount of remaining cytokines in the supernatant was quantified. As shown in **Figure 3.2 E-G**, when 1 mg of MΦ-NPs was added, 105.1 pg of IL-6, 4.3 pg of TNF-α, and 6.5 pg of IFN-γ were removed from the mixture, corresponding to a cytokine removal yields of 52.6%, 11.6%, and 14.8%, respectively. When 4 mg of MΦ-NPs was added, 194.4 pg of IL-6, 6.7 pg of TNF-α, and 13.9 pg of IFN-γ were removed from the mixture, corresponding to a cytokine removal yields of 97.2%, 18.1%, and 31.6%, respectively. These quantification results suggest that the MΦ-NPs can effectively remove various types of proinflammatory cytokines in a concentration dependent manner.

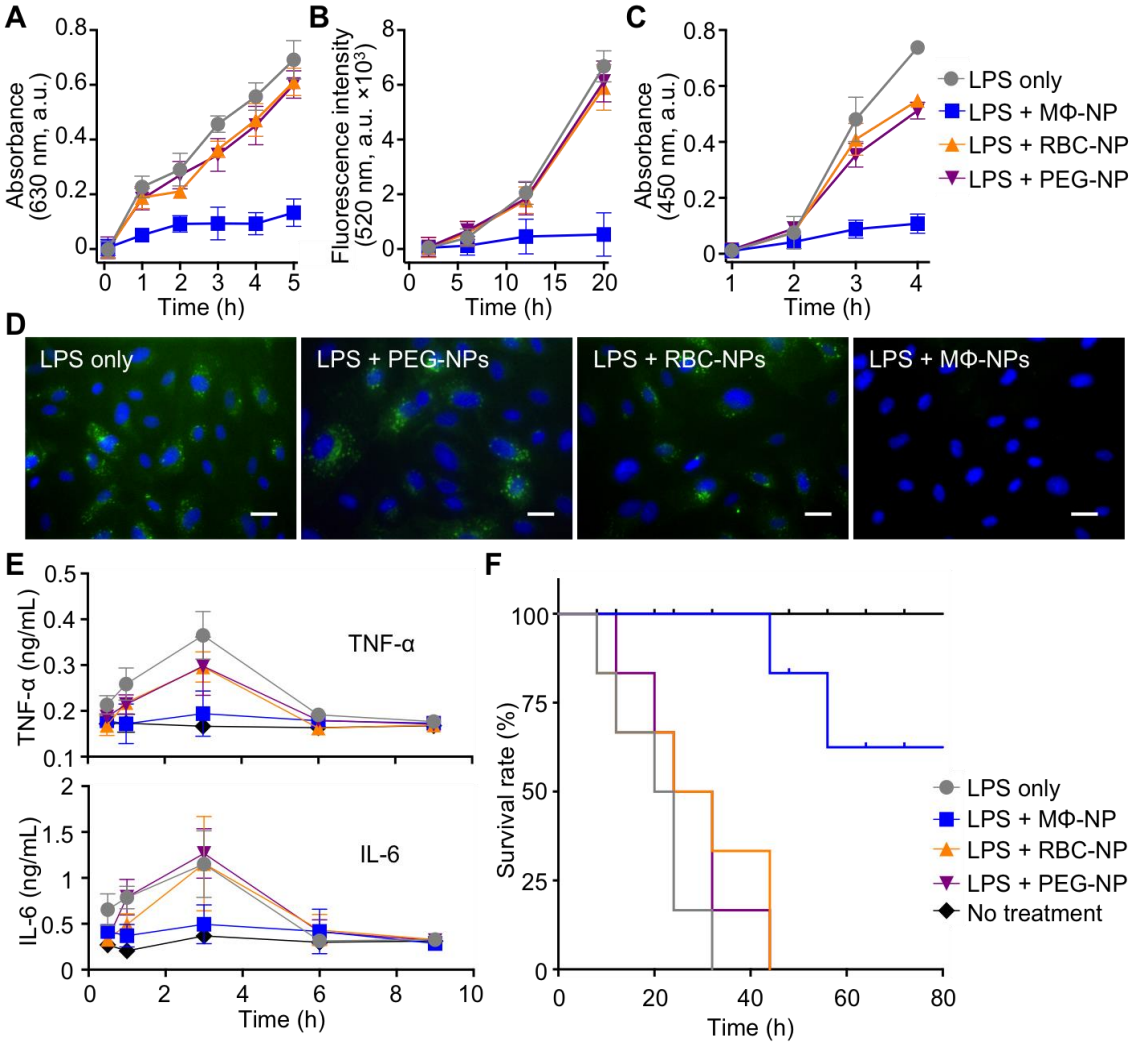

Figure 3.3 In vitro and in vivo LPS neutralization with MΦ-NPs. (A-C) LPS-inducible cell functions, including (A) TLR4 activation on HEK293 cells, (B) intracellular nitric oxide (iNO) production from J774 macrophages, and (C) E-selectin expression of HUVECs, were studied by stimulating corresponding cells with LPS alone or LPS mixed with MΦ-NPs, RBC-NPs, or PEG-NPs, respectively. (D) Fluorescent images collected from samples in (C) after 4 h of incubation. Cells were stained with mouse anti-human E-selectin, followed by staining with anti-mouse IgG Alexa 488-conjugates (green) and DAPI (blue). Scale bars = 5 μm. Three samples were used in each group. (E-F) For in vivo evaluation, (E) levels of inflammatory cytokines, including TNF-α and IL-6, in plasma (n=6) and (F) survival (n=10) were studied after injecting mice with LPS alone or LPS mixed with MΦ-NPs, RBC-NPs, or PEG-NPs. Untreated mice were also included as a control group.

Following the LPS and proinflammatory cytokine removal studies, we investigated the ability of MΦ-NPs to neutralize the function of LPS in vitro. Among various cell receptors, TLR4 receptor is well known to interact with LPS and induce an inflammatory response (27-29). To evaluate the neutralization, we used engineered HEK293 TLR4 reporter cells that produce

secreted embryonic alkaline phosphatase (SEAP) in response to TLR4 activation (**Figure 3.3A**). When free LPS was added into the cell culture, within 5 h, pronounced TLR4 activation was observed. However, when LPS was incubated with MΦ-NPs prior to their addition to the culture, TLR4 activation was abrogated. To confirm that the neutralization was specific to MΦ-NPs, we also used RBC-NPs and PLGA nanoparticles functionalized with synthetic polyethylene glycol (PEG-NPs). Incubation of LPS with these two control nanoparticle formulations was ineffective in inhibiting TLR4 activation. LPS is also known to induce the overproduction of intracellular nitric oxide (iNO) by inducible NO synthase in various cell types, including macrophages (10). As a recognized marker of proinflammatory responses, the strong release of iNO may trigger inflammatory cascades in activated cells. We investigated LPS neutralization by examining the attenuation of LPS-induced iNO production by MΦ-NPs (**Figure 3.3B**). Cells incubated with free LPS showed a continual increase of iNO, whereas LPS incubated with MΦ-NPs was unable to enhance iNO production, implying a clear inhibitory effect. This effect was absent when LPS was incubated with RBC-NPs or PEG-NPs, further confirming the neutralization specificity of MΦ-NPs.

Endothelial cells are known to rapidly respond to a minute amount of LPS exposure, which rapidly induces the expression of the cell adhesion molecule E-selectin (32). As such, we used LPS-mediated induction of E-selectin on human umbilical vein endothelial cells (HUVECs) to further investigate LPS neutralization by MΦ-NPs. In the study, cultured cells were incubated with LPS, and the levels of E-selectin expression were quantified by an enzyme immunoassay. As shown in **Figure 3.3C**, the addition of LPS at a concentration of 10 ng/mL caused a continuous increase of E-selectin expression. However, when the LPS was added together with 1 mg/mL of MΦ-NPs, E-selectin expression remained at a level comparable to untreated cells. The addition of control nanoparticle groups, including RBC-NPs and PEG-NPs, was unable to inhibit the overexpression of E-selectin, confirming the specificity of MΦ-NPs in LPS neutralization. Three hours after adding LPS, cells were also stained with antibodies to

fluorescently label E-selectin. Under the microscope, cells incubated with LPS alone, LPS with RBC-NPs, and LPS with PEG-NPs showed strong green fluorescence in the cytoplasmic and nuclear peripheral regions (**Figure 3.3D**). In contrast, little expression was observed on HUVECs incubated with LPS together with MΦ-NPs. These results further confirm the capability of MΦ-NPs in neutralizing LPS.

The LPS neutralization by MΦ-NPs was further evaluated in mice by examining the inhibition of acute inflammatory responses to endotoxin. In the study, LPS at a dosage of 5 μg/kg was injected intravenously via the tail vein of the mice (**Figure 3.3E**). Following the injection, blood was collected at various time points and the levels of inflammatory cytokines, including TNF-α, and IL-6, were quantified with ELISA. Cytokine levels increased and reached maximums at 3 h following injection of LPS alone. By 6 h, they returned to baseline levels. Remarkably, in the study group, where MΦ-NPs at a dosage of 80 mg/kg were injected immediately after the LPS, no increase in cytokine levels was observed. Both TNF-α and IL-6 remained at background levels during the course of the study, demonstrating potent LPS neutralization by the MΦ-NPs. Meanwhile, when MΦ-NPs were replaced with RBC-NPs or PEG-NPs for injection, the cytokine levels followed similar kinetics compared with the LPS only group.

We further validated MΦ-NPs for their LPS neutralization capability in vivo by monitoring the survival rate of mice when challenged with LPS. In the study, we first sensitized the mice with D-galactosamine hydrochloride via intraperitoneal injection at a dosage of 800 mg/kg to increase their sensitivity to the lethal effects of LPS (33). After 30 min of sensitization, LPS and nanoparticles were injected intravenously. As shown in **Figure 3.3F**, a single dose of LPS (5 μg/kg) showed 100% mortality by 32 h after the injection. Mice in the treatment groups received an intravenous injection of MΦ-NPs, RBC-NPs, or PEG-NPs at a dose of 200 mg/kg. In the group treated with MΦ-NPs, 60% of mice survived the lethal LPS challenge (n = 10). In contrast, RBC-NPs and PEG-NPs failed to improve the survival rate of the LPS-challenged mice, and

there was no significant difference in survival between these groups and the LPS only group. These results together validated the potential of MΦ-NPs as a novel endotoxin bioscavenger.

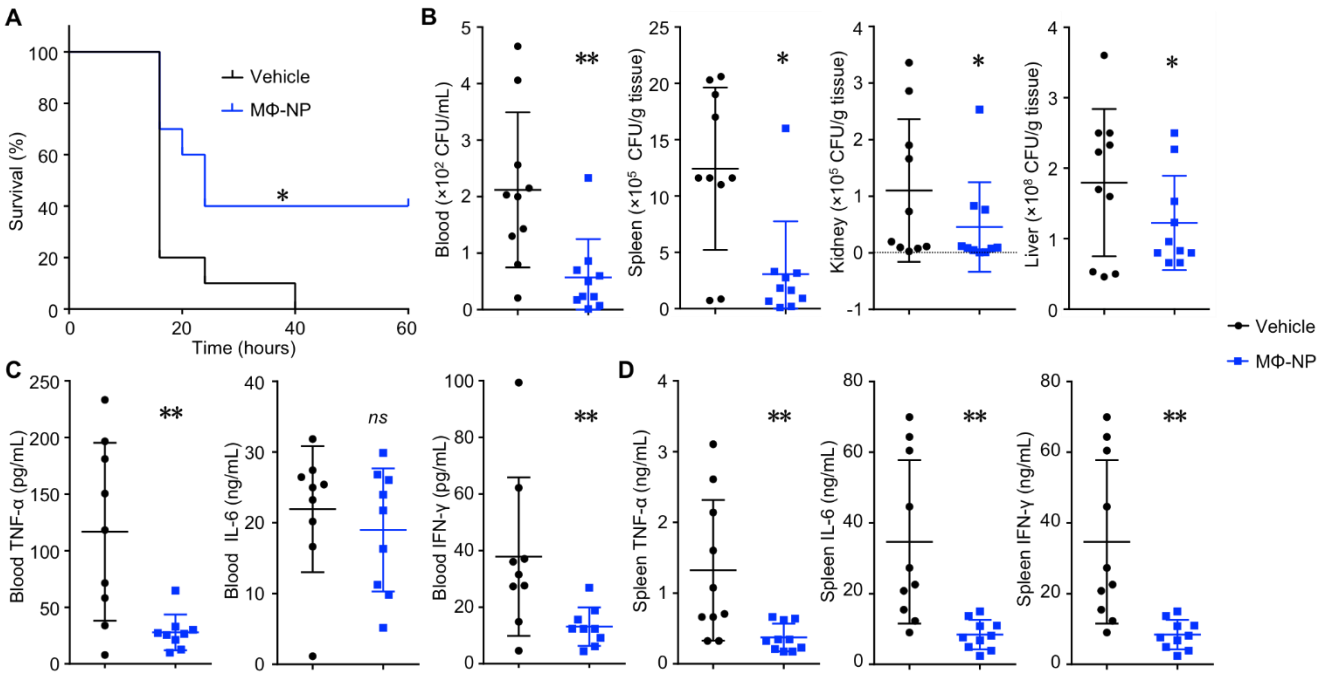

Figure 3.4. In vivo therapeutic efficacy of MΦ-NPs evaluated with a mouse bacteremia model. (A) Survival curve of mice with bacteremia after treatment with MΦ-NPs (n = 10). (B) Bacteria enumeration in blood, spleen, kidney, and liver at 4 h after MΦ-NPs were intraperitoneally injected. (C-D) Pro-inflammatory cytokines, including IL-6, TNF-α, and IFN-γ, from the blood and spleen were quantified with a cytometric bead array. (*ns* = not significant, **p* < 0.05, ***p* < 0.01)

Finally, the therapeutic potential of MΦ-NPs in vivo was examined in a mouse model of bacteria-induced systemic inflammation. Mice were challenged intraperitoneally with a lethal dose of *Escherichia coli* (1×10^7 CFU) and treated with either MΦ-NPs (300 mg/kg) or 10% sucrose solution as the control 30 min after bacterial challenge. In this lethal model, all animals in the control group treated with sucrose solution died, whereas four of ten animals treated with MΦ-NPs reached the experimental endpoint of 60 h, demonstrating a significant survival benefit ($p < 0.05$, **Figure 3.4A**). We then examined the bacterial colonization in key organs, including the blood, spleen, kidney, and liver, 4 h after bacterial injection. In the blood and spleen of the mice treated with MΦ-NPs, the bacterial counts were found to be significantly lower compared to those of the control group. Notably, the kidney and liver from the mice of both groups showed

comparable levels of bacterial counts (**Figure 3.4B**). Furthermore, the reduction of bacterial colonization in the blood and spleen conferred by MΦ-NPs corresponded with a significant reduction of pro-inflammatory cytokines, including IL-6, TNF-α, and IFN-γ, in these organs (**Figure 3.4C**).

In summary, we have demonstrated the therapeutic potential of MΦ-NPs for sepsis control through a two-step neutralization process: LPS neutralization in the first step followed by cytokine neutralization in the second step. MΦ-NPs function as an LPS and cytokine decoy, capable of inhibiting systemic inflammatory response and conferring a significant survival benefit during septic shock. The proposed MΦ-NPs represent an innovative and effective strategy for sepsis management. Unlike conventional endotoxin neutralization agents that compete with endotoxin binding pathways and thus cause toxicity, MΦ-NPs function as a toxin decoy to absorb endotoxins and divert them away from their cellular targets (i.e., macrophages), hence imposing minimum interference with the cells. Such a 'decoy strategy' also takes advantage of the common functionality of endotoxins binding to macrophages, thereby allowing for a 'universal' neutralization approach across different bacterial genus, species, and strains. The top-down fabrication of MΦ-NPs effectively replicates endotoxin-binding motifs on the target cells that are otherwise difficult to identify, purify, and conjugate. Coating macrophage membranes onto nanoparticle surfaces significantly increases the surface-to-volume ratio of given membrane materials, which is critical for efficient endotoxin neutralization. The concept of MΦ-NPs can be further expanded to develop other types of cell membrane-coated nanoparticles for a broader range of detoxification applications. Overall, MΦ-NPs as a new biomimetic detoxification strategy is promising and may ultimately improve the clinical outcome of sepsis patients, potentially shifting the current paradigm of clinical detoxification therapy.

MATERIALS AND METHODS

Macrophage membrane derivation.

The murine J774 cell line was purchased from the American Type Culture Collection (ATCC) and maintained in Dulbecco's Modified Eagle Medium (DMEM, Invitrogen) supplemented with 10% fetal bovine serum (FBS, Hyclone) and 1% penicillin-streptomycin (Invitrogen). Plasma membrane was collected according to a previously published centrifugation method(34). Specifically, cells were grown in T-175 culture flasks to full confluency and detached with 2 mM ethylenediaminetetraacetic acid (EDTA, USB Corporation) in phosphate buffered saline (PBS, Invitrogen). The cells were washed with PBS three times (500 × g for 10 min each) and the cell pellet was suspended in homogenization buffer containing 75 mM sucrose, 20 mM Tris-HCl (pH = 7.5, Mediatech), 2 mM $MgCl_2$ (Sigma Aldrich), 10 mM KCl (Sigma Aldrich), and 1 tablet of protease/phosphatase inhibitors (Pierce ThermoFisher). The suspension was loaded into a dounce homogenizer and the cells were disrupted with 20 passes. Then the suspension was spun down at 3,200 × g for 5 min to remove large debris. The supernatant was collected and centrifuged at 20,000 × g for 25 min, after which the pellet was discarded and the supernatant was centrifuged at 100,000 × g for 35 min. After the centrifugation, the supernatant was discarded and the plasma membrane was collected as an off-white pellet for subsequent experiments. Membrane protein content was quantified with a Pierce BCA assay (Life Technology).

MΦ-NP preparation and characterization.

MΦ-NPs were formulated in two steps. In the first step, approximately 80 nm polymeric cores were prepared using 0.67 dL/g carboxyl-terminated 50:50 poly(lactic-*co*-glycolic acid) (PLGA, LACTEL Absorbable Polymers) through a nanoprecipitation method. The PLGA polymer was first dissolved in acetone at a concentration of 10 mg/mL. Then 1 mL of the solution was added rapidly to 3 mL of water. For fluorescently labeled PLGA cores, 1,1'-dioctadecyl-3,3,3',3'-tetramethylindodicarbocyanine perchlorate (DiD, excitation/emission = 644 nm/665 nm, Life Technologies) was loaded into the polymeric cores at 0.1 wt%. The nanoparticle solution was then stirred in open air for 4 h to remove the organic solvent. In the second step, the collected

macrophage membranes were mixed with nanoparticle cores at a membrane protein-to-polymer weight ratio of 1:1. The mixture was sonicated with a Fisher Scientific FS30D bath sonicator at a frequency of 42 kHz and a power of 100 W for 2 min. Nanoparticles were measured for size and size distribution with dynamic light scattering (DLS, ZEN 3600 Zetasizer, Malvern). All measurements were done in triplicate at room temperature. Serum and PBS stabilities were examined by mixing 1 mg/mL of MΦ-NPs in water with 100% FBS and 2× PBS, respectively, at a 1:1 volume ratio. Membrane coating was confirmed with transmission electron microscopy (TEM). Briefly, 3 μL of nanoparticle suspension (1 mg/mL) was deposited onto a glow-discharged carbon-coated copper grid. Five minutes after the sample was deposited, the grid was rinsed with 10 drops of distilled water, followed by staining with a drop of 1 wt% uranyl acetate. The grid was subsequently dried and visualized using an FEI 200 kV Sphera microscope.

Membrane protein characterization.

MΦ-NPs were purified from free vesicles, membrane fragments, or unbound proteins by centrifugation at 16,000 × g. Macrophage cell lysates, membrane vesicles, and MΦ-NPs were mixed with lithium dodecyl sulfate (LDS) loading buffer to the same total protein concentration of 1 mg/mL as determined with a Pierce BCA assay (Life Technology). Electrophoresis was carried out with NuPAGE Novex 4-12% Bis-Tris 10-well minigels in MOPS running buffer with an XCell SureLock Electrophoresis System (Invitrogen). Western blot analysis was performed by using primary antibodies including rat anti-mouse CD14, rat anti-mouse CD126, rat anti-mouse CD130, rat anti-mouse CD284, armenian hamster anti-mouse CD120a, armenian hamster anti-mouse CD120b, and armenian hamster anti-mouse CD119 (Biolegend). Corresponding IgG-horseradish peroxidase (HRP) conjugates were used for the secondary staining. Films were developed with ECL western blotting substrate (Pierce) on a Mini-Medical/90 Developer (ImageWorks).

Lipopolysaccharides (LPS) and cytokines binding studies.

To study whether LPS binding with MΦ-NPs was dependent on LBP, CD14, or TLR4, the mixture of MΦ-NPs (1 mg/mL) and FITC-LPS (from *E. coli* O111:B4, Sigma, 125 ng/mL) in 1X PBS was added with FBS (10% as the source of LBP), anti-CD14 (Biolegend, 10 μg/mL), or anti-TLR4 (Invivogen, 10 μg/mL), respectively. The solution was incubated at 37°C for 30 min. Following the incubation, MΦ-NPs were spun down with ultracentrifugation (16,000 ×g). The fluorescence intensity from FITC-LPS remaining in the supernatant was measured. The fluorescence intensity from a FITC-LPS solution of 125 ng/mL served as 100%. The mixtures without adding FBS or antibodies were used as the controls. All experiments were performed in triplicate.

To quantify LPS removal with MΦ-NPs, MΦ-NPs (0.4 mg, 4 mg/mL) were mixed with LPS from *E. coli* K12 (Invivogen) with varying amount of 5, 10, 25, and 50 ng (50, 100, 250, and 500 ng/mL), respectively, in 1X PBS containing 10% FBS. In a parallel experiment, the removal was studied by fixing LPS amount at 50 ng (250 ng/mL) but varying the amount of MΦ-NPs at 0.1, 0.2, 0.3, and 0.4 mg (0.5, 1, 1.5, and 2 mg/mL), respectively. In both cases, the mixtures were incubated for 30 min and then spun down at 16,000 × g for 15 min to pellet the nanoparticles. The free LPS content in the supernatant was quantified by using LAL assay (Thermo Fisher Scientific) per manufacture's instruction. All experiments were performed in triplicate.

To determine MΦ-NP binding with cytokines, including IL-6, TNF-α, and IFN-γ, 100 μL of MΦ-NP samples (1 and 4 mg/mL) mixed with IL-6 (2000 pg/mL), TNF-α (370 pg/mL), or IFN-γ (880 pg/mL) in PBS containing 10% FBS were incubated at 37°C for 30 min. Following the incubation, the samples were centrifuged at 16,000 × g for 15 min to pellet the nanoparticles. Cytokine concentrations in the supernatant were quantified by using enzyme-linked immunosorbent assay (ELISA, Biolegend). All experiments were performed in triplicate.

LPS neutralization in vitro.

Murine toll-like receptor 4 (TLR4) reporter cells (HEK-Blue™ mTLR4 cells, Invivogen) were first used to determine LPS neutralization by MΦ-NPs. Cells were cultured in DMEM supplemented

with 10% FBS, 1% pen-strep, 100 μg/mL Normocin™, 2 mM L-glutamine, and 1× HEK-Blue™ selection (Invivogen). In the study, 2.5×10^4 cells were seeded in each well of a 96-well plate with 160 μL HEK-Blue™ detection medium, followed by adding 20 μL of 100 ng/mL LPS in PBS. Then 20 μL of nanoparticle solution of MΦ-NPs, RBC-NPs, or PEG-NPs (all at a concentration of 10 mg/mL), was added into each well. Control wells were added with 20 μL PBS. Cells without any treatment served as the background. The mixture was incubated for 12 h. Secreted embryonic alkaline phosphatase (SEAP) was quantified by measuring the absorbance at 630 nm with an Infinite M200 multiplate reader (Tecan). All experiments were performed in triplicate. Production of intracellular nitric oxide (iNO) was also used to evaluate LPS neutralization with MΦ-NPs. Briefly, 2×10^4 J774 cells were seeded in each well of a 96-well plate. The cells were incubated with 10 μM of 2', 7'-dichlorofluorescin-diacetate (DCFH-DA, Sigma) in culture medium for 1 h, and then washed 3 times with the culture medium. Then the wells were added with 180 μL of medium containing 10 ng/mL of LPS. Then 20 μL of nanoparticle solution of MΦ-NPs, RBC-NPs, or PEG-NPs (all at a concentration of 10 mg/mL), was added into each well. Control wells were added with 20 μL PBS. Cells without any treatment served as the background. The plate was incubated at 37°C for 5 h. The production of iNO was quantified by measuring the fluorescence intensity at 520 nm using an excitation wavelength of 485 nm (Infinite M200 multiplate reader, Tecan). All experiments were performed in triplicate.

LPS neutralization with MΦ-NPs was further evaluated by examining E-selectin expression on human umbilical vein endothelial cells (HUVECs). Specifically, HUVECs were cultured to confluence in a 96-well plate. Then 200 μL of LPS (250 ng/mL) mixed with MΦ-NPs, RBC-NPs, or PEG-NPs (4 mg/mL) in culture medium was added to the cells and the plate was incubated at 37°C. Cells added with LPS and PBS were used as controls. Three wells were used per sample. After 1, 2, 3, and 4 h of incubation at 37°C, medium was removed and cells were washed with PBS. Then the cells were fixed with 4% paraformaldehyde (Sigma) at room temperature for 15 min. Following the fixation, cells were washed twice with PBS and blocked

with 1% bovine serum albumin (BSA, Sigma). Subsequently, the reagent was decanted and 50 µL of primary antibody (mouse anti-human E-selectin, Biolegend, 1:10 dilution in 1% BSA) was added to each well and incubated at 37°C for 45 min. Wells were then rinsed three times with 1X PBS prior to the addition of 50 µl of secondary antibody (HRP-conjugated anti-mouse IgG, Biolegend, 1:10 dilution in 1% BSA) followed by an incubation for 45 min at 37°C. After this, wells were again rinsed three times with 1X PBS and after the final rinse, 100 µl of TMB (3,3',5,5'-tetramethylbenzidine) substrate solution was added to each well. The plate was incubated at 37°C followed by measuring the absorbance at 450 nm.

To visually examine E-selectin expression, cells following the same treatment as above experiment were incubated at 37°C for 4 h and rinsed twice with PBS, fixed with 4% paraformaldehyde for 15 min, permeabilized in 0.2% Triton X-100 (Sigma) in buffer for 10 min, and then incubated with 1% BSA in PBS for 30 min. Cells were then stained with mouse anti-human E-selectin for 1 h, washed 3 times with 1× PBS and then incubated with anti-mouse IgG Alexa 488-conjugates in 1% BSA in PBS for 1 h. Cell nuclei were stained with DAPI (1 mg/mL stock solution, Thermo Fisher Scientific). Fluorescence images were taken with an EVOS fluorescence microscope (Thermo Fisher Scientific).

Animal care and injections.

All animal studies were approved under the guidelines of the University of California San Diego (UCSD) Institutional Animal Care and Use Committee (IACUC). Mice were housed in an animal facility at UCSD under federal, state, local, and National Institutes of Health guidelines for animal care. In the study, no inflammation was observed at the sites of injection.

Pharmacokinetics and biodistribution studies.

The experiments were performed on 6-week old male ICR mice (Harlan Laboratories). To determine the circulation half-life, 150 µL of DiD-labeled MΦ-NPs (3 mg/mL) were injected intravenously through the tail vein. At 1, 15, 30 min, and 1, 2, 4, 8, 24, 48, 72 h post-injection, one drop of blood (~30 µL) was collected from each mouse via submandibular puncture with

heparin-coated tubes. Then 20 μL of blood was mixed with 180 μL PBS in a 96-well plate for fluorescence measurement. Pharmacokinetic parameters were calculated to fit a two-compartment model. For biodistribution study, 150 μL of DiD-labeled MΦ-NPs (3 mg/mL) were injected intravenously through the tail vein. At 24, 48, and 72 h post-injection, organs including the liver, kidneys, spleen, brain, lungs, heart, and blood were collected from six randomly selected mice. The collected organs were weighed and then homogenized in PBS for fluorescence measurement. All fluorescence measurements were carried out with an Infinite M200 multiplate reader (Tecan).

LPS neutralization in vivo.

The efficacy of MΦ-NPs in neutralizing LPS was first evaluated with a mouse endotoxemia model with 6-week old male BALB/c mice (Harlan). To evaluate the efficacy through cytokine production, mice were injected with 5 μg/kg LPS through the tail vein. After 15 min, MΦ-NPs, RBC-NPs, or PEG-NPs were injected at 200 mg/kg. Following the injections, blood samples (<30 μL) were collected at predetermined time points via submandibular puncture. Untreated mice and mice injected with LPS alone were used as controls. Cytokines, including IL-6 and TNF-α, in the plasma were quantified by ELISA as described above. In each group, 6 mice were used. To evaluate efficacy through survival, mice were first sensitized with D-galactosamine hydrochloride (Sigma Aldrich) via intraperitoneal injection at a dosage of 800 mg/kg. After 30 min of sensitization, LPS and nanoparticles were injected intravenously. Ten mice were used in each group.

LPS neutralization efficacy was also evaluated with a mouse bacteremia model. Specifically, 6-week old female C57BL/6 (Jackson labs) mice were injected intraperitoneally with 1×10^7 CFU of *Escherichia coli* UPEC CFT073 suspended in 100 μL of 1× PBS. After 30 min, mice were randomly placed into two groups (n = 10), and each mouse was injected with 500 μL of MΦ-NPs at a concentration of 10 mg/mL in 10% sucrose solution intraperitoneally. Mice were euthanized 4 h after the injection. Blood and organs were collected and homogenized with a Mini

Beadbeater-16 (BioSpec) in 1 mL of PBS. Proinflammatory cytokines in the blood, including IL-6, TNF-α, and IFN-γ, were quantified by a cytometric bead array per manufacturer's instruction (BD Biosciences). For bacterial enumeration, homogenized samples were serially diluted with PBS (from 10 to 107 folds) and plated onto agar plates. After 24 h of culture, bacterial colonies were counted. To evaluate efficacy through survival the same experimental procedure was carried out and survival monitored over a period of 60 hours (n = 10).

ACKNOWLEDGEMENTS

This work is supported by the National Science Foundation Grant DMR-1505699 (L.Z.), the Defense Threat Reduction Agency Joint Science and Technology Office for Chemical and Biological Defense under Grant Number HDTRA1-14-1-0064 (L.Z.), and NIH Grant RO1HL125352 (to V.N.) T.E. was supported through the UCSD NIH/NIGMS Training Program in Molecular and Cellular Pharmacology (T32GM007752).

Chapter 3, in full, is a reprint of the material as it appears in: Thamphiwatana KS*, Angsantikul P*, Escajadillo T*, Zhang Q, Olson J, Luk BT, Zhang S, Fang RH, Gao W, Nizet V, Zhang L. 2017. Macrophage-like nanoparticles concurrently absorbing endotoxins and proinflammatory cytokines for sepsis management. *PNAS*. 114:11488-11493. The dissertation author was one of the primary investigators and authors of this paper.

AUTHOR CONTRIBUTIONS

S.T., P.A., T.E., R.F., W.G., V.Z., and L.Z. conceived and designed the experiments; S.T., P.A., T.E., Q.Z., J.O., B.L., and S. Z. performed all the experiments. The manuscript was written by S.T., P.A., T.E., R.F., W.G., V.Z., and L.Z. All authors discussed the results and reviewed the manuscript.

REFERENCES

1. Angus DC, van der Poll T (2013) Severe sepsis and septic shock. *New Engl J Med* 369:840-851.

2. Cohen J (2002) The immunopathogenesis of sepsis. *Nature* 420:885-891.

3. Rittirsch D, Flierl MA, Ward PA (2008) Harmful molecular mechanisms in sepsis. *Nat Rev Immunol* 8:776-787.

4. Ranieri VM, Thompson BT, Barie PS, Dhainaur JF, Douglas IS, Finfer S, Gardlund B, Marshall JC, Rhodes A, Artigas A, Payen D, Tenhunen J (2012) Drotrecogin alfa (activated) in adults with septic shock. *New Engl J Med* 366:2055-2064.

5. Gaieski DF, Edwards JM, Kallan MJ, Carr BG (2013) Benchmarking the incidence and mortality of severe sepsis in the united states. *Crit Care Med* 41:1167-1174.

6. Yaroustovsky M, Plyushsc M, Popov D, Samsonova N, Abramyan M, Popok Z, Krotenko N (2013) Prognostic value of endotoxin activity assay in patients with severe sepsis after cardiac surgery. *J Inflammation* 10:article number e0129450.

7. Grandel U, Grimminger F (2003) Endothelial responses to bacterial toxins in sepsis. *Crit Rev Immunol* 23:267-299.

8. Peters K, Unger RE, Brunner J, Kirkpatrick CJ (2003) Molecular basis of endothelial dysfunction in sepsis. *Cardiovasc Res* 60:49-57.

9. Wang Y (2014) Attenuation of berberine on lipopolysaccharide-induced inflammatory and apoptosis responses in beta-cells via tlr4-independent JNK/NF-κB path. *Pharm Biol* 52:532-538.

10. Nishio K, Horie M, Akazawa Y, Shichiri M, Iwahashi H, Hagihara Y, Yoshida Y, Niki E, (2013) Attenuation of lipopolysaccharide (LPS)-induced cytotoxicity by tocopherols and tocotrienols. *Redox Biology* 1:97-103.

11. Brandenburg K, Wiese A (2004) Endotoxins: Relationships between structure, function, and activity. *Curr Top Med Chem* 4:1127-1146.

12. Gabrielli L, Capitoli A, Bini D, Taraballi F, Lupo C, Russo L, Cipolla L (2012) Recent approaches to novel antibacterials designed after LPS structure and biochemistry. *Curr Drug Targets* 13:1458-1471.

13. Kelesidis T, Falagas ME (2015) The safety of polymyxin antibiotics. *Expert Opin Drug Saf* 14:1687-1701.

14. Justo JA, Bosso JA (2015) Adverse reactions associated with systemic polymyxin therapy. *Pharmacotherapy* 35:28-33.

15. Cavaillon JM (2011) Polymyxin B for endotoxin removal in sepsis. *Lancet Infect Dis* 11:426-427.

16. Fujii T, Ganeko R, Kataoka Y, Featherstone R, Bagshaw SM, Furukawa TA (2016) Polymyxin B-immobilised haemoperfusion and mortality in critically ill patients with sepsis/septic shock: A protocol for a systematic review and meta-analysis. *Bmj Open* 6:article number e012908.

17. Raghavan R (2012) When access to chronic dialysis is limited: One center's approach to emergent hemodialysis. *Semin Dial* 25:267-271.

18. Zhang LF, Leroux JC (2015) Current and forthcoming approaches for systemic detoxification preface. *Adv Drug Del Rev* 90:1-2.

19. Hu CMJ, Fang RH, Wang KC, Luk BT, Thamphiwatana S, Dehaini D, Nguyen P, Angsantikul P, Wen CH, Kroll AV, Carpenter C, Ramesh M, Qu V, Patel SH, Zhu J, Shi W, Hofman FM, Chen TC, Gao W, Zhang K, Chien S, Zhang L (2015) Nanoparticle biointerfacing by platelet membrane cloaking. *Nature* 526:118-121.

20. Hu CMJ, Fang RH, Copp J, Luk BT, Zhang LF (2013) A biomimetic nanosponge that absorbs pore-forming toxins. *Nat Nanotechnol* 8:336-340.

21. Copp JA, Fang RH, Luk BT, Hu CM, Gao W, Zhang K, Zhang L (2014) Clearance of pathological antibodies using biomimetic nanoparticles. *Proc Natl Acad Sci U S A* 111:13481-13486.

22. Pang ZQ, Hu CM, Fang RH, Luk BT, Gao W, Wang F, Chuluun E, Angsantikul P, Thamphiwatana S, Lu W, Jiang X, Zhang L (2015) Detoxification of organophosphate poisoning using nanoparticle bioscavengers. *ACS Nano* 9:6450-6458.

23. Akira S, Takeda K, Kaisho T (2001) Toll-like receptors: Critical proteins linking innate and acquired immunity. *Nat Immunol* 2:675-680.

24. Medzhitov R (2001) Toll-like receptors and innate immunity. *Nat Rev Immunol* 1:135-145.

25. Schutt C (1999) Fighting infection: The role of lipopolysaccharide binding proteins cd14 and lbp. *Pathobiology* 67:227-229.

26. Triantafilou M, Triantafilou K (2002) Lipopolysaccharide recognition: Cd14, tlrs and the LPS-activation cluster. *Trends Immunol* 23:301-304.

27. Zanoni I, Ostuni R, Marek LR, Barresi S, Barbalat R, Barton GM, Granucci F, Kagan JC (2011) Cd14 controls the LPS-induced endocytosis of toll-like receptor 4. *Cell* 147:868-880.

28. Schilling JD, Machkovech HM, He L, Diwan A, Schaffer JE (2013) TLR-4 activation under lipotoxic conditions leads to synergistic macrophage cell death through a trif-dependent pathway. *J Immunol* 190:1285-1296.

29. Hagar JA, Powell DA, Aachoui Y, Ernst RK, Miao EA (2013) Cytoplasmic LPS activates caspase-11: Implications in tlr4-independent endotoxic shock. *Science* 341:1250-1253.

30. Martinon F, Chen X, Lee A-H, Glimcher LH (2010) TLR activation of the transcription factor XBP1 regulates innate immune responses in macrophages. *Nat Immunol* 11:411-418.

31. Spence S*,* Greene MK, Fay F, Hams E, Saunders SP, Hamid U, Fitzgerals M, Beck J, Bains BK, Smyth P, Themistou E, Small DM, Schmid D, O'Kane CM, Fitzgerals DC, Abdelghany SM, Johnston JA, Fallon PG, Burrows JF, McAuley DF, Kissenpfennig A, Scott CJ (2015)Targeting siglecs with a sialic acid-decorated nanoparticle abrogates inflammation. *Sci Transl Med* 7:article number 303ra140.

32. Unger RE, Peters K, Sartoris A, Freese C, Kirkpatrick CJ (2014) Human endothelial cell-based assay for endotoxin as sensitive as the conventional limulus amebocyte lysate assay. *Biomaterials* 35:3180-3187.

33. Roger T*,* Froidevaux C, Le Roy D, Reymond MK, Chanson AL, Mauri D, Burns K, Reiderer BM, Akira S, Calandra T (2009) Protection from lethal gram-negative bacterial sepsis by targeting toll-like receptor 4. *Proc Natl Acad Sci U S A* 106:2348-2352.

34. Fang RH*,* Hu CM, Luk BT, Gao W, Copp JA, Tai Y, O'Conner DE, Zhang L (2014) Cancer cell membrane-coated nanoparticles for anticancer vaccination and drug delivery. *Nano Lett* 14:2181-2188.

CHAPTER 4

Novel role for Sterol Regulatory Element Binding Protein-2 (SREBP-2) in the regulation of host cell susceptibility to the streptococcal toxin streptolysin-O

Tamara Escajadillo[1,2*], Lauren Popov [3*], Samira Dahesh[2], Jan E. Carette[3], Victor Nizet[1,2]

Biomedical Sciences Graduate Program[1], Department of Pediatrics, Division of Host-Microbe Systems and Therapeutics[2], UC San Diego, La Jolla, CA 92093. Department of Microbiology and Immunology, Stanford University School of Medicine, Stanford, CA 94305[3].

*These authors contributed equally

Keywords: *Streptococcus pyogenes*, group A *Streptococcus*, streptolysin O, pore-forming toxin, Haploid genetic screen, CRISPR-Cas9, sterol regulatory element binding protein-2, cholesterol, membrane, antivirulence therapy

PREFACE TO CHAPTER 4

Chapter 4 in a manuscript being prepared for submission. This works helps address Aims 3A-3D: Validate top novel “hits” by CRISPR KO in Hap1 cells and determine if the host cell protection is specific for the PFT SLO or is generalizable for other PFTs, analyze membrane dynamics, cholesterol homeostasis and cell death pathways associated with the SLO resistance phenotype in the SREBP2 knockout, determine if host cell protection conferred by SREBP2 inhibition is applicable to a macrophage cell line and the effect on inflammatory pathways, and screen for potential pharmacological inhibitors of SREBP2 that will mirror the phenotype observed in the genetic knockout.

Our work helps expand on the knowledge of host factors involved in mediating SLO toxicity and helps demonstrate the potential of using gene-trap mutagenesis and CRISPR-Cas9 deletions for the study of bacterial related disease pathogenesis.

ABSTRACT

Despite the timely use of antibiotics, Group A *Streptococcus* (GAS) continues to be one of the leading human bacterial pathogens responsible for considerable morbidity and mortality worldwide. The expression of the pore forming toxin streptolysin O (SLO) by virtually all GAS clinical isolates is associated with increased disease severity. In addition to the deceptive simplicity of pore formation, sub lethal doses have been shown to trigger inflammatory pathways and induce phagocytic cell dysfunction. To further our understanding of the downstream effects of SLO on host cells, we conducted a high-throughput genetic screen using mutagenized haploid human cells to discover novel host factors required for SLO cytotoxicity. Our screen identified a critical component of the cholesterol metabolic pathway, sterol regulatory element binging protein-2 (SREBP2) as the most significantly enriched gene, in addition to other genes in lipid regulatory pathways. In the present work, we describe a novel role for SREBP2 in modulating host cell susceptibility to SLO by decreasing the ability of the toxin to interact with the host plasma membrane. SREBP-2 knockout cells demonstrated decreased cholesterol and lipid raft availability in the membrane with concomitant reduction in SLO binding. Pharmacological inhibition of SREBP2 using betulinic acid mirrored the phenotype observed in the genetic knockout, suggesting the potential for pursuing SREBP2 as a candidate for anti-virulence-based GAS therapy.

INTRODUCTION

Streptococcus pyogenes, or group A *Streptococcus* (GAS), is a human-specific bacterial pathogen that colonizes nearly 20% of the population and remains a leading public health concern. GAS produces approximately 700 million human infections annually, ranging from mild pharyngitis and skin infections, to severe invasive diseases including sepsis and necrotizing fasciitis that exert high morbidity and mortality even with prompt administration of antibiotics (1). Invasive forms of GAS infection have increased in recent decades due in large part to the global dissemination of a hyperinvasive M1T1 GAS clone (2-4). The severity of GAS M1T1 clinical manifestations may be further potentiated by acquisition of functionally inactivating mutations the CovRS two-component regulatory system (5-9), leading to significant upregulations in several GAS virulence factors including the hyaluronic acid capsule and the potent pore-forming cytolytic toxin, streptolysin O (SLO) (10-12).

SLO is a member of the large family classically of so-called cholesterol-dependent cytolysins (CDCs), due to their ability to target cholesterol rich membranes through a cholesterol recognition/binding motif (CRM) on the tip of domain 4 and form large 30nm sized pores (13-15). Disruption of plasma membrane integrity by SLO induces multiple cell death pathways in keratinocytes and innate immune cells (16-19), prevents phagolysosome acidification to promote GAS intracellular survival (20), and impairs critical neutrophil cell functions such as oxidative burst, degranulations and extracellular trap (NET) formaiton (21). Inactivation of SLO by genetic manipulation (17, 22, 20, 23, 24), active or passive immunization (21), and bioengineered nanoparticle absorption (25, 26) attenuate GAS disease severity in invasive murine infection models. Indeed, such virulence factor-targeted strategies have become increasingly promising as adjunctive therapies to antibiotic treatment to reduce disease severity in systemic infection (27-30).

As an alternative to directly targeting a critical bacterial toxin virulence by blocking its production or binding/inactivating the molecule itself, one can also contemplate identifying mechanisms that target the host cell, in order to increase its resistance to toxin action, i.e. host cell “resilience”. In this regard, forward genetic screens have proven to be valuable tools for the unbiased approach to understanding diverse biological processes involved in host-pathogen interactions (31, 32). Recent advances in loss-of-function genetic techniques, including insertional mutagenesis in human haploid cells (HAP1), have uncovered genes that control susceptibility to pharmacological interventions (31, 33-37), and have recently revealed a role for an adherens junction protein, plekstrin-homology domain containing protein 7 (PLEKHA7), in mediating cytotoxicity of a bacterial pore-forming toxin -- α-toxin of *Staphylococcus aureus* (38).

In the present work, we use an unbiased high-throughput genetic screen in HAP1 cells to identify genes involved in SLO cytotoxicity. In this screen, the strongest hit identified is a key regulator of the cholesterol metabolic pathway, sterol regulatory element binding protein-2 (SREBP-2). CRISPR-Cas9 gene edited knockout of SREBP-2 increased cell survival after SLO intoxication and live GAS infection, in association deficient SLO host membrane-binding and altered membrane composition. This phenotype could be recapitulated by pharmacological inhibition of SREBP-2 using the natural product betulinic acid (BA), suggesting this pathway of cholesterol regulation as a target for reducing disease severity during invasive GAS infection.

RESULTS

Human Haploid Genetic Screen to Identify Host Factors Necessary for SLO Toxicity.

To increase our understanding of how the SLO toxin impacts host cell biology, we employed a live/dead genetic screen technique (38). Haploid human cells (HAP1) were treated with gene-trap retroviruses containing a strong adenoviral acceptor site and a marker gene

(green fluorescent protein, GFP), placed in reverse orientation of the retroviral backbone, to create knockout alleles in essentially all genes (35, 36).

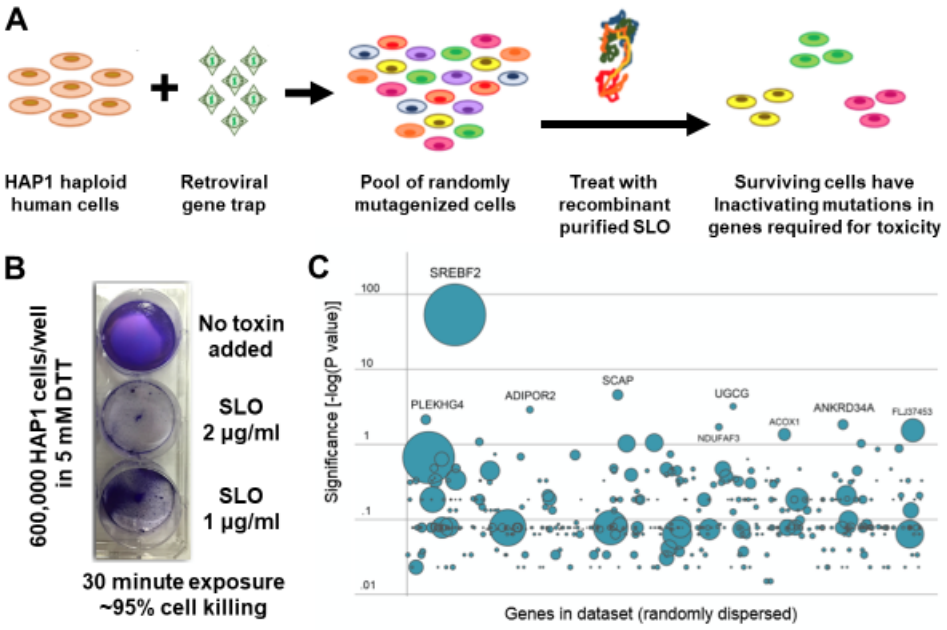

Figure 4.1. Haploid insertional mutagenesis screen and generation of CRISPR-Cas9 ΔSREBP2 sub-clones. (A) Schematic representation of retroviral gene trap insertion into haploid human cells creating a pool of randomly mutagenized cells, intoxicated with purified recombinant SLO and surviving cells having inactivating insertions in genes required for cytotoxicity. **(B)** Haploid cells (HAP1) were treated with 2 µg/ml and 1 µg/ml SLO in the presence of 5mM DTT for 30 min to determine host cell susceptibility, and colonies were grown up from single surviving cells post-intoxication. **(C)** Bubble plot where each bubble represents a gene, and bubble size corresponds to the number of independent gene-trap insertion events in the SLO-selected population. Y axis corresponds to the enrichment significance of each insertion compared to the non-selected control population.

The pool of randomly mutagenized cells was then intoxicated with purified recombinant SLO, with surviving cells determined to be toxin-resistant (**Figure 4.1A-B**). The gene trap insertion sites in the SLO-selected population were then compared to a control library not exposed to the toxin, allowing us to identify 15 genes that were significantly enriched ($P<0.05$) in the SLO-treated population (**Figure 4.1C, Supplementary Table 4.1**).

The haploid mutant viability screen uncovered several genes involved in host cell cholesterol homeostasis, but which have never previously been identified in the context of SLO toxicity. The single most enriched gene in the dataset was SREBP-2 ($P=2.55 \times 10^{-53}$) followed

by the SREBP cleavage-activating protein, SCAP ($P=2.65x10^{-5}$) (**Figure 4.1C, Supplementary Table 4.1**). Unlike SREBP-1 isoforms -1a and -1c, which are primarily involved in the regulation of fatty acid metabolism, SREBP-2 preferentially regulates cholesterol metabolism. SCAP is both a sterol sensor an escort protein for SREBP-2 from the endoplasmic reticulum to the Golgi apparatus, whereupon proteolytic cleavage allows SREBP-2 to stimulate sterol biosynthesis (39, 40).

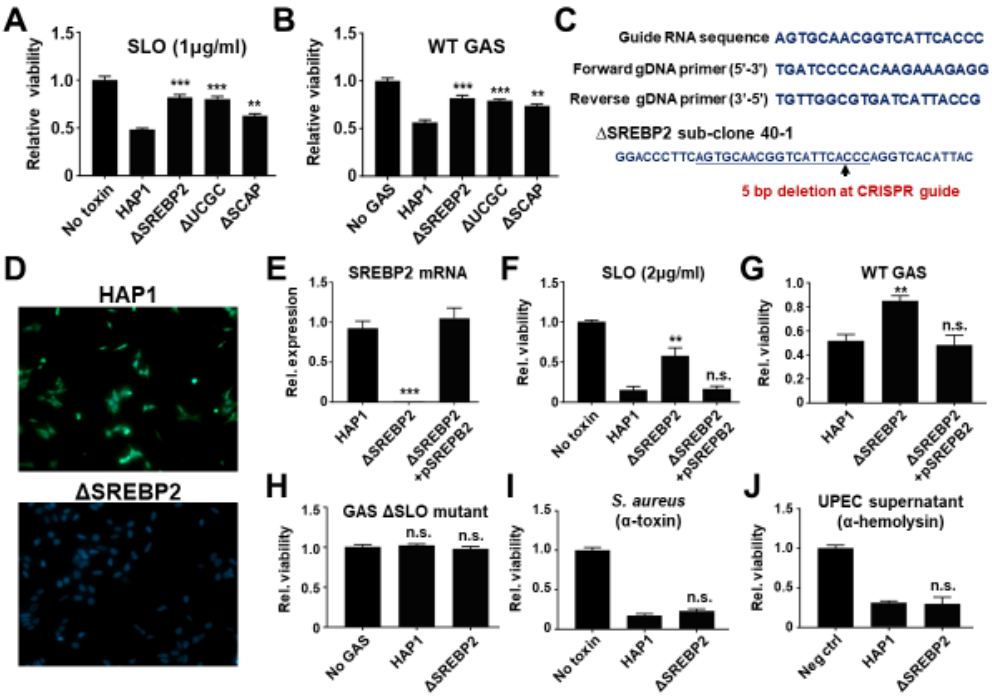

Figure 4.2. Validation of effect of SREBP2 knockout on cellular susceptibility to GAS and bacterial toxins. WT, ΔSREBP2, ΔUGCG, and ΔSCAP cells were **(A)** intoxicated with 1 µg/mL purified recombinant SLO in the presence of 10mM DTT for 15 min or **(B)** infected with WT M1 GAS at MOI = 5 for 2 h, followed by removal of media and incubation with Cell-Titer Glo intracellular ATP determining reagent. Results are from experiments performed in triplicate and reported as mean +/- SEM from at least 3 experiments. **(C)** CRISPR-Cas9 target guide sites in a HAP ΔSREBP2 sub-clones sequenced and compared with WT sequence, with guide target sequences indicated in bold and underlined text. **(D)** Immunofluorescent microscopy analysis of SREBP2 in WT and ΔSREBP2 cells using an antibody against SREBP2 (green) and DAPI (blue) for nuclear visualization. **(E)** SREBP2 mRNA expression was assessed using q-PCR for WT, ΔSREBP2 and SREBP2 +SREBP2-FLAG cells and compared to GAPDH housekeeping gene. WT, ΔSREBP2 and SREBP2 +SREBP2-FLAG cells were **(F)** intoxicated with 2 µg/mL purified recombinant SLO in the presence of 10mM DTT for 15 min, infected with **(G)** WT M1 GAS M1 or **(H)** an isogenic ΔSLO mutant at MOI = 5 for 2 h, **(I)** intoxicated with *Staphylococcus aureus* α-toxin for 1 h, or **(J)** co-incubated with uropathogenic *E. coli* cell-free supernatant for 2 h. In each case, treatment was followed by removal of media and incubation with Cell-Titer Glo intracellular ATP-determining reagent to enumerae viable cells compared to uninfected controls. Results are from experiments performed in triplicate and reported as mean +/- SEM from at least 3 experiments.

Other screen hits were known to be involved in other aspects of lipid biogenesis or metabolism, such as UDP-glucose ceramide glycosyltransferase (UGCG), which generates glucosylceramide, the precursor for all glycosphingolipids (41), and ADIPOR2, a cellular receptor for adiponectin, which promotes ceramide degradation and modulates cellular glucose and lipid pathways (42).

Bacterial pore-forming toxins such as *S. aureus* α-toxin and aerolysin of *Aeromonas hydrophila* provoke inflammasome assembly, thereby rendering caspase-1 proteolytically active, which in turn can process SREBPs to their active form (43). SREBPs have been hypothesized to facilitate membrane repair and promote cell viability (43); indeed, loss of SREBP-1 in macrophages was linked to increased apoptosis in response to challenge with purified α-toxin (44-46). Given that loss of SREBP-2 was the single most enriched mutation in our unbiased haploid cell screen selecting for SLO resistance, rather than SLO sensitivity, we proceeded to further characterize this curious finding.

CRISPR/Cas9-Engineered SREBP2 Knockout Reduces Susceptibility to SLO Toxicity.

CRISPR/Cas9 gene editing was used to independently generate HAP1 knockout sub-clone cell lines for SREBP-2 and two additional gene candidates (SCAP, UCCG) identified in the original screen. Compared to unmodified HAP1 parent cells, CRISPR/Cas9 targeting of each of the three genes yielded HAP1 sub-clones with significantly increased viability after exposure to purified SLO (**Figure 4.2A**) or to live wild-type (WT) GAS expressing the toxin (**Figure 4.2B**). The sequenced SREBP2 knockout sub-clone (ΔSREBP2) was identified to contain a 5-base pair deletion at the CRISPR guide site (**Figure 4.2C**). Inactivating deletion in the ΔSREBP2 sub-clone was further validated at the protein level by loss of immunofluorescent detection of SREBP2 (**Figure 4.2D**). Knockout of SREBP-2 eliminated SREBP2 RNA expression, which could be restored by stably transforming the cells with a human SREBP2-FLAG expression construct *in trans* (ΔSREBP2 +SREBP2-FLAG) (**Figure 4.2E**); SREBP1 gene

expression was not affected (**Supplementary Figure S 4.1A**) The increased resistance of ΔSREBP2 cells to both purified recombinant SLO and live WT GAS was reversed when the gene defect was corrected by plasmid expression of SREBP (**Figure 4.2 F,G**).

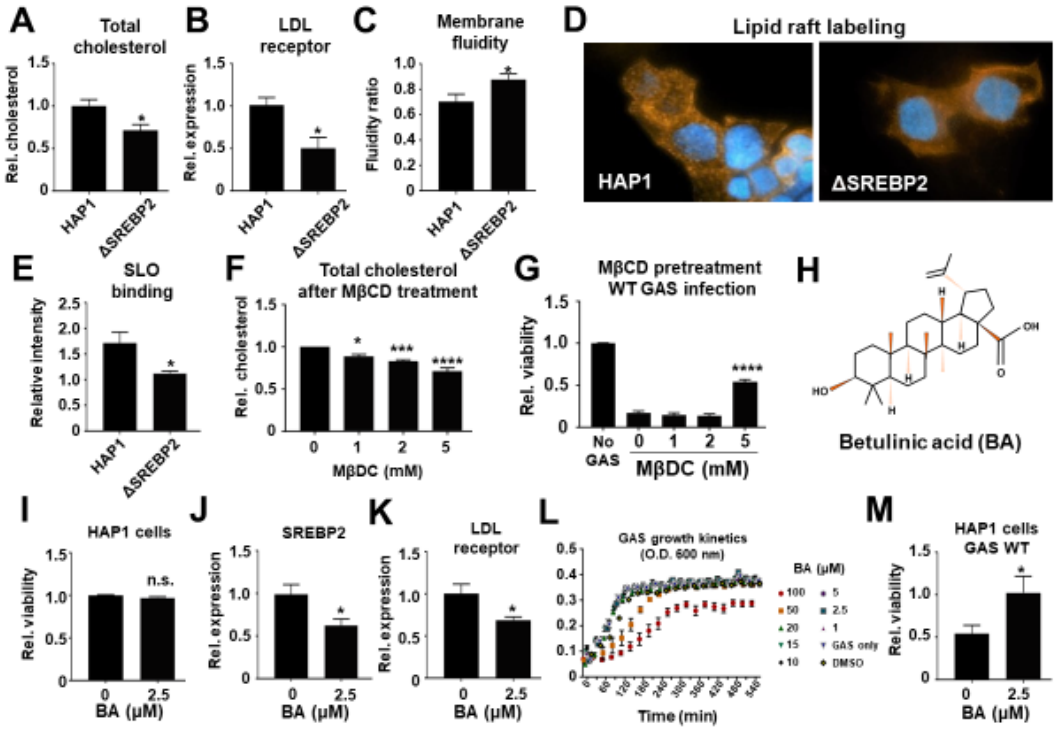

Figure 4.3. Characterization of cellular effects of SREBP2 knockout and betulinic acid treatment. **(A)** Presence of total cholesterol/cholesteryl esters assessed by absorbance at 570nm wavelength and graphed as relative to WT Haploid cells. **(B)** LDLR mRNA expression was assessed using q-PCR for WT and ΔSREBP2 and compared to GAPDH housekeeping gene. **(C)** Membrane fluidity determined as ratio of excimer to monomer fluorescence present in WT ΔSREBP2 cells. **(D)** Incorporation of fluorescent CT-B conjugate (orange) into membrane shown as well-defined clusters (WT) or uniformly distributed dye (ΔSREBP2) along with DAPI nuclear stain (blue). **(E)** Cell surface incorporation of SLO on WT, and ΔSREBP2 HAP1 cells as measured by flow cytometric analysis of fluorescently stained SLO. **(F)** Presence of total cholesterol/cholesteryl esters after MβCD pre-treatment for 15 min of WT Haploid cells and read by absorbance at 570nm wavelength. **(G)** Relative survival of 15 min MβCD pre-treated WT Haploid cells after infection with WT GAS M1 5448 at MOI = 5 for 2 h. Results are from experiments performed in triplicate and reported as mean +/- SEM from at least 3 experiments. **(H)** Molecular structure of pentacyclic triterpenoid betulinic acid. **(I)** Effect on viability of WT HAP1 after 20 h of 2.5μM BA or DMSO pre-treatment measured by luminescence. mRNA expression of **(J)** SREBP2 and **(K)** LDLR after 20-hour pre-treatment of WT HAP1 with 2.5μM BA or DMSO control, normalized to GAPDH. **(L)** Effect of BA at concentration ranges of 1-100μM on growth of WT GAS M1 5448 in RPMI + 20%FBS. **(M)** Relative survival of WT HAP1 treated with DMSO or BA for 20 h followed by infection with WT GAS M1 5448 at MOI of 10 for 2 h. Results are from experiments performed in triplicate and reported as mean +/- SEM from at least 3 experiments.

The specificity of the observed SREBP-2 effect to the particular pore-forming CDC SLO was tested in a number of ways. First, no significant change was observed in SLO toxicity to

HAP1 cells upon deletion of ADAM10, a surface receptor important for the pore-forming activity *S. aureus* α-toxin, but which is not known to be involved in the SLO mechanisms of action (**Supplementary Figure S 4.1B**). Susceptibility of ΔSREBP2 cells to injury when infected with a mutant strain of GAS lacking SLO did not differ from the parent HAP1 cells (**Figure 4.2H**). Finally, deletion of SREBP-2 did not confer resistance to recombinant *S. aureus* α-toxin (**Figure 4.2I**) nor cell free supernatants of an *Escherichia coli* strain expressing the pore-forming HlyA hemolysin (**Figure 4.2J**).

Membrane Alterations Associated with SREBP2 Inhibition.

The interaction of CDCs with the membrane surface of host cells is dependent on the structure of the sterols and the lipid environment. CDCs will preferentially bind to membranes with an optimal lipid environment surrounding cholesterol and require that the cholesterol contain an intact 3-hydroxyl with no significant alterations to the ring structure (13, 47-50). We found that ΔSREBP2 cells exhibited an approximately 35% reduction in the total amount of available cholesterol as quantified to include both free cholesterol and cholesteryl esters (**Figure 4.3A**). ΔSREBP2 cells also showed a significant reduction in the expression of the low-density lipoprotein receptor (LDLR), a key regulator of cholesterol uptake in cells, and a classical SREBP-2 target gene (40, 51, 52) (**Figure 4.3B**). These changes were accompanied by an increase in membrane fluidity (**Figure 4.3C**), a term used to describe local membrane dynamics that are heavily influenced by the presence of cholesterol, where the presence of cholesterol on the surface of the bilayer decreases the fluidity of the membrane due to organization of liquid-ordered (l_o) phases (53, 54).

Detergent-insoluble membrane domains, termed lipid rafts, are generally defined as sphingolipid and sterol-rich domains that exist in the l_o state, with the presence of cholesterol a determinant for their formation (55-59). Our studies revealed a reduction in the number of lipid rafts in ΔSREBP2 cells, as determined by the presence of distinctly immuno-stained puncta

versus undefined dispersed staining (**Figure 4.3D**). We next analyzed the binding of SLO to the membrane of the ΔSREBP2 cells using flow cytometry and observed a slight, yet significant, reduction in SLO surface binding when compared to the WT (**Figure 4.3E**). Pre-treatment with 5mM methyl-β-cyclodextrin (MBCD), the most widely used method for acute cholesterol depletion (60) achieved a similar reduction in cholesterol (~30%) to that seen in ΔSREBP2 cells (**Figure 4.3F**), without apparent cytotoxicity (**Supplementary Figure S 4.1C**). MBCD pre-treatment at 5mM also yielded in a similar fold increase in cell viability upon live GAS infection as earlier seen with loss of SREBP-2 (**Figure 4.3G**), suggesting that cholesterol depleting membrane alterations secondary to SREBP-2 knockdown are significant factors associated with decreased HAP1 cell susceptibility to SLO toxicity.

Pharmacological Inhibition of SREBP2 Reduces SLO Toxicity.

Betulinic acid (BA) is a naturally occurring pentacyclic triterpenoid found abundantly in the plant kingdom that has been studied for its wide range of pharmacological effects on cancer, malaria, viruses and inflammation (61, 62) (**Figure 4.3H**). BA inhibits expression of genes involved in cholesterol efflux, including ABCA1, after treatment of cells for 24 h (63). Its precursor, betulin, inhibits SREBP2 processing, and reduces levels of genes involved in cholesterol biosynthesis, including SREBP2, by approximately 30%, consistent with the known ability the transcription factor to regulate its own gene expression (64). Higher concentrations of BA (20 and 10 μM) impacted cell viability of HAP1 cells, but no significant toxicity was observed at lower concentrations (5 and 2.5 μM) (**Supplementary Figure S 4.1D, Figure 4.3I**). We observed an inhibitory effect of 2.5μM BA on SREBP2 expression, with a 20 h pre-treatment yielding an approximate 40% reduction in expression of SREBP2 and its target gene LDLR (**Figure 4.3 J, K**). BA did not inhibit growth of GAS bacteria, even at concentrations that displayed toxicity to mammalian cells (**Figure 4.3L**). Guided by these parameters, we observed a significant increase in cell viability in HAP1 cells pretreated with 2.5μM BA then subsequently

challenged with WT GAS expressing the SLO toxin (**Figure 4.3M**). These results suggest the potential for reducing SLO induced host cell damage by pharmacological targeting of SREBP2.

DISCUSSION

Severe cases of invasive GAS disease have increased dramatically over the past few decades, with cutaneous/soft tissue infections and necrotizing fasciitis representing a significant proportion of these dangerous clinical syndromes. Despite the availability of antibiotics, surgical intervention through drainage, debridement or amputation is often necessary not only to control the spread of the infection but to save the life of the patient (1, 65, 66). Adjunctive therapies to target key GAS virulence factors driving the pathological process provide a promising avenue to improve patient outcomes. Indeed, anti-virulence and vaccination strategies designed to bind or sequester the SLO toxin attenuate GAS disease severity in murine models of infection (17, 21, 25). Here we posited that by better understanding of host factors necessary for SLO toxicity, we could exploit this knowledge to make host cells more resilient to GAS induced damage or functional impairment.

Cellular cholesterol has been studied in the context of SLO since the toxin and other members of the CDC family share a strong dependence on the presence of membrane cholesterol to exert their pore-forming effects (14, 67, 68). Cholesterol plays a significant role in maintaining plasma membrane integrity, for which precise homeostatic control of the cholesterol biosynthetic process is necessary, a process controlled in large part by a feedback system regulated by SREBP2 (40, 69, 70). As a key component of cell structural integrity, wholescale cholesterol depletion would be incompatible with survival, and the partial decrease in cellular cholesterol observed in ∆SREBP2 cells indicates that additional regulatory pathways exist as a failsafe to maintain a threshold cholesterol level essential for cell viability.

Previous work revealed that upon significant cholesterol depletion, SLO membrane binding remains relatively unaffected, whereas formation of the pre-pore complex is effectively

interrupted, so that membrane damage is averted (71). Additional recent studies identified the presence of glycan-binding sites within domain 4 of SLO and showed that administration of the purified glycan lacto-N-neotetraose (LNnT) robustly inhibited SLO lysis of red blood cells (72). In the context of our studies, reduced cellular toxicity (**Figure 4.2F-G**) and SLO membrane binding (**Figure 4.3E**) could be secondary to the observed alterations in membrane lipid raft formation in ΔSREBP2 cells (**Figure 4.3D**). Lipid raft domains are implicated in numerous biological functions, and cholesterol can influence domain association and biological activity of other factors that co-isolate with these detergent-resistant membranes (58, 59, 73, 74). Modifications in host cell membranes due to SREBP2 knockout-induced depletion of cholesterol could influence protein and carbohydrate presentation within the lipid raft domains, precluding key interactions of SLO with any potential receptor that facilitates membrane binding and pore formation. Future structural biochemistry studies using mutated or truncated versions of SLO that are still capable of binding to the membrane, but do not induce toxicity (75), may be instructive in this regard.

Plant natural products have served as a basis for medicinal systems since early recorded history and continue to play a key role in pharmaceutical development (76, 77). Many naturally occurring bioactive pentacyclic triterpenoids, including BA, possess medically significant pharmacological activity, ranging from anti-cancer (78, 79) to anti-bacterial (77) to cholesterol lowering (63, 64).

A BA-induced reduction in SREBP2 expression was sufficient to increase host cell survival upon SLO intoxication (**Figure 4.4F**). While there are reported concentration-dependent alterations of erythrocyte membrane shape with BA and its analogues (80), the concentrations required were significantly higher than we employed. While other plant-derived compounds may directly inhibit microbial toxin-mediated cell damage (81), this has generally been tested by co-incubation with the toxin; in contrast our approach removed BA prior to SLO toxin or GAS

infection challenge and employed concentrations with no direct effect on bacterial growth (**Figure 4.4E**). Other reported SREBP2 inhibitors, including miR-33 (82), could potentially reproduce or augment this effect. It is important to note that total knockout of SREBP2 in mice results in an embryonic lethal phenotype, with additional aberrations in limb bud development and cellular autophagy (83-85). thus, its pharmacological targeting requires careful analysis. Nevertheless, BA is under active investigation as a selective anti-cancer agent, with documented activity against multiple tumor cell lines, even at doses of 10μM (86, 87). Phase I clinical trials on the safety and tolerability of topical BA on cutaneous melanoma are ongoing including a 20% BA ointment formulation (ClinicalTrials.gov #NCT00346502), a dosing exposure above that effective here in augmenting SLO toxin resistance.

Through these studies we demonstrated the effectiveness of a haploid human cell based insertional mutagenesis screen, coupled with CRISPR-Cas9 targeted gene deletion, to identify novel host factors associated with SLO toxicity. We expanded knowledge of a mechanism wherein toxicity is reduced by SREBP2 deletion to modulate host cell cholesterol and show further that this regulatory factor can also be pharmacologically inhibited by the investigational agent BA. Since many infectious diseases, including human immunodeficiency virus-1 (HIV-1) and *Mycobacterium tuberculosis* rely on lipids and lipid membrane structures to gain access to host tissues, lipid targeted therapy is being increasingly explored to neutralize the pathologic processes (56). The present study provides proof-of-principle of such a target pathway for adjunctive therapy of severe toxin-driven GAS infection where host cell protection is crucial for resolution of disease.

METHODS

Bacterial strains and chemical reagents.

GAS M1T1 serotype M1T1 5448 was isolated from a patient with necrotizing fasciitis and toxic shock syndrome (88). Isogenic M1T1 5448 ΔSLO mutant was described previously (17). GAS strains were propagated using Todd Hewitt broth (THB) or agar (THA) at 37 °C. *E. coli* UPEC CFT073 was grown to and OD_{600} = 0.5, spun down by centrifugation, and cell free supernatant collected for use in mammalian cell assay. Recombinant *S. aureus* α-toxin was purchased from IBT Bioservices (#1401-002) and 1µg toxin used in cell assays. MBCD and BA were purchased from Sigma (catalog #M7439 and #B8936, respectively). MBCD was resuspended to a 100mM working solution in PBS and used in a final concentration range of 1-5mM. BA was resuspended to a 2 mM working solution in DMSO and used in concentration range of 1-100µM.

Expression and purification of recombinant SLO.

SLO gene was cloned into vector pET15b and transformed into BL21 DE3 *E. coli*. Bacteria expressing SLO were cultured in 1L lysogeny broth (LB) and incubated at 37°C with shaking. Expression was induced in cultures at 0.7 A_{600} with 0.5 mM isopropyl 1-thio-β-D-galactopyranoside (Bio-Vectra) and maintained at 30 °C for 4 h. Bacterial pellets were disrupted by sonication, and soluble 6×histidine-tagged SLO was purified using nickel-nitrilotriacetic acid-agarose (Invitrogen). Fractions corresponding to full-length SLO were pooled and further purification achieved using Amicon ultra centrifugal filters (Millipore Sigma). Protein was monitored by SDS-PAGE, and quantified by $A_{280,}$ and frozen in aliquots at –80°C. Assays were performed in the presence of 10 mM dithiothreitol (reducing conditions).

Mammalian cell culture

Human haploid (HAP1) cells and isogenic knockout sub-clone lines were grown in Iscove's modified Dulbecco's Medium (IMDM) (HyClone) supplemented with 10% (vol/vol) FBS, 1× penicillin/streptomycin (Gibco), and 2 mM L-glutamine. HEK-293T cells were used for lentivirus

generation and cultured in DMEM (HyClone) supplemented with 10% FBS, 1× penicillin/streptomycin (Gibco), and 2 mM L-glutamine.

Haploid human cell genetic screen.

HAP1 cells were mutagenized with a retroviral gene trap to cause inactivating mutations throughout the genome, and a genetic screen performed as previously described (35, 36). Approximately 10^8 gene-trap mutagenized cells were treated with 2 μg/mL SLO for 48 h. Following selection, surviving HAP1 colonies were expanded and pooled. Genomic DNA from the surviving, expanded cell population was isolated using the QIAamp DNA mini kit (Qiagen). Gene-trap insertion sites were recovered by linear amplification of genomic DNA sequences flanking the pro-viral DNA insertions and mapped to the human genome by deep sequencing. For each gene, enrichment of inactivating gene-trap insertions in the SLO selected pool over an unselected control dataset was determined by a one-sided Fisher's exact test and corrected for false discovery rate as previously described.

Genome engineering and SREBP2 cloning.

CRISPR targeting sequences were designed using the Feng Zhang Lab (Broad Institute of MIT, Cambridge, MA) CRISPR design tool (crispr.mit.edu). Using the Gibson Assembly Reaction (New England BioLabs), oligos corresponding to the guide RNA sequences (**Supplementary Table 4.2**) directly cloned into the Zhang Lab Cas9-expressing plasmid px458 (Addgene plasmid 48138) (89). HAP1 cells were transfected with guide RNA encoding px458 plasmids using Lipofectamine 2000 per manufacturer's guidelines (Life Technologies). At 48 h post-transfection, cells were single-cell sorted based on GFP expression using a BD InFlux cell sorter at the Stanford Shared FACS facility into 96-well tissue plates containing cell culture growth media. Single-cell sub-clones were expanded, and genomic DNA isolated for sequence-

based genotyping of the targeted exonic sites using sequencing primers listed in **Figure 4.1C**. Sub-clones containing frame-shift or large indels were selected for further experimentation, and when possible, the gene knockout was confirmed by immunofluorescent microscopy. Multiple independent sub-clones for each gene knockout were isolated and tested to confirm the reported phenotypes.

Cell Viability Assays

For quantification of cellular ATP as an indicator of metabolic activity and cell viability, opaque-walled 96-well plates with were prepared using HAP1 cells seeded at density 2 x 10^4 cells/well, and infected with GAS WT or ΔSLO mutant strains at MOI = 5 and 10 for 2 h or SLO + 10mM DTT for 15 min at 37°C. After incubation, media was removed and 100 µl of CellTiter-Glo® reagent added to wells, mixed for 2 min on an orbital shaker to induce cell lysis, and incubated at RT x 10 min to stabilize the luminescent signal then recorded using SpectraMax M3 plate reader/ SoftMax Pro plate reader and software.

Immunostaining of SREBP2.

For microscopic visualization of protein abundance, WT and ∆SREBP2 HAP1 cells were plated at 1x10^5 in 12-well plates with coverslips on day prior to staining. Cells were fixed with 4% paraformaldehyde and stained with anti-SREBP2 antibody (1:200 dilution, Santa Cruz) in PBS + 1% bovine serum albumin (BSA, Sigma-Aldrich) at room temperature for 1 h, followed by incubation with goat anti-rabbit Alexa 488 antibody (1:500 dilution, Life Technologies) for 30 min. Cells were counterstained with ProlongGold + 4',6'-diamidino-2-phenylindole (DAPI, Invitrogen) and imaged on a fluorescent microscope. Representative, randomized images (n=3) were taken for each condition and individualized experiment. Imaging was performed using Zeiss LSM 700 confocal microscope.

RNA extraction and qPCR.

WT and ΔSREBP2 HAP1 cells were sub-cultured into 12-well plates one day prior to experiment. Total RNA was isolated using RNeasy Mini Kit (Qiagen, Germantown, MD), and amplified in triplicate using KAPA SYBR FAST qPCR kit (Sigma-Aldrich) and the following primer sets: SREBP2 Forward: 5'-CACCACTCCGCAGCAGACGAGGA-3', SREBP2 Reverse: 5'-GTGACCGGCTGTACCTGGGA-3', SREBP1 Forward: 5'-GCAAGGCCATCGACTACATT-3', SREBP1 Reverse: 5'-GGTCAGTGTGTCCTCCACCT-3', LDLR Forward:5'-CAGATATCATCAACGAAGC-3' LDLR Reverse: 5'-CCTCTCACACCAGTTCACTCC-3', GAPDH Forward: 5'-TCCGGGAAACTGTGGCGTGA-3', GAPDH Reverse: 5'-GGAAGGCCATGCCAGTGAGC-3'. Gene expression was normalized to GAPDH mRNA content and calculated using the ΔΔ cycle threshold (ΔΔCT) method.

Total cholesterol determination.

WT and ΔSREBP2 HAP1 cells were sub-cultured into 6-well plates and total cholesterol and cholesteryl ester content determined using assay kit from BioVision (catalog #K603). Briefly, samples were prepared with or without 15 min MBCD pre-treatment by extraction with 200 µl chloroform:isopropanol:NP-40 (7:11:0.1), transferred to 1.5ml Eppendorf tubes and spun at 15,000 x g for 10 min. Liquid (organic phase) was transferred to a new tube, air dried to remove chloroform, and put under vacuum for 1 hour to remove trace organic solvent. Dried lipids were dissolved with 200 µl cholesterol assay buffer, sonicated and vortexed until homogeneous, 50 µl of extracted sample + 50 µl reaction mix added to 96 well plate and incubated in the dark for 1 hour at 37º. Absorbance was read at 570 nm using SpectraMax M3 plate reader/ SoftMax Pro plate reader and software and ratio determined by comparing to un-treated WT control.

Membrane fluidity assay.

WT and ΔSREBP2 HAP1 cells were sub-cultured into 96-well opaque white bottom plates and membrane fluidity assessed using a membrane fluidity kit (ABCAM ab189819). Cells were

incubated with labeling solution containing Fluorescent Lipid Reagent and Pluronic F-127 for 20 minutes at RT in the dark, washed 2X, and resuspended in perfusion buffer. Fluorescence emission was read at both 400 and 460-470nm with excitation at 360nm using SpectraMax M3 plate reader/ SoftMax Pro plate reader and software, and ratio of excimer to monomer fluorescence determined (Ie/Im).

Lipid rafts visualization.

WT and ΔSREBP2 HAP1 cells were sub-cultured into 12-well plates with coverslips and stained using the Vybrant Alexa Fluor 555 Lipid Raft Labeling Kit (ThermoFisher catalog #V34404). Briefly, cells were labeled with fluorescent cholera toxin subunit B (CT-B) conjugate for 10 min at 4^{o}C, crosslinked with anti-CT-B antibody and fixed with 4% paraformaldehyde. Cells were then mounted onto coverslips with DAPI-ProLong Gold antifade mountant (ThermoFisher catalog #P36931). And visualized using Zeiss LSM 700 confocal microscope. Representative, randomized images (n=3) were taken for each condition and individualized experiment. Lipid rafts were determined by visualization of distinct orange puncta versus unspecific dispersion of orange fluorescence.

Flow cytometry analysis of SLO binding.

WT and ΔSREBP2 HAP1 cells were sub-cultured into 12-well plates and treated with 0.25-0.5μg/ml purified recombinant SLO for 15 min. Cells were washed and transferred to Eppendorf tubes, spun down and resuspended in 4% paraformaldehyde for 20 min. Samples were washed twice with PBS+ centrifugation at 500xg for 10 min and resuspended in 1% BSA in PBS with anti-SLO antibody (1:200, ABCAM ab23501) for 1 h on ice. Samples were again and resuspended in goat anti-rabbit Alexa 488 antibody (1:500 dilution, Life Technologies) for 30 min, washed again and resuspended in 1 ml 1% BSA in PBS. Analysis was performed by flow cytometry (FACS Canto) and quantification using FlowJo software.

Bacterial growth curve analysis.

Overnight stationary phase cultures of GAS in THB were centrifuged at 4000x g for 10 min and resuspended in 300 ml RPMI 1640 medium (Invitrogen) supplemented with 20% fetal bovine serum (FBS; Gibco) heat-inactivated (HI) at 70°C for 30 min. The bacterial concentrate was used to adjust 10 ml of RPMI + 20% HI FBS to a starting optical density at 600 nm (OD600) of 0.01, and concentrations of BA or DMSO control were added. Growth at 37°C under static conditions was monitored by measuring the OD600 for 24 h.

Statistical analysis Error data represent standard errors of the means (SEM) of the results from experimental duplicates, triplicates, or quadruplets. Statistical analysis was performed using Student's unpaired two-tailed t test. Comparisons among three or more samples were evaluated using one-way analysis of variance (ANOVA) followed by Dunnett's or Tukey's test (Graph Pad Prism).

SUPPLEMENTARY FIGURES

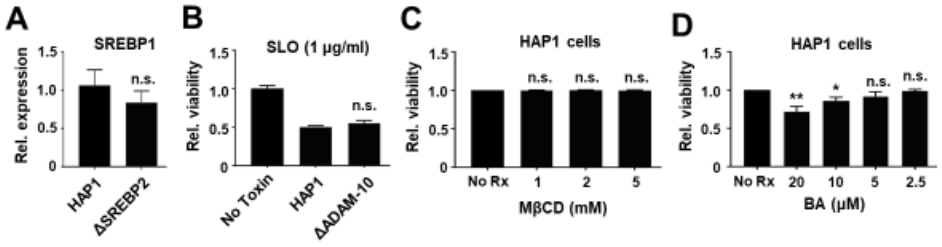

Figure S 4.1. (A) SREBP1 mRNA expression was assessed using q-PCR for WT cells treated with 2.5μM BA or negative control DMSO and compared to GAPDH housekeeping gene. **(B)** No change in susceptibility of ΔADAM-10 HAP1 cells vs. WT parent cells to SLO toxicity. **(C)** Effect of 1,2 and 5mM 15-minute MBCD pre-treatments on viability of WT HAP1 cells **(D)** Effect of 20 h pre-treatment of WT HAP1 cells with 20, 10, 5 and 2.5μM BA concentrations as determined by Cell-Titer Glo luminescent reagent. Results are from experiments performed in triplicate and reported as mean +/- SEM from at least 3 experiments.

Table 4.1. Inactivating gene-trap insertions. Inactivating insertions mapped in a SLO–selected HAP1 cell population compared with gene-trap insertions mapped in a control, unselected HAP1 cell population. Total unique retroviral inserts mapped in toxin library = 104,923 and in control library = 268,515.

GENE SYMBOL	GENE NAME	# of insertions in selected library	# of insertions in control library	P-value (uncorrected)	P-value (corrected for multiple hypothesis testing)	Fold-enrichment of insertions in selected library
SREBF2	Sterol Regulatory Element Binding Factor 2	198	63	2.07E-57	2.55E-53	8.043081934
SCAP	SREBP Cleavage-Activating Protein	33	15	5.99E-09	2.65E-05	5.630157353
UGCG	UDP-Glucose Ceramide Glucosyltransferase	20	6	3.36E-07	0.000690244	8.530541445
ADIPOR2	Adiponectin Receptor 2	22	9	9.04E-07	0.001314189	6.255730393
PLEKHG4	Puratrophin-1	31	23	6.15E-06	0.00758075	3.449305889
ANKRD34A	Ankyrin Repeat Domain-containing protein 34A	32	26	1.36E-05	0.015226865	3.14973838
NDUFAF3	NADH Dehydrogenase (Ubiquinone) complex 1, Assembly Factor 3	22	13	1.92E-05	0.019685681	4.330890272
FLJ37453	Uncharacterized LOC729614	74	100	3.20E-05	0.030317166	1.893780201
ACOX1	Peroxisomal acyl-coenzyme A oxidase 1	39	40	5.08E-05	0.044765288	2.495183373
NF2	Neurofibromin 2	25	20	0.00010047	0.082566008	3.198953042

Table 4.2. CRISPR guide RNA sequences. Selected CRISPR guides for top hit genes revealed in insertional mutagenesis screen.

CRISPR guide name	official guide # from GeckoV2 Library	guide sequence
SCAP-05	HGLibB_42805	ACAGCCCTGAAAGC CGCTGC
SCAP-04	HGLibB_42804	GTGGACTCTGACCG CAAACA
UCGC-50	HGLibA_60150	CCGATTACACCTCAA CAAGA
UCGC-97	HGLibB_52797	GATGTATGTAAGAA GCTTCT
ADIPOR2-80	HGLibB_00980	ATACAGTGATGAAG CTCCTC
ADIPOR2-84	HGLibA_00984	CTTACAAGCCCATCA TGCTA
ADIPOR1-79	HGLibB_00979	CCTGCAAGCCCACC ACGCCA
ADIPOR1-80	HGLibA_00980	CTGCCATCATTGTG GCGCAG
SREBF2-39	HGLibA_54239	TCAGCACCACTCCG CAGACG
SREBF2-40	HGLibA_54240	AGTGCAACGGTCAT TCACCC
ADAM10-1	n/a	TGATGATGGCGTAC TTGGTC

ACKNOWLEDGEMENTS

This work was supported by the NIH grants R01AI077780 and R01HL125352 (V.N.). T.E. was supported through the UCSD NIH/NIGMS Training Program in Molecular and Cellular Pharmacology (T32GM007752) and PhRMA Foundation Fellowship. J.E.C. is a David and Lucile Packard Foundation fellow and is funded by NIH Grant DP2 AI104557.

Chapter 4 is a prepared manuscript ready for submission: Tamara Escajadillo, Lauren Popov, Samira Dahesh, Jan E Carette, Victor Nizet. Novel role for Sterol Regulatory Element Binding Protein-2 (SREBP-2) in the regulation of host cell susceptibility to the streptococcal toxin streptolysin-O. The dissertation author is one of the primary investigators and authors of this paper.

REFERENCES

1. Walker MJ, Barnett TC, McArthur JD, Cole JN, Gillen CM, Henningham A, et al. Disease manifestations and pathogenic mechanisms of Group A Streptococcus. *Clin Microbiol Rev.* 2014;27(2):264-301.

2. LaRock CN, Dohrmann S, Todd J, Corriden R, Olson J, Johannssen T, et al. Group A streptococcal M1 protein sequesters cathelicidin to evade innate immune killing. *Cell Host Microbe.* 2015;18(4):471-7.

3. Aziz RK, and Kotb M. Rise and persistence of global M1T1 clone of Streptococcus pyogenes. *Emerg Infect Dis.* 2008;14(10):1511-7.

4. Tart AH, Walker MJ, and Musser JM. New understanding of the group A Streptococcus pathogenesis cycle. *Trends Microbiol.* 2007;15(7):318-25.

5. Aziz RK, Pabst MJ, Jeng A, Kansal R, Low DE, Nizet V, et al. Invasive M1T1 group A Streptococcus undergoes a phase-shift in vivo to prevent proteolytic degradation of multiple virulence factors by SpeB. *Mol Microbiol.* 2004;51(1):123-34.

6. Cole JN, McArthur JD, McKay FC, Sanderson-Smith ML, Cork AJ, Ranson M, et al. Trigger for group A streptococcal M1T1 invasive disease. *FASEB J.* 2006;20(10):1745-7.

7. Maamary PG, Ben Zakour NL, Cole JN, Hollands A, Aziz RK, Barnett TC, et al. Tracing the evolutionary history of the pandemic group A streptococcal M1T1 clone. *FASEB J.* 2012;26(11):4675-84.

8. Li J, Zhu H, Feng W, Liu M, Song Y, Zhang X, et al. Regulation of inhibition of neutrophil infiltration by the two-component regulatory system CovRS in subcutaneous murine infection with group A streptococcus. *Infect Immun.* 2013;81(3):974-83.

9. Walker MJ, Hollands A, Sanderson-Smith ML, Cole JN, Kirk JK, Henningham A, et al. DNase Sda1 provides selection pressure for a switch to invasive group A streptococcal infection. *Nat Med.* 2007;13(8):981-5.

10. Sumby P, Whitney AR, Graviss EA, DeLeo FR, and Musser JM. Genome-wide analysis of group a streptococci reveals a mutation that modulates global phenotype and disease specificity. *PLoS Pathog.* 2006;2(1):e5.

11. Shiseki M, Miwa K, Nemoto Y, Kato H, Suzuki J, Sekiya K, et al. Comparison of pathogenic factors expressed by group A Streptococci isolated from patients with streptococcal toxic shock syndrome and scarlet fever. *Microb Pathog.* 1999;27(4):243-52.

12. Ato M, Ikebe T, Kawabata H, Takemori T, and Watanabe H. Incompetence of neutrophils to invasive group A streptococcus is attributed to induction of plural virulence factors by dysfunction of a regulator. *PLoS One.* 2008;3(10):e3455.

13. Farrand AJ, Hotze EM, Sato TK, Wade KR, Wimley WC, Johnson AE, et al. The cholesterol-dependent cytolysin membrane-binding interface discriminates lipid

environments of cholesterol to support beta-barrel pore insertion. *The Journal of biological chemistry.* 2015;290(29):17733-44.

14. Feil SC, Ascher DB, Kuiper MJ, Tweten RK, and Parker MW. Structural studies of Streptococcus pyogenes streptolysin O provide insights into the early steps of membrane penetration. *Journal of molecular biology.* 2014;426(4):785-92.

15. Tweten RK. Cholesterol-dependent cytolysins, a family of versatile pore-forming toxins. *Infect Immun.* 2005;73(10):6199-209.

16. Cywes Bentley C, Hakansson A, Christianson J, and Wessels MR. Extracellular group A Streptococcus induces keratinocyte apoptosis by dysregulating calcium signalling. *Cellular microbiology.* 2005;7(7):945-55.

17. Timmer AM, Timmer JC, Pence MA, Hsu LC, Ghochani M, Frey TG, et al. Streptolysin O promotes group A Streptococcus immune evasion by accelerated macrophage apoptosis. *The Journal of biological chemistry.* 2009;284(2):862-71.

18. Keyel PA, Roth R, Yokoyama WM, Heuser JE, and Salter RD. Reduction of streptolysin O (SLO) pore-forming activity enhances inflammasome activation. *Toxins.* 2013;5(6):1105-18.

19. Chandrasekaran S, and Caparon MG. The NADase-negative variant of the Streptococcus pyogenes toxin NAD(+) glycohydrolase induces JNK1-mediated programmed cellular necrosis. *mBio.* 2016;7(1):e02215-15.

20. Bastiat-Sempe B, Love JF, Lomayesva N, and Wessels MR. Streptolysin O and NAD-glycohydrolase prevent phagolysosome acidification and promote group A Streptococcus survival in macrophages. *mBio.* 2014;5(5):e01690-14.

21. Uchiyama S, Dohrmann S, Timmer AM, Dixit N, Ghochani M, Bhandari T, et al. Streptolysin O rapidly impairs neutrophil oxidative burst and antibacterial responses to group A Streptococcus. *Frontiers in immunology.* 2015;6:581.

22. Cole JN, Barnett TC, Nizet V, and Walker MJ. Molecular insight into invasive group A streptococcal disease. *Nature reviews Microbiology.* 2011;9(10):724-36.

23. Limbago B, Penumalli V, Weinrick B, and Scott JR. Role of streptolysin O in a mouse model of invasive group A streptococcal disease. *Infect Immun.* 2000;68(11):6384-90.

24. Ikebe T, Ato M, Kobayashi K, and Watanabe H. [Mechanism behind streptococcus toxic shock-like syndrome onset--immune evasion and bacterial properties]. *Kansenshogaku zasshi The Journal of the Japanese Association for Infectious Diseases.* 2009;83(5):485-9.

25. Escajadillo T, Olson J, Luk BT, Zhang L, and Nizet V. A red blood cell membrane-camouflaged nanoparticle counteracts streptolysin O-mediated virulence phenotypes of invasive group A Streptococcus. *Frontiers in pharmacology.* 2017;8:477.

26. Zhang Y, Gao W, Chen Y, Escajadillo T, Ungerleider J, Fang RH, et al. Self-assembled colloidal gel using cell membrane-coated nanosponges as building blocks. *ACS Nano.* 2017;11(12):11923-30.

27. Cegelski L, Marshall GR, Eldridge GR, and Hultgren SJ. The biology and future prospects of antivirulence therapies. *Nature reviews Microbiology.* 2008;6(1):17-27.

28. Clatworthy AE, Pierson E, and Hung DT. Targeting virulence: a new paradigm for antimicrobial therapy. *Nature chemical biology.* 2007;3(9):541-8.

29. Munguia J, and Nizet V. Pharmacological targeting of the host-pathogen interaction: Alternatives to classical antibiotics to combat drug-resistant superbugs. *Trends in pharmacological sciences.* 2017;38(5):473-88.

30. Thamphiwatana S, Angsantikul P, Escajadillo T, Zhang Q, Olson J, Luk BT, et al. Macrophage-like nanoparticles concurrently absorbing endotoxins and proinflammatory cytokines for sepsis management. *Proceedings of the National Academy of Sciences of the United States of America.* 2017;114(43):11488-93.

31. Lee CC, Carette JE, Brummelkamp TR, and Ploegh HL. A reporter screen in a human haploid cell line identifies CYLD as a constitutive inhibitor of NF-kappaB. *PLoS One.* 2013;8(7):e70339.

32. Puschnik AS, Majzoub K, Ooi YS, and Carette JE. A CRISPR toolbox to study virus-host interactions. *Nature reviews Microbiology.* 2017;15(6):351-64.

33. Blomen VA, Majek P, Jae LT, Bigenzahn JW, Nieuwenhuis J, Staring J, et al. Gene essentiality and synthetic lethality in haploid human cells. *Science (New York, NY).* 2015;350(6264):1092-6.

34. Pillay S, and Carette JE. Hunting viral receptors using haploid cells. *Annual review of virology.* 2015;2(1):219-39.

35. Carette JE, Guimaraes CP, Varadarajan M, Park AS, Wuethrich I, Godarova A, et al. Haploid genetic screens in human cells identify host factors used by pathogens. *Science (New York, NY).* 2009;326(5957):1231-5.

36. Carette JE, Guimaraes CP, Wuethrich I, Blomen VA, Varadarajan M, Sun C, et al. Global gene disruption in human cells to assign genes to phenotypes by deep sequencing. *Nat Biotechnol.* 2011;29(6):542-6.

37. Guimaraes CP, Carette JE, Varadarajan M, Antos J, Popp MW, Spooner E, et al. Identification of host cell factors required for intoxication through use of modified cholera toxin. *The Journal of cell biology.* 2011;195(5):751-64.

38. Popov LM, Marceau CD, Starkl PM, Lumb JH, Shah J, Guerrera D, et al. The adherens junctions control susceptibility to Staphylococcus aureus alpha-toxin. *Proceedings of the National Academy of Sciences of the United States of America.* 2015;112(46):14337-42.

39. Jeon TI, and Osborne TF. SREBPs: metabolic integrators in physiology and metabolism. *Trends in endocrinology and metabolism: TEM.* 2012;23(2):65-72.

40. Horton JD, Goldstein JL, and Brown MS. SREBPs: activators of the complete program of cholesterol and fatty acid synthesis in the liver. *The Journal of clinical investigation.* 2002;109(9):1125-31.

41. Ichikawa S, Sakiyama H, Suzuki G, Hidari KI, and Hirabayashi Y. Expression cloning of a cDNA for human ceramide glucosyltransferase that catalyzes the first glycosylation step of glycosphingolipid synthesis. *Proceedings of the National Academy of Sciences of the United States of America.* 1996;93(22):12654.

42. Sharma AX, and Holland WL. Adiponectin and its hydrolase-activated receptors. *J Nat Sci.* 2017;3(6).

43. Gurcel L, Abrami L, Girardin S, Tschopp J, and van der Goot FG. Caspase-1 activation of lipid metabolic pathways in response to bacterial pore-forming toxins promotes cell survival. *Cell.* 2006;126(6):1135-45.

44. Oishi Y, Spann NJ, Link VM, Muse ED, Strid T, Edillor C, et al. SREBP1 contributes to resolution of pro-inflammatory TLR4 signaling by reprogramming fatty acid metabolism. *Cell metabolism.* 2017;25(2):412-27.

45. Osborne TF, and Espenshade PJ. Evolutionary conservation and adaptation in the mechanism that regulates SREBP action: what a long, strange tRIP it's been. *Genes & development.* 2009;23(22):2578-91.

46. Im SS, and Osborne TF. Protection from bacterial-toxin-induced apoptosis in macrophages requires the lipogenic transcription factor sterol regulatory element binding protein 1a. *Molecular and cellular biology.* 2012;32(12):2196-202.

47. Flanagan JJ, Tweten RK, Johnson AE, and Heuck AP. Cholesterol exposure at the membrane surface is necessary and sufficient to trigger perfringolysin O binding. *Biochemistry.* 2009;48(18):3977-87.

48. Heuck AP, Hotze EM, Tweten RK, and Johnson AE. Mechanism of membrane insertion of a multimeric beta-barrel protein: perfringolysin O creates a pore using ordered and coupled conformational changes. *Molecular cell.* 2000;6(5):1233-42.

49. Nelson LD, Johnson AE, and London E. How interaction of perfringolysin O with membranes is controlled by sterol structure, lipid structure, and physiological low pH: insights into the origin of perfringolysin O-lipid raft interaction. *The Journal of biological chemistry.* 2008;283(8):4632-42.

50. Zitzer A, Bittman R, Verbicky CA, Erukulla RK, Bhakdi S, Weis S, et al. Coupling of cholesterol and cone-shaped lipids in bilayers augments membrane permeabilization by the cholesterol-specific toxins streptolysin O and Vibrio cholerae cytolysin. *The Journal of biological chemistry.* 2001;276(18):14628-33.

51. Briggs MR, Yokoyama C, Wang X, Brown MS, and Goldstein JL. Nuclear protein that binds sterol regulatory element of low density lipoprotein receptor promoter. I. Identification of the protein and delineation of its target nucleotide sequence. *The Journal of biological chemistry.* 1993;268(19):14490-6.

52. Wong J, Quinn CM, and Brown AJ. SREBP-2 positively regulates transcription of the cholesterol efflux gene, ABCA1, by generating oxysterol ligands for LXR. *The Biochemical journal.* 2006;400(3):485-91.

53. Subczynski WK, Pasenkiewicz-Gierula M, Widomska J, Mainali L, and Raguz M. High cholesterol/low cholesterol: Effects in biological membranes: A review. *Cell biochemistry and biophysics.* 2017;75(3-4):369-85.

54. Subczynski WK, and Wisniewska A. Physical properties of lipid bilayer membranes: relevance to membrane biological functions. *Acta biochimica Polonica.* 2000;47(3):613-25.

55. Abboud R, Charcosset C, and Greige-Gerges H. Biophysical methods: complementary tools to study the influence of human steroid hormones on the liposome membrane properties. *Biochimie.* 2018.

56. Dumas F, and Haanappel E. Lipids in infectious diseases - The case of AIDS and tuberculosis. *Biochimica et biophysica acta.* 2017;1859(9 Pt B):1636-47.

57. Megha, Bakht O, and London E. Cholesterol precursors stabilize ordinary and ceramide-rich ordered lipid domains (lipid rafts) to different degrees. Implications for the Bloch hypothesis and sterol biosynthesis disorders. *The Journal of biological chemistry.* 2006;281(31):21903-13.

58. Simons K, and Ikonen E. Functional rafts in cell membranes. *Nature.* 1997;387(6633):569-72.

59. Xu X, and London E. The effect of sterol structure on membrane lipid domains reveals how cholesterol can induce lipid domain formation. *Biochemistry.* 2000;39(5):843-9.

60. Mahammad S, and Parmryd I. Cholesterol depletion using methyl-beta-cyclodextrin. *Methods in molecular biology (Clifton, NJ).* 2015;1232:91-102.

61. Costa JF, Barbosa-Filho JM, Maia GL, Guimaraes ET, Meira CS, Ribeiro-dos-Santos R, et al. Potent anti-inflammatory activity of betulinic acid treatment in a model of lethal endotoxemia. *International immunopharmacology.* 2014;23(2):469-74.

62. Yogeeswari P, and Sriram D. Betulinic acid and its derivatives: a review on their biological properties. *Current medicinal chemistry.* 2005;12(6):657-66.

63. Zhao GJ, Tang SL, Lv YC, Ouyang XP, He PP, Yao F, et al. Antagonism of betulinic acid on LPS-mediated inhibition of ABCA1 and cholesterol efflux through inhibiting nuclear factor-kappaB signaling pathway and miR-33 expression. *PLoS One.* 2013;8(9):e74782.

64. Tang JJ, Li JG, Qi W, Qiu WW, Li PS, Li BL, et al. Inhibition of SREBP by a small molecule, betulin, improves hyperlipidemia and insulin resistance and reduces atherosclerotic plaques. *Cell metabolism.* 2011;13(1):44-56.

65. O'Brien KL, Beall B, Barrett NL, Cieslak PR, Reingold A, Farley MM, et al. Epidemiology of invasive group a streptococcus disease in the United States, 1995-1999. *Clinical*

infectious diseases : an official publication of the Infectious Diseases Society of America. 2002;35(3):268-76.

66. Stevens DL, and Bryant AE. In: Ferretti JJ, Stevens DL, and Fischetti VA eds. *Streptococcus pyogenes : Basic Biology to Clinical Manifestations*. Oklahoma City (OK): University of Oklahoma Health Sciences Center; 2016.

67. Giddings KS, Zhao J, Sims PJ, and Tweten RK. Human CD59 is a receptor for the cholesterol-dependent cytolysin intermedilysin. *Nature structural & molecular biology.* 2004;11(12):1173-8.

68. Alouf JE. Cholesterol-binding cytolytic protein toxins. *International journal of medical microbiology : IJMM.* 2000;290(4-5):351-6.

69. Eberle D, Hegarty B, Bossard P, Ferre P, and Foufelle F. SREBP transcription factors: master regulators of lipid homeostasis. *Biochimie.* 2004;86(11):839-48.

70. Ye J, and DeBose-Boyd RA. Regulation of cholesterol and fatty acid synthesis. *Cold Spring Harbor perspectives in biology.* 2011;3(7).

71. Giddings KS, Johnson AE, and Tweten RK. Redefining cholesterol's role in the mechanism of the cholesterol-dependent cytolysins. *Proceedings of the National Academy of Sciences of the United States of America.* 2003;100(20):11315-20.

72. Shewell LK, Harvey RM, Higgins MA, Day CJ, Hartley-Tassell LE, Chen AY, et al. The cholesterol-dependent cytolysins pneumolysin and streptolysin O require binding to red blood cell glycans for hemolytic activity. *Proceedings of the National Academy of Sciences of the United States of America.* 2014;111(49):E5312-20.

73. Ge M, Field KA, Aneja R, Holowka D, Baird B, and Freed JH. Electron spin resonance characterization of liquid ordered phase of detergent-resistant membranes from RBL-2H3 cells. *Biophysical journal.* 1999;77(2):925-33.

74. Silvius JR, del Giudice D, and Lafleur M. Cholesterol at different bilayer concentrations can promote or antagonize lateral segregation of phospholipids of differing acyl chain length. *Biochemistry.* 1996;35(48):15198-208.

75. Chiarot E, Faralla C, Chiappini N, Tuscano G, Falugi F, Gambellini G, et al. Targeted amino acid substitutions impair streptolysin O toxicity and group A Streptococcus virulence. *mBio.* 2013;4(1):e00387-12.

76. Cragg GM, and Newman DJ. Natural products: a continuing source of novel drug leads. *Biochimica et biophysica acta.* 2013;1830(6):3670-95.

77. Silva LN, Zimmer KR, Macedo AJ, and Trentin DS. Plant natural products targeting bacterial virulence factors. *Chemical reviews.* 2016;116(16):9162-236.

78. Newman DJ, and Cragg GM. Natural products as sources of new drugs over the 30 years from 1981 to 2010. *Journal of natural products.* 2012;75(3):311-35.

79. Alakurtti S, Makela T, Koskimies S, and Yli-Kauhaluoma J. Pharmacological properties of the ubiquitous natural product betulin. *European journal of pharmaceutical sciences : official journal of the European Federation for Pharmaceutical Sciences.* 2006;29(1):1-13.

80. Ziegler HL, Franzyk H, Sairafianpour M, Tabatabai M, Tehrani MD, Bagherzadeh K, et al. Erythrocyte membrane modifying agents and the inhibition of Plasmodium falciparum growth: structure-activity relationships for betulinic acid analogues. *Bioorganic & medicinal chemistry.* 2004;12(1):119-27.

81. Upadhyay A, Mooyottu S, Yin H, Nair MS, Bhattaram V, and Venkitanarayanan K. Inhibiting microbial toxins using plant-derived compounds and plant extracts. *Medicines (Basel, Switzerland).* 2015;2(3):186-211.

82. Fernandez-Hernando C, and Moore KJ. MicroRNA modulation of cholesterol homeostasis. *Arterioscler Thromb Vasc Biol.* 2011;31(11):2378-82.

83. Shimano H, Shimomura I, Hammer RE, Herz J, Goldstein JL, Brown MS, et al. Elevated levels of SREBP-2 and cholesterol synthesis in livers of mice homozygous for a targeted disruption of the SREBP-1 gene. *The Journal of clinical investigation.* 1997;100(8):2115-24.

84. Seo YK, Jeon TI, Chong HK, Biesinger J, Xie X, and Osborne TF. Genome-wide localization of SREBP-2 in hepatic chromatin predicts a role in autophagy. *Cell metabolism.* 2011;13(4):367-75.

85. Vergnes L, Chin RG, de Aguiar Vallim T, Fong LG, Osborne TF, Young SG, et al. SREBP-2-deficient and hypomorphic mice reveal roles for SREBP-2 in embryonic development and SREBP-1c expression. *Journal of lipid research.* 2016;57(3):410-21.

86. Fulda S. Betulinic Acid for cancer treatment and prevention. *Int J Mol Sci.* 2008;9(6):1096-107.

87. Ehrhardt H, Fulda S, Fuhrer M, Debatin KM, and Jeremias I. Betulinic acid-induced apoptosis in leukemia cells. *Leukemia.* 2004;18(8):1406-12.

88. Chatellier S, Ihendyane N, Kansal RG, Khambaty F, Basma H, Norrby-Teglund A, et al. Genetic relatedness and superantigen expression in group A streptococcus serotype M1 isolates from patients with severe and nonsevere invasive diseases. *Infect Immun.* 2000;68(6):3523-34.

89. Ran FA, Hsu PD, Wright J, Agarwala V, Scott DA, and Zhang F. Genome engineering using the CRISPR-Cas9 system. *Nature protocols.* 2013;8(11):2281-308.

CHAPTER 5

CONCLUSIONS

Bacterial infections continue to be a significant cause of morbidity and mortality worldwide due to the escalating prevalence of antimicrobial resistance. Therefore, there is an acute need to develop innovative strategies to combat the global threat of antibiotic resistance. Among the most promising approaches include boosting host immune cell function and neutralizing key pathogen virulence factors.

While the contribution of PFTs to the pathogenicity and severity of bacterial disease has been appreciated, significant exploration into the mechanisms of exploiting this knowledge for the improvement of clinical outcomes is still lacking. PFT neutralization as adjunctive therapy to classical antibiotic treatments has the potential to be a low risk, high reward approach due to many factors including the possibility of reducing selective pressure on the bacteria while preserving the normal flora and immune system capable of independently combating disease.

This dissertation project offers evidence that disarming bacterial pathogens through inhibition of their PFTs or other bacterial toxins at any stage of secretion and or interaction with the host may constitute a viable treatment option when the use of classical antibiotics is insufficient. This final chapter of the dissertation will summarize the evidence of novel strategies for bacterial detoxification presented herein and advances our understanding and knowledge of bacterial toxin induced disease states. This chapter will further suggest future studies to continue to complement these strategies in an effort to make these approaches a viable and clinically significant means of combating bacterial burden in disease.

SUMMARY OF RESULTS

Prior to the beginning of the projects listed in this dissertation, there existed a limited number of strategies for targeting bacterial toxins as a strategy for combating clinical disease

Table 5.1. Therapies involving inactivation of pore forming toxins.

GENERAL MECHANISM OF PFT INACTIVATION	SUB-CLASSIFICATION	PFT	THERAPY
DIRECT BINDING/INHIBITION OF TOXIN ASSEMBLY: ANTIBODIES	MONOCLONAL ANTIBODIES	Hla	mAbs: MEDI4893 from MedImmune LLC, LTM14(Foletti et al. (2013); mAbs 2A3 and LC10 (Hua et al. 2014, Tkaczyk et al. 2012); mAbs 7B8 and 1A9 (Ragle and Bubeck Wardenburg 2009)
		Hla, leukocydins (LukED LukSF-PV, HlgAB, HlgCB)	AR-301 (Salvecin™) from Aridis Pharmaceuticals, Inc.; ASN-1 and ASN-2 (Rouha et al. (2018), ASN100 (Arsanis Inc)
		LukS-PV, LukF-PV, γ-hemolysin C (HlgC)	HCAbs(Laventie et al. 2011)
		PLY	mAbs: PLY-4 PLY-7 (Suarez-Alvarez et al. (2003); **LeX/sLeX antibodies(Shewell et al. 2014)**
		ALO	mAbs 64F8 and 80C9 (Nakouzi et al. 2008)
DIRECT BINDING/INHIBITION OF TOXIN ASSEMBLY: OTHER SMALL MOLECULES	SMALL MOLECULES	Hla	baicalin (Qiu et al. (2012) apigenin, chrysin, kaempferol, luteolin, and quercetin; *trans*-resveratrol and betulinic acid(Cho et al. 2015)Orolyxin A (Dong et al. 2013); morin hydrate(Wang et al. 2015b); Oroxylin A 7-O-glucuronide (OLG) and Oroxin B (ORB) (Qiu et al. 2013)
			peptides: IYGSKANRQTDK(Rani et al. 2014)
		PLY	**β-Sitosterol (Li et al. (2015), apigenin (Song et al. (2016); LeX/sLeX antibodies(Shewell et al. 2014)** Amentoflavone (Zhao et al. (2017); Verbascoside(Zhao et al. 2016)
		SLO	allicin (Arzanlou and Bohlooli 2010); lacto-*N*-neotetraose (LNnT)(Shewell et al. 2014)
		LLO	Finestin Wang et al. (2015a), 4-Cyclopent-3-enyl-6, 7-dihydroxy-8-hydroxymethyl-nona-2, 8-dienylideneamino)-penta-1,4-dien-3-one(Ghafari et al. 2017)
DIRECT BINDING/INHIBITION THROUGH DECOY CAPTURE	LIPOSOMES NANOPARTICLES	Hla, potential broad spectrum	(Ch:Sm) liposomes, (Ch:Sm+Sm) liposomes(Henry et al. 2015)
		PLY, potential broad spectrum	CAL02 (Combioxin SA)
		Hla, SLO, LLO, potential broad spectrum	RBC-coated nanoparticles (Hu et al. 2013a)
ALTERATION OF HOST CELL RECEPTORS/UPTAKE INHIBITION	PEPTIDES STATINS	Hla	GI254023X (ADAM10 inhibitor) (Inoshima, Wang and Bubeck Wardenburg 2012, Ludwig et al. 2005)
		ILY	ILY peptide (residues 438-452)(Johnson et al. 2013);rILYd4(Cai et al. 2014)
		LukED	Maraviroc (CCR5 agonist) (Alonzo et al. 2013)
		PLY, SLO, tetanolysin	Simvastatin (Statt et al. 2015, Rosch et al. 2010)
PORE BLOCKAGE	CHEMICAL COMPOUNDS SMALL MOLECULES	Hla	β-cyclodextrins (Yannakopoulou et al. 2011); β-cyclodextrin derivative: IB201(Ragle, Karginov and Bubeck Wardenburg 2010); ANBOβCD (Karginov et al. 2007); Cu(isapn) and perclorate—[Cu(isapn)]$(ClO_4)_2$—or sulfonate—[Cu(isapn)]$(SO_4)_2$(Melo et al. 2016)
		Etx	N-cycloalkylbenzamide, furo[2,3-b]quinoline, and 6H- anthra[1,9-cd]isoxazol
INCREASE HOST RESILIANCE TO TOXIN	MEMBRANE REPAIR VACCINES	PLY	AP301 (TNF-derived TIP peptide) and JI-34 (GHRH agonist) (Lucas et al. 2013); pneumolysin toxoid (dPly) (Alexander et al. 1994); Δ6 PLY (Kirkham et al. 2006);CbpA peptide–L460D pneumolysoid (Mann et al. 2014);
		Hla	IFN-α (increase in lipid metabolism)(Yarovinsky et al. 2008) ; Hla_{H35L} (Bubeck Wardenburg and Schneewind 2008); AT62 (Adhikari et al. 2012); chimeric bivalent IsdB/Hla(Zuo et al. 2013)
		LukS-PV and LukF-PV	LukS-Mut9/LukF-Mut1 (Karauzum et al. 2013)
		Hla, potential broad spectrum	Nanotoxoids (Hu et al. 2013b)
		SLO	rSLOmut (Uchiyama et al. 2015)
		Etx	Y30A-Y196A(Bokori-Brown et al. 2014)
		LLO	LLO W492A, LLO W491-492A(Michel et al. 1990, Hernandez-Flores and Vivanco-Cid 2015)

and improving patient outcomes, which can be found summarized in **Table 5.1.** This dissertation expands the number of potential therapies being developed pertaining to toxin neutralization by focusing on two general mechanisms of action: inhibition through decoy capture and increase in host cell resilience.

As fully discussed in Chapter 2 of this dissertation, utilizing a nanoparticle formulation derived from red blood cells (RBC s) previously studied in the context of the purified Staphylococcus aureus PFT alpha-toxin in vitro (Hu et al. 2013), this dissertation expands the proven application of nanosponges in toxin neutralization to the GAS virulence factor SLO, with studies using purified toxin, live bacteria, and a murine model of infection. This proof of principle involving nanoparticle strategies was further evolved to incorporate the use of macrophage derived nanoparticles for the concurrent absorption and detoxification of both bacterial toxins and proinflammatory cytokines, which are key players in the development of sepsis. These results, described extensively in Chapter 3, can potentially be envisioned to apply to any bacterial pathogen involved in septic disease states.

Chapter 4 expanded on the knowledge of host factors involved in mediating SLO toxicity by describing the use of a CRISPR-based mutagenized haploid cell genetic screen. Through this method, we discovered gene candidates involved in cholesterol metabolism whose reduced expression promotes resistance to SLO cytotoxicity. Individual “hits” were validated by CRISPR knockdown, including a regulator of cholesterol homeostasis SREBP2, and downstream effects and possible mechanisms of host cell resilience were described in detail.

FUTURE DIRECTIONS

This thesis dissertation has shown that inactivation of bacterial toxins, both through the use of engineered nanoparticles and inactivation of host factors required for toxicity, may present viable therapeutic options for patients facing clinically significant disease states where the use of antibiotics is not enough. Inactivation of bacterial toxins can present a relief for the host immune system when faced with overwhelming infection and allow the natural immunity to function at a higher rate due to reduced destruction of host cells. Both strategies can be further developed to target multiple toxins on the same bacteria or similar toxins from different bacteria,

in an effort to expand treatment options when timing is critical, and the specific disease state is unknown.

ACKNOWLEDGEMENTS

Chapter 5 is a portion of a review article being prepared for submission as: Escajadillo T & Nizet V. Targeting bacterial pore forming toxins: implications for virulence based adjunctive therapy for invasive bacterial infections. The dissertation author is the primary author of this paper.

REFERENCES

1. Adhikari, R. P., H. Karauzum, J. Sarwar, L. Abaandou, M. Mahmoudieh, A. R. Boroun, H. Vu, T. Nguyen, V. S. Devi, S. Shulenin, K. L. Warfield & M. J. Aman (2012) Novel structurally designed vaccine for S. aureus alpha-hemolysin: protection against bacteremia and pneumonia. *PLoS One,* 7**,** e38567.

2. Alexander, J. E., R. A. Lock, C. C. Peeters, J. T. Poolman, P. W. Andrew, T. J. Mitchell, D. Hansman & J. C. Paton (1994) Immunization of mice with pneumolysin toxoid confers a significant degree of protection against at least nine serotypes of Streptococcus pneumoniae. *Infect Immun,* 62**,** 5683-8.

3. Alonzo, F., 3rd, L. Kozhaya, S. A. Rawlings, T. Reyes-Robles, A. L. DuMont, D. G. Myszka, N. R. Landau, D. Unutmaz & V. J. Torres (2013) CCR5 is a receptor for Staphylococcus aureus leukotoxin ED. *Nature,* 493**,** 51-5.

4. Arzanlou, M. & S. Bohlooli (2010) Inhibition of streptolysin O by allicin - an active component of garlic. *J Med Microbiol,* 59**,** 1044-9.

5. Bokori-Brown, M., C. A. Hall, C. Vance, S. P. Fernandes da Costa, C. G. Savva, C. E. Naylor, A. R. Cole, A. K. Basak, D. S. Moss & R. W. Titball (2014) Clostridium perfringens epsilon toxin mutant Y30A-Y196A as a recombinant vaccine candidate against enterotoxemia. *Vaccine,* 32**,** 2682-7.

6. Bubeck Wardenburg, J. & O. Schneewind (2008) Vaccine protection against Staphylococcus aureus pneumonia. *J Exp Med,* 205**,** 287-94.

7. Cai, B., S. Xie, F. Liu, L. C. Simone, S. Caplan, X. Qin & N. Naslavsky (2014) Rapid degradation of the complement regulator, CD59, by a novel inhibitor. *J Biol Chem,* 289**,** 12109-25.

8. Cho, H. S., J. H. Lee, M. H. Cho & J. Lee (2015) Red wines and flavonoids diminish Staphylococcus aureus virulence with anti-biofilm and anti-hemolytic activities. *Biofouling,* 31**,** 1-11.

9. Dong, J., J. Qiu, Y. Zhang, C. Lu, X. Dai, J. Wang, H. Li, X. Wang, W. Tan, M. Luo, X. Niu & X. Deng (2013) Oroxylin A inhibits hemolysis via hindering the self-assembly of alpha-hemolysin heptameric transmembrane pore. *PLoS Comput Biol,* 9**,** e1002869.

10. Foletti, D., P. Strop, L. Shaughnessy, A. Hasa-Moreno, M. G. Casas, M. Russell, C. Bee, S. Wu, A. Pham, Z. Zeng, J. Pons, A. Rajpal & D. Shelton (2013) Mechanism of action and in vivo efficacy of a human-derived antibody against Staphylococcus aureus alpha-hemolysin. *J Mol Biol,* 425**,** 1641-54.

11. Ghafari, S., M. Komeilian, M. S. Hashemi, S. Oushani, G. Rigi, B. Rashidieh, K. Yarahmadi & F. Khoddam (2017) Molecular docking based screening of Listeriolysin-O for improved inhibitors. *Bioinformation,* 13**,** 160-163.

12. Henry, B. D., D. R. Neill, K. A. Becker, S. Gore, L. Bricio-Moreno, R. Ziobro, M. J. Edwards, K. Muhlemann, J. Steinmann, B. Kleuser, L. Japtok, M. Luginbuhl, H. Wolfmeier, A. Scherag, E. Gulbins, A. Kadioglu, A. Draeger & E. B. Babiychuk (2015) Engineered liposomes sequester bacterial exotoxins and protect from severe invasive infections in mice. *Nat Biotechnol,* 33**,** 81-8.

13. Hernandez-Flores, K. G. & H. Vivanco-Cid (2015) Biological effects of listeriolysin O: implications for vaccination. *Biomed Res Int,* 2015**,** 360741.

14. Hu, C. M., R. H. Fang, J. Copp, B. T. Luk & L. Zhang (2013a) A biomimetic nanosponge that absorbs pore-forming toxins. *Nat Nanotechnol,* 8**,** 336-40.

15. Hu, C. M., R. H. Fang, B. T. Luk & L. Zhang (2013b) Nanoparticle-detained toxins for safe and effective vaccination. *Nat Nanotechnol,* 8**,** 933-8.

16. Hua, L., J. J. Hilliard, Y. Shi, C. Tkaczyk, L. I. Cheng, X. Yu, V. Datta, S. Ren, H. Feng, R. Zinsou, A. Keller, T. O'Day, Q. Du, L. Cheng, M. Damschroder, G. Robbie, J. Suzich, C. K. Stover & B. R. Sellman (2014) Assessment of an anti-alpha-toxin monoclonal antibody for prevention and treatment of Staphylococcus aureus-induced pneumonia. *Antimicrob Agents Chemother,* 58**,** 1108-17.

17. Inoshima, N., Y. Wang & J. Bubeck Wardenburg (2012) Genetic requirement for ADAM10 in severe Staphylococcus aureus skin infection. *J Invest Dermatol,* 132**,** 1513-6.
18. Johnson, S., N. J. Brooks, R. A. Smith, S. M. Lea & D. Bubeck (2013) Structural basis for recognition of the pore-forming toxin intermedilysin by human complement receptor CD59. *Cell Rep,* 3**,** 1369-77.

19. Karauzum, H., R. P. Adhikari, J. Sarwar, V. S. Devi, L. Abaandou, C. Haudenschild, M. Mahmoudieh, A. R. Boroun, H. Vu, T. Nguyen, K. L. Warfield, S. Shulenin & M. J. Aman (2013) Structurally designed attenuated subunit vaccines for S. aureus LukS-PV and LukF-PV confer protection in a mouse bacteremia model. *PLoS One,* 8**,** e65384.

20. Karginov, V. A., E. M. Nestorovich, F. Schmidtmann, T. M. Robinson, A. Yohannes, N. E. Fahmi, S. M. Bezrukov & S. M. Hecht (2007) Inhibition of S. aureus alpha-hemolysin and B. anthracis lethal toxin by beta-cyclodextrin derivatives. *Bioorg Med Chem,* 15**,** 5424-31.

21. Kirkham, L. A., A. R. Kerr, G. R. Douce, G. K. Paterson, D. A. Dilts, D. F. Liu & T. J. Mitchell (2006) Construction and immunological characterization of a novel nontoxic protective pneumolysin mutant for use in future pneumococcal vaccines. *Infect Immun,* 74**,** 586-93.

22. Laventie, B. J., H. J. Rademaker, M. Saleh, E. de Boer, R. Janssens, T. Bourcier, A. Subilia, L. Marcellin, R. van Haperen, J. H. Lebbink, T. Chen, G. Prevost, F. Grosveld & D. Drabek (2011) Heavy chain-only antibodies and tetravalent bispecific antibody neutralizing Staphylococcus aureus leukotoxins. *Proc Natl Acad Sci U S A,* 108**,** 16404-9.

23. Li, H., X. Zhao, J. Wang, Y. Dong, S. Meng, R. Li, X. Niu & X. Deng (2015) beta-sitosterol interacts with pneumolysin to prevent Streptococcus pneumoniae infection. *Sci Rep,* 5**,** 17668.

24. Lucas, R., I. Czikora, S. Sridhar, E. Zemskov, B. Gorshkov, U. Siddaramappa, A. Oseghale, J. Lawson, A. Verin, F. G. Rick, N. L. Block, H. Pillich, M. Romero, M. Leustik, A. V. Schally & T. Chakraborty (2013) Mini-review: novel therapeutic strategies to blunt actions of pneumolysin in the lungs. *Toxins (Basel),* 5**,** 1244-60.

25. Ludwig, A., C. Hundhausen, M. H. Lambert, N. Broadway, R. C. Andrews, D. M. Bickett, M. A. Leesnitzer & J. D. Becherer (2005) Metalloproteinase inhibitors for the disintegrin-like metalloproteinases ADAM10 and ADAM17 that differentially block constitutive and phorbol ester-inducible shedding of cell surface molecules. *Comb Chem High Throughput Screen,* 8**,** 161-71.

26. Mann, B., J. Thornton, R. Heath, K. R. Wade, R. K. Tweten, G. Gao, K. El Kasmi, J. B. Jordan, D. M. Mitrea, R. Kriwacki, J. Maisonneuve, M. Alderson & E. I. Tuomanen (2014) Broadly protective protein-based pneumococcal vaccine composed of pneumolysin toxoid-CbpA peptide recombinant fusion protein. *J Infect Dis,* 209**,** 1116-25.

27. Melo, M. C., L. R. Teixeira, L. Pol-Fachin & C. G. Rodrigues (2016) Inhibition of the hemolytic activity caused by Staphylococcus aureus alpha-hemolysin through isatin-Schiff copper(II) complexes. *FEMS Microbiol Lett,* 363**,** fnv207.

28. Michel, E., K. A. Reich, R. Favier, P. Berche & P. Cossart (1990) Attenuated mutants of the intracellular bacterium Listeria monocytogenes obtained by single amino acid substitutions in listeriolysin O. *Mol Microbiol,* 4**,** 2167-78.

29. Nakouzi, A., J. Rivera, R. F. Rest & A. Casadevall (2008) Passive administration of monoclonal antibodies to anthrolysin O prolong survival in mice lethally infected with Bacillus anthracis. *BMC Microbiol,* 8**,** 159.

30. Qiu, J., X. Niu, J. Dong, D. Wang, J. Wang, H. Li, M. Luo, S. Li, H. Feng & X. Deng (2012) Baicalin protects mice from Staphylococcus aureus pneumonia via inhibition of the cytolytic activity of alpha-hemolysin. *J Infect Dis,* 206**,** 292-301.

31. Qiu, J., D. Wang, Y. Zhang, J. Dong, J. Wang & X. Niu (2013) Molecular modeling reveals the novel inhibition mechanism and binding mode of three natural compounds to staphylococcal alpha-hemolysin. *PLoS One,* 8**,** e80197.

32. Ragle, B. E. & J. Bubeck Wardenburg (2009) Anti-alpha-hemolysin monoclonal antibodies mediate protection against Staphylococcus aureus pneumonia. *Infect Immun,* 77**,** 2712-8.

33. Ragle, B. E., V. A. Karginov & J. Bubeck Wardenburg (2010) Prevention and treatment of Staphylococcus aureus pneumonia with a beta-cyclodextrin derivative. *Antimicrob Agents Chemother,* 54**,** 298-304.

34. Rani, N., V. Saravanan, P. T. V. Lakshmi & A. Annamalai (2014) Inhibition of Pore Formation by Blocking the Assembly of Staphylococcus aureus α-Hemolysin Through a Novel Peptide Inhibitor: an In Silco Approach. *International Journal of Peptide Research and Therapeutics,* 20**,** 575-583.

35. Rosch, J. W., A. R. Boyd, E. Hinojosa, T. Pestina, Y. Hu, D. A. Persons, C. J. Orihuela & E. I. Tuomanen (2010) Statins protect against fulminant pneumococcal infection and cytolysin toxicity in a mouse model of sickle cell disease. *J Clin Invest,* 120**,** 627-35.

36. Rouha, H., S. Weber, P. Janesch, B. Maierhofer, K. Gross, I. Dolezilkova, I. Mirkina, Z. C. Visram, S. Malafa, L. Stulik, A. Badarau & E. Nagy (2018) Disarming Staphylococcus aureus from destroying human cells by simultaneously neutralizing six cytotoxins with two human monoclonal antibodies. *Virulence,* 9**,** 231-247.

37. Shewell, L. K., R. M. Harvey, M. A. Higgins, C. J. Day, L. E. Hartley-Tassell, A. Y. Chen, C. M. Gillen, D. B. James, F. Alonzo, 3rd, V. J. Torres, M. J. Walker, A. W. Paton, J. C. Paton & M. P. Jennings (2014) The cholesterol-dependent cytolysins pneumolysin and streptolysin O require binding to red blood cell glycans for hemolytic activity. *Proc Natl Acad Sci U S A,* 111**,** E5312-20.

38. Song, M., L. Li, M. Li, Y. Cha, X. Deng & J. Wang (2016) Apigenin protects mice from pneumococcal pneumonia by inhibiting the cytolytic activity of pneumolysin. *Fitoterapia,* 115**,** 31-36.

39. Statt, S., J. W. Ruan, L. Y. Hung, C. Y. Chang, C. T. Huang, J. H. Lim, J. D. Li, R. Wu & C. Y. Kao (2015) Statin-conferred enhanced cellular resistance against bacterial pore-forming toxins in airway epithelial cells. *Am J Respir Cell Mol Biol,* 53**,** 689-702.

40. Suarez-Alvarez, B., M. Garcia-Suarez Mdel, F. J. Mendez & J. R. de los Toyos (2003) Characterisation of mouse monoclonal antibodies for pneumolysin: fine epitope mapping and V gene usage. *Immunol Lett,* 88**,** 227-39.

41. Tkaczyk, C., L. Hua, R. Varkey, Y. Shi, L. Dettinger, R. Woods, A. Barnes, R. S. MacGill, S. Wilson, P. Chowdhury, C. K. Stover & B. R. Sellman (2012) Identification of anti-alpha toxin monoclonal antibodies that reduce the severity of Staphylococcus aureus dermonecrosis and exhibit a correlation between affinity and potency. *Clin Vaccine Immunol,* 19**,** 377-85.

42. Uchiyama, S., S. Dohrmann, A. M. Timmer, N. Dixit, M. Ghochani, T. Bhandari, J. C. Timmer, K. Sprague, J. Bubeck-Wardenburg, S. I. Simon & V. Nizet (2015) Streptolysin O Rapidly Impairs Neutrophil Oxidative Burst and Antibacterial Responses to Group A Streptococcus. *Front Immunol,* 6**,** 581.

43. Wang, J., J. Qiu, W. Tan, Y. Zhang, H. Wang, X. Zhou, S. Liu, H. Feng, W. Li, X. Niu & X. Deng (2015a) Fisetin inhibits Listeria monocytogenes virulence by interfering with the oligomerization of listeriolysin O. *J Infect Dis,* 211**,** 1376-87.

44. Wang, J., X. Zhou, S. Liu, G. Li, L. Shi, J. Dong, W. Li, X. Deng & X. Niu (2015b) Morin hydrate attenuates Staphylococcus aureus virulence by inhibiting the self-assembly of alpha-hemolysin. *J Appl Microbiol,* 118**,** 753-63.

45. Yannakopoulou, K., L. Jicsinszky, C. Aggelidou, N. Mourtzis, T. M. Robinson, A. Yohannes, E. M. Nestorovich, S. M. Bezrukov & V. A. Karginov (2011) Symmetry requirements for effective blocking of pore-forming toxins: comparative study with alpha-, beta-, and gamma-cyclodextrin derivatives. *Antimicrob Agents Chemother,* 55**,** 3594-7.

46. Yarovinsky, T. O., M. M. Monick, M. Husmann & G. W. Hunninghake (2008) Interferons increase cell resistance to Staphylococcal alpha-toxin. *Infect Immun,* 76**,** 571-7.

47. Zhao, X., H. Li, J. Wang, Y. Guo, B. Liu, X. Deng & X. Niu (2016) Verbascoside Alleviates Pneumococcal Pneumonia by Reducing Pneumolysin Oligomers. *Mol Pharmacol,* 89**,** 376-87.

48. Zhao, X., B. Liu, S. Liu, L. Wang & J. Wang (2017) Anticytotoxin Effects of Amentoflavone to Pneumolysin. *Biol Pharm Bull,* 40**,** 61-67.

49. Zuo, Q. F., L. Y. Yang, Q. Feng, D. S. Lu, Y. D. Dong, C. Z. Cai, Y. Wu, Y. Guo, J. Gu, H. Zeng & Q. M. Zou (2013) Evaluation of the protective immunity of a novel subunit fusion vaccine in a murine model of systemic MRSA infection. *PLoS One,* 8**,** e81212.